2012

Surface-modified PLGA nanoparticles for targeted drug delivery to neurons

Jingyan Li
Louisiana State University and Agricultural and Mechanical College, jli54@lsu.edu

SURFACE-MODIFIED PLGA NANOPARTICLES FOR TARGETED DRUG DELIVERY TO NEURONS

A Thesis

Submitted to the graduate faculty of the
Louisiana State University and
Agricultural and Mechanical College
in partial fulfillment of the requirements for degree of
Master of Science in Biological
and Agricultural Engineering

in

the Department of Biological and Agricultural Engineering

by
Jingyan Li
B.S. East China University of Science and Technology, 2010
December 2012

ACKNOWLEDGMENTS

I would not complete this thesis without the support and guidance from many people. I would like to thank all of them and express my appreciation to them.

I would like to express my sincere gratitude to my major advisor, Dr. Cristina Sabliov whose encouragement, guidance and support in both research and life were important for the accomplishment of this work. She was always willing to help with patience and caring. I want to thank her for all of these, and especially to her assistance in with my research planning and writing papers. A special thank goes out to Dr. Jolene Zheng, my co-advisor whose advice and guidance on *C.elegans* were also vital to the completion of my thesis. Also, I would like to thank my committee members, Dr. Daniel Hayes and Dr. Roger A Laine for reviewing my research project.

I would like to thank Carlos Astete for his guidance on synthesis of nanoparticles, to Dr. Ying Xiao for her advice on nanoparticles characterization by transmission electron microscopy (TEM), and to Dr. Rafael Cueto for his advice on nanoparticles characterization by dynamic light scattering (DLS).

I must also thank all my co-workers and graduate students who I met here and who became my friends. A special thanks to Carlos Astete, Cong Chen, Erica Muse, Mengdie Zhou and Chenfei Gao for being around when I was alone in a foreign country. I will never forget you.

Finally I want to thank my family for being supportive.

This work was supported by the LSU AgCenter Biotechnology Interdisciplinary Team (BAIT) Program and Pennington Biomedical Research Center/Pennington Biomedical Research Center/Reilly Family Foundation (RFF).

TABLE OF CONTENTS

LIST OF TABLES

LIST OF FIGURES

ABSTRACT

The blood-brain barrier (BBB), which protects the central nervous system (CNS) from unnecessary substances, is a challenging obstacle in the treatment of CNS disease such as Parkinson's Disease (PD). Many therapeutic agents such as hydrophilic and macromolecular drugs cannot overcome the BBB. One promising solution is the employment of polymeric nanoparticles (NPs) such as poly (lactic-co-glycolic acid) (PLGA) NPs as drug carrier. Over the past few years, significant breakthroughs have been made in developing suitable poly (lactic-co-glycolic acid) (PLGA) and poly (lactic acid) (PLA) nanoparticles for drug delivery across the BBB.

Recent advances on PLGA/PLA NPs enhanced neural delivery of drugs were reviewed and presented in the second chapter of the thesis. Both *in vitro* and *in vivo* studies were included in the review. From this review, it was learned that cellular uptake and therapeutic efficacy of drugs delivered with modified PLGA/PLA NPs were enhanced compared to free drugs or drugs delivered by unmodified PLGA NPs; no significant *in vitro* cytotoxicity was observed for PLGA NPs and PLA NPs. Surface modification of PLGA/PLA NPs by coating with surfactants/polymers or covalently conjuged with targeting ligands has been confirmed to enhance drug delivery across the BBB. Most unmodified PLGA NPs showed low brain uptake (<1%), which confirms the safety of PLGA/PLA NPs used for other purposes than treating CNS diseases.

For the second part of the thesis, wheat germ agglutinin (WGA), a lectin was conjugated to PLGA nanoparticles (PLGA-tWGA NPs, 221 nm) to improve DAergic neuron delivery in *C.elegans*. PLGA-tWGA NPs did not show a significant effect on pumping rate and life span of *C. elegans* at low concentration (<3 mg/ml). Fluorescent studies of GFP-DAergic neurons revealed

that pumping rate and area of GFP-DAergic neurons of worms treated with a high concentrations PLGA-tWGA NPs (>3mg/ml) was significantly decreased. Number and mean intensity of GFP-DAergic neurons also decreased, but no significant difference was found compared with control group. Co-localization of the fluorescent particles with the GFP-DAergic neurons of treated worms proved the targeting property of PLGA-tWGA nanoparticles to DAergic neurons. Enhanced targeted delivery of PLGA-tWGA NPs to neurons compared with tWGA and PLGA-t NPs confirmed that PLGA-tWGA NPs had the potential to act as targeted neural delivery systems for the treatment of PD.

CHAPTER 1. INTRODUCTION

1.1. Parkinson's disease

It is estimated that about 1–2% of the population over 65 years suffer from Parkinson's disease (PD), the second most common neurodegenerative disease after Alzheimer's disease (Alves, Forsaa et al. 2008). PD is a neurodegenerative disorder of the central nervous system, which impairs motor skills, cognitive processes, and other functions. Clinical symptoms of PD include both motor and non-motor symptoms such as bradykinesia, hypokinesia, and rigidity. These symptoms are known as Parkinsonism, which is essential for clinical diagnosis in PD. According to current studies, nigral dopamine deficiency-related dysfunction of the basal ganglia is regarded as the cause of the major PD symptoms (Wolters 2009).

The cause of the disease however is unknown. PD's symptoms result from the greatly reduced activity of dopamine-secreting cells while the cells in the pars compacta region of the substantia nigra die (Obeso, Rodriguez-Oroz et al. 2008). Pathologically, the disease is characterized by the accumulation of alpha-synuclein protein forming inclusions called Lewy bodies. The loss of function mechanisms in Parkinson's the brain cells are varied (Obeso, Rodriguez-Oroz et al. 2010). It is proposed that genetic mutations are not the only triggering factor of PD. "Pathogen theory" proposed by Braak's group is somehow reasonable considering the major gastrointestinal (GI) dysfunctions of PD patients and prevalence of PD in vegetarians (Ho, Woo et al. 1989). In this theory, it is proposed that an "unknown pathogen" penetrates the GI wall and enters the central nervous system (CNS) via retrograde transport through the the vagus nerve to cause PD (Braak, Rub et al. 2003).

Because dopamine cannot across Blood Brain Barrier (BBB), current treatments are effective at managing motor symptoms through the use of levodopa (L-DOPA), dopamine agonists and Monoamine oxidase B (MAO-B) inhibitors (Schapira 2005). However, drug delivery to the brain remains limited because of the blood-brain barrier (BBB). Take L-DOPA as an example, only 5-10% of L-DOPA orally administered is able to cross the blood-brain barrier. The remaining is often metabolised to dopamine by enzymes, i.e. decarboxylases, in the stomach or blood, causing a wide variety of side effects, such as nausea, dyskinesias and stiffness (Factor 2008).

To reduce the harmful side effects of drug such as L-DOPA associated with systemic accumulation, improved delivery systems must be developed for treatment of PA. Among the advanced technology, nanotechnology appears promising in developing drug delivery systems of targeting and controlled-release characteristics beneficial for drug delivery (Linazasoro 2008).

1.2. Nanoparticles as drug delivery vehicles

The advantages of nanoparticles as drug delivery systems include time controlled drug delivery, reduced drug toxicity, improved bioavailability and enhanced therapeutic efficacy and biodistribution (Ravi Kumar 2000). Nanoparticles can also protect the sensitive drugs from degradation by environmental factors such as stomach acid and enzymes (Jores, Mehnert et al. 2004). Polymeric nanoparticles range in size from about 10-1000nm (Kreuter 2001), and can be modified with different ligands such as antibodies to create a smart targeting delivery system. Polymeric nanoparticles of a size around or less than 300 nm coated with surfactants have been proved to be able to transport drugs across the BBB (Schroeder, Sommerfeld et al. 1998).

Poly (lactic-co-glycolic acid) (PLGA) is a copolymer which is used in a host of Food and Drug Administration (FDA) approved therapeutic devices. It is synthesized by means of random

ring-opening co-polymerization of two different monomers. PLGA is a common-used biodegradable polymer as its degradation by hydrolysis in the body produces the original monomers, lactic acid and glycolic acid which are by-products of various metabolic pathways. The degradation time of PLGA is controlled by the ratio of the two monomers: the higher the content of glycolide units, the less time required. However, the copolymer with 50:50 monomers ratio exhibits the fastest degradation. Because of its minimal toxicity and ability of controlling the release of the drug, PLGA is suitable for drug delivery (Astete and Sabliov 2006). PLGA nanoparticles are versatile among nanopariculate systems because of their biocompatibility for drug targeting at the cellular level (Mohamed and van der Walle 2008).

During the formation of the PLGA nanoparticles, L-DOPA is encapsulated within the polymer matrix and it is released upon degradation. Thus, the side-effects of the drug would be reduced as noted with conventional oral delivery systems (Pillay, Pillay et al. 2009).

In addition, to further improve the delivery efficacy of L-DOPA; a targeted drug system is designed by conjugating PLGA with the lectin: wheat germ agglutinin (WGA).

1.3. Lectins

Lectins are sugar-binding proteins or glycoproteins that are highly specific for reversible binding to sugar moieties. Lectins were discovered by Peter Hermann Stillmark working with castor bean extracts 100 years ago. Lectins are found throughout nature, in plants (i.e. legumes, seeds, nightshades, grains, wheat, and nuts) and other foods such as dairy food, as well as in insects, and the human body (Kennedy, Palva et al. 1995; Bies, Lehr et al. 2004; Sharon and Lis 2004).

Carbohydrates acting as structural components of the human body are widely distributed in tissues especially on the cell surface, and are involved in diverse biological processes such as cell

adhesion, inflammation, cell activation (Bies, Lehr et al. 2004; Sharon and Lis 2004). These carbohydrates display specific sugar moieties for binding different kinds of lectins. Lectins are hardy proteins; they are resistant to stomach acid and digestive enzymes. Moreover, they can bind to gut wall, damage the epithelial cells, change gut permeability, pass through the gut into general circulation with other non-lectin proteins, and cause allergic reactions (Ni and Tizard 1996). Thus, some plant and animal lectins are severely toxic to humans.

It is their specific binding ability that makes nontoxic lectins suitable as pro-drug entities; lectins have been conjugated with drugs to enhance drug absorption in the gastrointestinal tract or to target drug to a certain kind of cells including intestine cells, cancer cells and brain endothelial cells (Bies, Lehr et al. 2004). Chunxia Wang's group has designed wheat germ agglutinin-conjugated PLGA nanoparticles for enhanced intracellular delivery of paclitaxel to colon cancer cells. Conjugated PLGA nanoparticles demonstrated 1.67 fold in the Caco-2 (30% of uptake) and 1.48 fold HT-29 (40% of uptake) cells more than non-targeted nanoparticles (Wang, Ho et al. 2010). Xiaoling Gao et al. developed an enhanced delivery of vasoactive intestinal peptide with nanoparticles conjugated with wheat germ agglutinin (Gao, Wu et al. 2007). The delivery of incorporated vasoactive intestinal peptide by PLGA nanoparticles and WGA conjugated PLGA nanoparticles was greatly improved 3.5 to 4.7 folds and 5.6 to 7.7 folds respectively when compared to the free drug. Wen Z. et al conjugated odorranalectin (OL) to PEG-PLGA nanoparticles to improve nose-to-brain drug delivery in the treatment of central neuron systems disorders(Wen, Yan et al. 2011).

Targeting delivery is a key challenge in PD therapy. Many severe side effects induced by the undesirable distribution of any antiparkinsonian drug in health tissues greatly limits the

maximal allowable dose of the drug. If the non-pathogenic lectins can deliver drugs to the nervous system, the dosage of the drugs may be minimized, and its side effects reduced.

Various lectins have been used as components of oral drug delivery systems including tomato lectin, peanut agglutinin and wheat germ agglutinin (WGA) (Gao, Wu et al. 2007). WGA comes from Triticum vulgaris, and shows a special affinity to N-Acetyl-glucosamine (GlcNAc) and sialic acid which are the major glycoproteins on the surface of most cells. WGA is regarded as a promising carrier for oral drugs because of its biochemical characteristics and non-toxic property(Irache, Durrer et al. 1994). In solution, wheat germ agglutinin exists as a heterodimer with a molecular weight of approximately 38,000 daltons, normally cationic under physiological conditions. The uptake and anterograde axonal transport of WGA has been confirmed in prior work (Margolis, Marchand et al. 1981).

1.4. *Caenorhabditis elegans*

Caenorhabditis elegans (*C.elegans*) is a 1 mm long, transparent nematode (Wintle and Van Tol 2001) of several advantages for laboratory study including short generation time (3.5 days), and ease of growth which allow for rapid and inexpensive production of animals (Wood 1988). *C. elegans,* with a simple, well characterized nervous system consisting of 302 neurons, is a useful model organism for the study of neuron systems (Albeg, Smith et al. 2011). It is found that the human genome contains only 20% more genes that the *C. elegans* genome according to the completion of the *C. elegans* genome and those of mouse and human (Hillier, Coulson et al. 2005). In addition to the genome, the worm's neurons contain almost all the known signaling and neurotransmitter systems found in vertebrates, including different molecular pathways involved in the production of numerous neurotranmitters such as glutamate, acetylcholine, and dopamine (DA) (Bargmann 1998; Nass and Blakely 2003).

C.elegans is a model commonly used to study neuron drug delivery (Braungart, Gerlach et al. 2004; Nass, Merchant et al. 2008) as the hermaphroditic *C.elegans* organism contains only eight dopamine neurons, thereby largely simplifying a wide array of investigations (Nass, Hall et al. 2002). Worms that express the green fluorescent protein (GFP) can be used when the *in vivo* visualization of cellular processes is necessary. Other advantages of using *C.elegans* in laboratory studies include a short generation time, and ease of growth (Wood 1988; Riddle 1997; Wintle and Van Tol 2001).

1.5. Objectives

1. Conduct and write a review paper on PLA/PLGA nanoparticles for delivery of drugs across the blood-brain barrier.

    a) Assessment of cytotoxicity, cellular uptake, and therapeutical efficacy of PLA/PLGA nanoparticles *in vitro*.

    b) Investigation of brain uptake, location in the brain, and therapeutical efficacy of unmodified and modified PLA/PLGA nanoparticles via systemic administration with rats or mice *in vivo*.

2. Development of WGA conjugated PLGA nanoparticles for enhanced neuron delivery in *C.elegans*.

    a) Synthesis of TRITC conjugated poly (lactide-co-glycolide) nanoparticles (PLGA-t NPs) and tWGA conjugated PLGA nanoparticles (PLGA-tWGA NPs) by emulsion evaporation method, with PVA as surfactant.

    b) Charaterization of PLGA-t NPs and PLGA-tWGA NPs in terms of size, size distribution, zeta potential (DLS), morphology (TEM) and conjugation efficiency.

c) Analysis of the effect of tWGA, PLGA-t NPs and PLGA-tWGA NPs on pumping rate, size, and number, intensity and area of GFP-DAergic neurons with *C.elegans*.

1.6. References

Albeg, A., C. J. Smith, et al. (2011). "C. elegans multi-dendritic sensory neurons: morphology and function." Mol Cell Neurosci **46**(1): 308-317.

Alves, G., E. B. Forsaa, et al. (2008). "Epidemiology of Parkinson's disease." J Neurol **255 Suppl 5**: 18-32.

Astete, C. E. and C. M. Sabliov (2006). "Synthesis and characterization of PLGA nanoparticles." J
Biomater Sci Polym Ed **17**(3): 247-289.

Bargmann, C. I. (1998). "Neurobiology of the Caenorhabditis elegans genome." Science **282**(5396): 2028-2033.

Bies, C., C. M. Lehr, et al. (2004). "Lectin-mediated drug targeting: history and applications." Adv Drug Deliv Rev **56**(4): 425-435.

Braak, H., U. Rub, et al. (2003). "Idiopathic Parkinson's disease: possible routes by which vulnerable neuronal types may be subject to neuroinvasion by an unknown pathogen." J Neural Transm **110**(5): 517-536.

Braungart, E., M. Gerlach, et al. (2004). "Caenorhabditis elegans MPP+ model of Parkinson's disease for high-throughput drug screenings." Neurodegener Dis **1**(4-5): 175-183.

Factor, S. A. (2008). "Current status of symptomatic medical therapy in Parkinson's disease." Neurotherapeutics **5**(2): 164-180.

Gao, X., B. Wu, et al. (2007). "Brain delivery of vasoactive intestinal peptide enhanced with the nanoparticles conjugated with wheat germ agglutinin following intranasal administration." J Control Release **121**(3): 156-167.

Hillier, L. W., A. Coulson, et al. (2005). "Genomics in C-elegans: So many genes, such a little worm." Genome Research **15**(12): 1651-1660.
Ho, S. C., J. Woo, et al. (1989). "Epidemiologic study of Parkinson's disease in Hong Kong." Neurology **39**(10): 1314-1318.

Irache, J. M., C. Durrer, et al. (1994). "Preparation and characterization of lectin-latex conjugates for specific bioadhesion." Biomaterials **15**(11): 899-904.

Jores, K., W. Mehnert, et al. (2004). "Investigations on the structure of solid lipid nanoparticles (SLN) and oil-loaded solid lipid nanoparticles by photon correlation spectroscopy, field-flow fractionation and transmission electron microscopy." J Control Release **95**(2): 217-227.

Kennedy, J. F., P. M. G. Palva, et al. (1995). "Lectins, Versatile Proteins of Recognition - a Review." Carbohydrate Polymers **26**(3): 219-230.

Kreuter, J. (2001). "Nanoparticulate systems for brain delivery of drugs." Adv Drug Deliv Rev **47**(1): 65-81.
Linazasoro, G. (2008). "Potential applications of nanotechnologies to Parkinson's disease therapy." Parkinsonism Relat Disord **14**(5): 383-392.

Margolis, T. P., C. M. Marchand, et al. (1981). "Uptake and anterograde axonal transport of wheat germ agglutinin from retina to optic tectum in the chick." J Cell Biol **89**(1): 152-156.

Mohamed, F. and C. F. van der Walle (2008). "Engineering biodegradable polyester particles with specific drug targeting and drug release properties." J Pharm Sci **97**(1): 71-87.

Nass, R. and R. D. Blakely (2003). "The Caenorhabditis elegans dopaminergic system: opportunities for insights into dopamine transport and neurodegeneration." Annu Rev Pharmacol Toxicol **43**: 521-544.

Nass, R., D. H. Hall, et al. (2002). "Neurotoxin-induced degeneration of dopamine neurons in Caenorhabditis elegans." Proc Natl Acad Sci U S A **99**(5): 3264-3269.

Nass, R., K. M. Merchant, et al. (2008). "Caenohabditis elegans in Parkinson's disease drug discovery: addressing an unmet medical need." Mol Interv **8**(6): 284-293.

Ni, Y. and I. Tizard (1996). "Lectin-carbohydrate interaction in the immune system." Vet Immunol Immunopathol **55**(1-3): 205-223.

Obeso, J. A., M. C. Rodriguez-Oroz, et al. (2008). "Functional organization of the basal ganglia: therapeutic implications for Parkinson's disease." Mov Disord **23 Suppl 3**: S548-559.

Obeso, J. A., M. C. Rodriguez-Oroz, et al. (2010). "Missing pieces in the Parkinson's disease puzzle." Nat Med **16**(6): 653-661.

Pillay, S., V. Pillay, et al. (2009). "Design, biometric simulation and optimization of a nano-enabled scaffold device for enhanced delivery of dopamine to the brain." Int J Pharm **382**(1-2): 277-290.

Ravi Kumar, M. N. (2000). "Nano and microparticles as controlled drug delivery devices." J Pharm Pharm Sci **3**(2): 234-258.

Riddle, D. L. (1997). C. elegans II. Plainview, N.Y., Cold Spring Harbor Laboratory Press.

Schapira, A. H. (2005). "Present and future drug treatment for Parkinson's disease." J Neurol Neurosurg Psychiatry **76**(11): 1472-1478.

Schroeder, U., P. Sommerfeld, et al. (1998). "Nanoparticle technology for delivery of drugs across the blood-brain barrier." J Pharm Sci **87**(11): 1305-1307.

Sharon, N. and H. Lis (2004). "History of lectins: from hemagglutinins to biological recognition molecules." Glycobiology **14**(11): 53R-62R.

Wang, C., P. C. Ho, et al. (2010). "Wheat germ agglutinin-conjugated PLGA nanoparticles for enhanced intracellular delivery of paclitaxel to colon cancer cells." Int J Pharm **400**(1-2): 201-210.

Wen, Z., Z. Yan, et al. (2011). "Odorranalectin-conjugated nanoparticles: preparation, brain delivery and pharmacodynamic study on Parkinson's disease following intranasal administration." J Control Release **151**(2): 131-138.

Wintle, R. F. and H. H. Van Tol (2001). "Dopamine signaling in Caenorhabditis elegans-potential for parkinsonism research." Parkinsonism Relat Disord **7**(3): 177-183.

Wolters, E. (2009). "Non-motor extranigral signs and symptoms in Parkinson's disease." Parkinsonism Relat Disord **15 Suppl 3**: S6-12.

Wood, W. B. (1988). The Nematode Caenorhabditis elegans. Cold Spring Harbor, N.Y., Cold Spring Harbor Laboratory.

CHAPTER 2. PLA/PLGA NANOPARTICLES FOR DELIVERY OF DRUGS ACROSS THE BLOOD-BRAIN BARRIER: A REVIEW

2.1. Introduction

Treatment of central nervous system (CNS) diseases including Alzheimer's disease, Parkinson's disease, Huntington's disease, schizophrenia, HIV infection of the brain and brain tumors remain limited due to the low transport of drugs across the blood-brain barrier (BBB) (Wohlfart, Gelperina et al. 2011). The BBB is composed of special endothelial cells with tight junctions, pericytes, astrocytes and microglial cells (Begley 2004); tight junctions (TJ) are formed by complex network of proteins and linked with cytoskeleton to restrict passage of substance from bloodstream to the brain (Chen and Liu 2011).

Only a small amount of water-soluble molecules diffuse paracellularly through the TJ. Small lipid soluble molecules enter transcellularly through the lipid membrane. Cell-mediated transcytosis is another recently identified route for entering the brain through the BBB; for example, some pathogens such as HIV or *Cryptococcal* could enter the BBB via cell-mediated transcytosis (Park 2008; Chen and Liu 2011). For other substances, adsorptive transcytosis and specific receptor-mediated are the main transport routes across the BBB (Chen and Liu 2011). Adsorptive-mediated transcytosis (AMT) is induced by the interaction between the negatively charged membrane surface and a positively charged substance. Receptor-mediated transcytosis (RMT) is a selective uptake of a specific substance. The expression of different transporters such as transferring receptors, insulin receptors, and lipoprotein receptors could help the internalization of molecules (Chen and Liu 2011).

Many therapeutic agents for CNS disease such as hydrophilic drugs and macromolecular drugs cannot transport through the impermeable tight junctions of the BBB (Mistry, Stolnik et al. 2009). Therefore, invasive and non-invasive methods were employed to enhance brain delivery

of drugs. Compared to invasive methods which include changing the permeability of the BBB, or direct intracerebral infusion and implantation of the drug, non-invasive methods such as systemic administration are preferred (Wohlfart, Gelperina et al. 2011).

For systemically administered drugs, the goal for the drug delivery system is to cross the BBB in sufficient concentrations without a negative impact on the function of the BBB. A number of drug carriers have been developed to improve brain delivery of drugs, and among carriers, nanoparticles (NP) have been receiving an increased attention because of their unique properties (Chen and Liu 2011). Biodegradable polymeric nanoparticles, as a stable drug carrier have been well studied for drug delivery. The advantages of polymeric nanoparticles as drug delivery systems include time controlled drug deliver, reduced drug toxicity, improved bioavailability, and enhanced therapeutic efficacy of the entrapped drug (Patel, Zhou et al. 2011). Brain delivery can be achieved by well-designed and modified polymeric nanoparticles. Blank polymeric nanoparticles are fabricated from polymers such as poly (lactic-co-glycolic acid) (PLGA) with surfactants such as poly (vinyl alcohol) (PVA) and others as stabilizer. Characteristics of polymeric nanoparticles such as size, zeta potential and hydrophilicity can be controlled by surface modification such as surfactant coating to enhance brain uptake. In addition, ligands known to target BBB surface receptors such as transferring, insulin, and lipoprotein receptors can be linked to the surface of the polymeric nanoparticles to provide targeted brain delivery and improved nanoparticles uptake (Rip, Schenk et al. 2009).

Both *in vitro* and *in vivo* studies have been conducted to study cytotoxicity and effectiveness of polymeric nanoparticles designed for delivery of drugs to the CNS. Prior to complex and expensive *in vivo* studies, *in vitro* studies on cytotoxicity, cellular uptake, endocytosis mechanism, and drug efficiency of drug delivery system were investigated with

different cell lines such as brain endothelial cells and glioma cells. Next, *in vivo* studies performed on mice and rats were used to study brain uptake, location of nano carriers and therapeutic efficacy of the entrapped drug.

Aspects of nanoparticle synthesis, general properties, mechanisms of action and potential pitfalls of nanoparticles for drug delivery to the central nervous system have been reviewed over the past years (Kreuter 2001; Olivier 2005; Roney, Kulkarni et al. 2005; Silva 2007; Wohlfart, Gelperina et al. 2011). Recent findings on polymeric nanoparticles, as brain delivery carriers are available in the literature as well (Patel, Zhou et al. 2011; Costantino and Boraschi 2012). However, to the authors' knowledge, no reviews have been specifically and solely dedicated to the effect of nanoparticle properties on delivery of drugs to the brain with PLGA/PLA nanoparticles; this aspect was only partially mentioned or briefly discussed in the previous review papers. The goal of this review is to highlight the recent developments on PLGA or poly (lactic acid) (PLA) nanoparticles designed for neural delivery, with emphasis on nanoparticle cytotoxicity, therapeutic efficacy of the entrapped drug, and brain uptake of PLGA and PLA nanoparticles as a function of their properties.

In this review, a literature search was conducted on the subject of PLGA/PLA NPs and brain delivery of drugs using PubMeb, ScienceDirect and Springerlink databases. The following key words were used in the search: polymeric/PLGA nanoparticles, brain delivery, blood-brain barrier, central nervous system, and neuron delivery. Relevant papers were selected based on whether it is PLGA/PLA NPs and systemic administration with the goal of delivering drugs across the BBB. In total, 29 papers on PLGA/PLA nanoparticles for drug delivery across the BBB were used in this review.

The papers are summarized with an emphasis on NP characteristics (core polymer, emulsifier, surface modification, loaded drug, size, zeta potential), the *in vitro* and *in vivo* models used, methods, and significant findings. The information is compiled in Table 2.1. The discussion section following the summaries is divided into two sections: *in vitro* studies and *in vivo* studies. For the *in vivo* studies, the percentage (%) brain uptake over 24 h was calculated as percentage of dose administered per animal, and plotted versus time (h). Potential effects of nanoparticle properties such as size, dose and administration on brain uptake of different nanoparticles were compared and discussed.

2.2. Summaries of cited papers

Tsai, Chien et al. (2011):

The tissue distribution and BBB distribution of curcumin and PLGA nanoparticles entrapped with curcumin (C-NPs) (163 nm) in all organs and regions of the brain in rats were studied. After intravenous administration of 25 mg/kg of free curcumin and C-NPs in male Sprague-Dawley rats, a 500 μl blood sample was obtained at 15, 30 and 60 min. The organs tested including liver, heart, spleen, lung, kidney and brain were removed, and the brain was dissected. Free curcumin distributed more in liver (9.0 min μg/ml) and kidney (12.0 min μg/ml) than in other organs, indicating that it might be cleared and metabolized. When curcumine was administered as C-NPs, a significant amount of curcumin was found in the spleen and lung instead of liver and kidney, which implied that NPs helped to provide a more efficient distribution to organs than free curcumin. Both formulations were able to cross the BBB whereas C-NPs showed significantly higher distribution than free curcumin. The significantly increased half-life ($t_{1/2}$/min) and mean residence time (MRT/min) confirmed that PLGA NPs prolonged the retention time of curcumin in the cerebral cortex and the hippocampus by 2.0 and 1.8-fold

respectively, while no significant difference was found in the other brain regions (Tsai, Chien et al. 2011)

Mittal et al. (2011):

Oral delivery of estradiol to the brain in rats was evaluated for Tween 80 (T80) coated PLGA nanoparticles synthesized with different concentration of initial T-80 concentrations. Five concentrations of T80 (T1-T5, 1%, 2%, 3%, 4% and 5%, v/v to total suspension volume) were coated on the PLGA NPs surface with Didodecyl dimethyl ammonium bromide (DMAB) as emulsifier to form NPs with a size range of 138 nm to 172 nm. The integrity of the coating was evaluated at 2 h for simulated gastric fluid (SGF) and 6 h for simulated intestinal fluid (SIF) to evaluate stability of T80 coating at pH 1.2 and at pH 7.4. The percentage of remaining T80 coating for T1- and T5-NPs in SGF was 77.3% and 43.7%, while the percentage of that in SIF was 65.6% and 37.8% respectively. T1- and T4-coated PLGA nanoparticles (138 nm, 157 nm respectively) were selected for the oral administration in rats to observe the effect of T80 coating concentration on uptake. After oral administration in male Sprague-Dawley rats for 24 h, PLGA nanoparticles coated with 4% T80 showed more effective delivery of estradiol to rat brain (1.969 ±0.197 ng/g tissue) as compared to uncoated NPs (1.105 ±0.136 ng/g tissue), and almost similar level of brain estradiol as that achieved by intramuscular administration of same dose (200 µg/rat) of free drug (2.123 ±0.370 ng/g tissue). Two behavior tests were performed in an ovariectomized (OVX) rat model of Alzeimer's disease (AD) including an open field test which used to evaluate the motor functions of the rats, and elevated plus maze test which was used to measure fear or anxiety. The tests were carried out after 6 weeks of treatment with T80-PLGA NPs. Behavior tests showed that the NP treatment effectively attenuated the anxiety-related behavior of the rats over the sham (control) group.

Table 2.1 Summaries of NP characteristics (core polymer, emulsifier, surface modification, loaded drug, fluorescent marker, size and zeta potential), animal study and result

Core polymer	Emulsifier	Surface modification	Loaded drug	Fluorescent marker	Size (nm)	Zeta potential (mV)	Animal study	Result	Ref
PLGA	PVA		Curcumin		163	-12.5	*In vivo*: Male Sprague-Dawley rats, i.v. administration	Significantly increased retention times of curcumin in the cerebral cortex and hippocampus	Tsai, Chien et al. 2011
PLGA	DMAB		estradiol		134.7	68.5, pH 4.1	*In vitro*: simulated gastric fluid and intestinal fluid	T-80 coat was stable in simulated gastric gluid and intestinal fluid	Mittal, Carswell et al. 2011
		1% T80			138.8	19.2, pH 5.6			
		2% T80			141.8	7.7, pH 7.2			
		3% T80			153.1	-1.1, pH 7.2	*In vivo*: male sprague-Dawley rats, oral administration (1%,4% T80-NPs); i.v. (1% T80-NPs)	Orally administrated T-80 coated nanoparticles reached higher levels after 24 h than uncoated drugs, and similar to those after same does of intramuscular drug injection	
		4% T80			157	-3.6, pH 7.2			
		5% T80			172.4	-6.5, pH 7.2			
PLGA	PVA		doxorubicin		238.6	11.8	*In vivo*: tumor-bearing male Wistar rats, tail vein injection	Loperamide loaded PVA-stabilized PLGA nanoparticles coated with poloxamer proved the highest and longlasting anti-tumor(glioblastoma) effect in rats	Gelperina, Maksimenko et al. 2010
	PVA	F68			243.4	6			
	PVA	T80			239.9	8.2			
	HSA				401.7	9.5			
	HSA	F68			408.6	8.1			
	HSA	T80			412	16.2			
	PVA		loperamide		177.7	-11.4			
	PVA	F68			168.5	-17.9			
	PVA	T80			166.9	-25			
	HSA				288.9	-11.9			
	HSA	F68			287.7	-17.5			
	HSA	T80			292.4	-18.9			
PLA					162.1	-29.5	*In vivo*: mice, tail vein injection	T80 coat was necessary for brain targeting. Free FITC, T80 and blank NPs were not observed in brain tissues	Sun, Xie et al. 2004
				FITC-dextran	194.2	-13.4			
		T80		FITC-dextran	202.6	-10.17, pH 7.4			

(Table 2.1 cont'd)

PLGA	PVA		docetaxel		227.7	-27.5	*In vitro*: C6 glioma cell line, cytotoxicity studies	The lowest IC50 was achieved after 72 h by the F68-PVA-NPs	Kulkarni and Feng 2011
	TPGS				222.3	-41.3			
	PVA	F68			235.5	-23.8			
	PVA	T80			250.2	-21.3			
	PVA	F127			242.5	-22.4			
	PVA			coumarin-6	177	-31.1	*In vitro*: MDCK cells uptake studies	*In vitro*: TPGS coated PLGA Nps showed 1.5-fold higher cellular uptake than PVA-emulsified NPs. F68-coated PLGA NPs displayed the highest uptake compared with T80, F127 coated NPs.	
	TPGS				165	-38.5			
	PVA	F68			196	-20.2			
	PVA	T80			194	-23.1	*In vivo*: male sprague-Dawley rats, tail vein injection	F68-coated PLGA nanoparticles also demonstrated highest brain accumulation over those with T80 and F127	
	PVA	F127			188	-20.6			
PLGA	PVA			coumarin-6	269.3	-21.2	*In vivo*: Male Wister rats, carotid artery/jugular administration	Carotid artery administration of all NPs showed higher brain distribution than those after jugular vein administration. T80-PLGA NP prolonged circulation time in the blood. CS-PLGA NP and T80-PLGA NP proved high brain distribution than uncoated and F68 coated NPs. CLSM studies demonstrated only T80-PLGA cross the BBB and located in the parenchyma.	Tahara, Miyazaki et al. 2011
		T80			231.7	-20.3			
		F68			252.2	-19.8			
		chitosan (CS)			396.2	6.1			
PLGA	TPGS		loperamide		173.5	-24.9	*In vitro*: rat brain endothelial cell and C6 co-cultures	P188-coated NPs showed better permeability than P80-coated NPs (1.47 fold); no toxicity	Chen, Hsieh et al. 2011
PLGA-PEG-PLGA					152.3	-0.5			
		P80			149	1.5	*In vivo*: male ICR mice, tail vein injection	Hot-plate test and formalin test for the antinociceptive effects studies. P188 NPs showed better effect over P80 NPs followed by PEP NP and blank NP	
		P188			147	3.1			
PLGA				coumarin-6	224.2	-22.4	*In vivo*: male SD rats, tail vein injection	P188-coated NPs distributed more in the brain than P80-coated NPs. Surfactant-coated NPs showed enhanced brain delivery over uncoated; pegylated NPs showed increasing distribution than blank NPs	
PLGA-PEG-PLGA					196.5	-0.4			
		P80			190	1.2			
PLGA-PEG-PLGA	TPGS	P188			200	2.4			

(Table 2.1 cont'd)

PLGA				coumarin-6	215	n/r	*In vitro*: MDCK cells uptake studies; C6 glioma cells cytotoxicity study (entrapped paclitaxel instead of coumarin-6)	The additives of P80 and TPGS during synthesis helped to improve cellular uptake more than surface coated nanoparticles; P80 emulsified NPs showed lowest cell viability	Xie, Lei et al. 2010
	PEG				225	n/r			
	TPGS				248	n/r			
	P80				256	n/r			
	F127				234	n/r			
		PEG			239	n/r			
		TPGS			245	n/r			
		F127			251	n/r			
PLA-b-PEG	n/r		Amphoteric in B (AmB)		120	n/r	*In vivo*: Cryptococcal Meningitis-bearing mice, intravenous administration	Enhance the stability and entrapment efficiency. Brain targeting and cross the BBB	Ren, Xu et al. 2009
		T80			120	n/r			
PLGA	TPGS			coumarin-6	94.7	-22.3	*In vitro*: cytotoxicity in SH-SY5Y cells by MTT assay	no significant cytotoxic effects	Wang, Wang et al. 2010
		trimethylated chitosan (TMC)			136.8	17.7	*In vivo*: CD-1 wild-type mice, caudal veins injection	Accumulated in the periventricular region of the cortex and the third ventricle, mechanism was absorptive-mediated transcytosis	
			coenzyme Q_{10}		99.6	-18.3	*In vivo*: APP/PS1 double transgenic mice, caudal veins injection	behavior tests, senile plaque and biochemical parameters were confirmed superior to the blank NPs	
		TMC			146.7	21			
PLGA	TPGS				250	n/r	*In vitro*: PC 12 cell line	No cytotoxicity, the more TPGS on the surface, the more effective therapeutic effects	Jalali, Moztarzadeh et al. 2011
PLGA	PVA			coumarin-6	267.7	-7.6, at pH 7	*In vitro*: Polarized MDCK cell monolayers	Selectively target the intracellular Aβ antigen	Jaruszewski, Ramakrishnan et al. 2012
		Chitosan			217.3	32.0, at pH 7			
		Chitosan, anti-Aβ antibody			265	16.8, at pH 7			
PEG-PLA	Sodium Cholate		sulpiride	rodomine B	218	-39	*In vivo*: male Sprague Dawley rats, injection in caudal vein	Faster clearance from the plasma and a high biodistribution in brain	Parikh, Bommana et al. 2010
		Alexa Fluor 488-labeled CBSA			329	-19			
		BSA			308	n/r			
PEG-PLA				coumarin-6	100	-16.8	*In vitro*: coculture of brain endothelial cells (BCEC) and astrocytes	Permeability of CBSA-NPs was higher than blank NPs, and decreased while incubated with free CBSA	Lu, Wan et al. 2007
		BSA		coumarin-6	97.4	-16.2			
		CBSA		coumarin-6	105	-13/-12.2/-9	*In vivo*: male BALB/c mice, tail vein injection	absorptive mediated transcytosis (AMT) process while no brain targeting of native BSA	

(Table 2.1 cont'd)

PLGA RG503H	F68			fluorescein-linked	212	-17.1, pH7.4	In vivo: Rat Brain Perfusion Technique; rat femoral vein injection	Not able to cross the BBB, localized into the blood vessels	Costantino, Gandolfi et al. 2005
		peptide 1		fluorescein-linked	170	-6.9, pH7.4		Penetrate into cerebral parenchima	
		peptide 2		fluorescein-linked	162	-8.6, pH7.4		Reach CNS after systemic admnistration	
		peptide 2		tetramethylrhodamine-linked	211	-14.6, pH7.4		Reach CNS after systemic admnistration	
		peptide 3		fluorescein-linked	178	-15.2, pH7.4		Penetrate into cerebral parenchima	
		peptide 4		fluorescein-linked	191	-6.1, pH7.4		Not able to cross the BBB	
		peptide 5		fluorescein-linked	185	-9.9, pH7.4		Penetrate into cerebral parenchima	
PEG-PLGA	n/r			coumarin-6	109.3	-23.4	*In vitro*: bEnd.3 cells, a model of the BBB	Significantly higher bEnd.3 cells uptake and brain delivery	Li, Peng et al. 2011
		12-amino-acid-peptide (Pep TGN)			121.5	-18.3	*In vivo*: male nude mice intravenously infection	Significantly higher brain delivery	
PLA	PVA		^{3}H-ritonavir		300	-19.3	*In vitro*: MDCK cells over-expressing (MDCK-MDR1) and non-P-gp-expressing (MDCK-wt)	TAT-NPs showed 40-fold increasing uptake than free ritonavir, similar with unconjugated NP in MDCK-MDR1 cells	Rao, Reddy et al. 2008
		trans-activation transcriptor (TAT) peptide	^{3}H-ritonavir		340	2.4	*In vivo*: male mice, tail veil injection	800-fold higher brain ritonavir level than free ritonavir and 7-dold higher than unconjugated NP	
				coumarin-6	n/r	n/r	*In vivo*: male mice, tail veil injection	Located within the parenchyma	
PLGA	F68	SA-g7	loperamide		180	-22.8, pH 7.4	*In vivo*: male albino Wistar-Hannover rats, tail vein injection	Significantly increase the central opioid activity of LOP for 24 h than other nanodelivery system	Tosi, Vergoni et al. 2010
		g7	loperamide		155	15.2, pH 7.4			
				rhodamine-123	187	-21.7, pH 7.4		SA-g7 NPs can cross the BBB, prolonged retention time	
		SA-g7		rhodamine-123	197	-15.9, pH 7.4			
		g7		rhodamine-123	169	-18.9, pH 7.4			
		SA-g7		tetramethylrhodamine (TMR)-linked	154	-24.2, pH 7.4			

(Table 2.1 cont'd)

PLGA	PVA	Tet-1 peptide	curcumin		150-200	-30 to -20	*In vitro*: cytotoxicity on LAG cells; uptake on GI-1 glioma cells	no significant cytotoxic effects; Tet-1 conjugated NPs showed increased uptake compared to unconjugated NPs	Mathew, Fukuda et al. 2012
PEG-PLGA	n/r		paclitaxel		168	n/r	*In vitro*: RG2 glioma cells	Higher cytoxicity in RG2 cells due to increased microtubule stabilization than uncoated NP	Geldenhuys, Mbimba et al. 2011
		2% glutathione	paclitaxel		237.6	n/r			
				coumarin-6	n/r	n/r	*In vivo*: mice	Higher brain uptake	
PLGA	n/r			Dil	79.2	-44.2, pH 7	*In vitro*: coculture of brain endothelial cells (BCEC) and astrocytes	Cellular endocytosis of Tf-NPs was 20-fold greater than blank NPs; 2-fold greater than BSA-NPs. T20-NPs showed strong toxicity	Chang, Jallouli et al. 2009
		Tween 20		Dil	80.9	-21.4, pH 7			
		BSA		Dil	88.8	-33.1, pH 7			
		FITC-labelled transferrin		Dil	90.2	-32.5, pH 7			
PLA-TPGS	TPGS			coumarin-6	228.6	-30	*In vitro*: C6 glioma cell line	Increasing uptake; non-specific endocytosis pathway and active receptor-mediated Tf/TfR endocytosis	Gan and Feng 2010
		Transferrin (Tf)		coumarin-6	245.8	-29	*In vivo*: Male Sprague -Dawley rats, intravenous	Much higher concentration of coumarin 6 in the brain than non-conjugated NPs;	
			Docetaxel		121.6	-36.5	*In vitro*: C6 cells	Cell viability and TC_{50} were determined, Tf-TPGS-PLA showed most efficient drug delivery	
		Transferrin (Tf)	Docetaxel		137.6	-31.1			
PLGA	PVA		temozolomide		112.9	-35.3	*In vitro*: 8 human cancer cell lines of six different cancer tissues	Tf-PEG-PLGA NPs and PEG-PLGA NPs showed higher cytotoxicity than PLGA NPs	Jain, Chasoo et al. 2011
PEG-PLGA					117.2	-4.2			
		Transferrin (Tf)			121	-4.3			
		Transferrin (Tf)		coumarin-6	n/r	n/r	*In vivo*: albino rats, i.v. administration	Tf-PEG-PLGA was located within the brain parenchyma	
PLGA	DODAB and P80	Transferrin (Tf)	nevirapine		170-200	30-40	*In vitro*: HBMECs, cytotoxicity and permeability	Tf and DODAB had effect on cell viability, and permeability of Tf-NPs with 67% DODAB reached highest	Kuo, Lin et al. 2011
				fluorescein isothiocyante conjugated dextran 7000			*In vitro*: HBMECs, uptake	Tf-PLGA NPs showed higher uptake than unconjugated NPs	

(Table 2.1 cont'd)

PEG-PLGA	n/r				92	n/r	*In vitro*: RG2 glioma cells	Enhanced cellular uptake compared to unconjugated NPs and free Tempol	Carroll, Bhatia et al. 2010
		transferrin antibody (OX 26)		coumarin-6	105	n/r		More effective in preventing cell viability compared to unconjugated NPs and free Tempol	
			tempol						
PLGA	PVA	glycopeptides for BBB crossing	$ZnSO_4$	tetramethylrhodamine-linked	190-210	-0.5 to -10	*In vitro*: neurons/glial cultures	PLGA NPs were not toxic. Glycopeptides conjugated NPs enhanced endocytosis	Grabrucker, Garner et al. 2011
		NCAM1 antibody		tetramethylrhodamine-linked			*In vitro*: NCAM1 labeled microtubule associated protein positive cells and CD44 labeled glial cells	NCAM-NPs targeted more to neurons stained for MAP2, less to glial cells	
		CD44 antibody		tetramethylrhodamine-linked				CD44-NPs targeted to glial cells more, and decreased targeting to neurons	
PEG-PLGA	Sodium Cholate				90	-24			Hu, Shi et al. 2011
		lactoferrin		coumarin-6	95	n/r	*In vitro*: bEnd.3 cells, a model of the BBB	significantly increased uptake in bEnd.3 cells; Clathrin mediated endocytosis; low toxicity	
							In vivo: KM mice, injection in caudal vein	2.49 times of coumarin-6 accumulation in the brain	
			urocortin (UCN)		120	-14	*In vivo*: 6-OHDA rats model of PD, injection in caudal vein	Enhanced delivery and theraputical effect of UCN-Loaded Lf-NPs was proved	
							In vivo: BALB/c mice, injection in caudal vein	Transient acute dose-related inflammatory reactions in liver, spleen and kidney	
PLGA	didecyl dimethylammonium bromide (DDAB)	poly-(γ-glutamic acid) (γ-PGA) (6 kDa)	saquinavir (SQV)		188	-28	*In vitro*: a monolayer of human brain-microvascular endothelial cells (HBMECs) with human astrocyte (HA)	A higher grafting efficiency and a lower molecular weight of γ-PGA increased the peameability of SQV cross the BBB, enhance the endocytosis and expression of ornithine decarboxylase (ODC)	Kuo and Yu 2011
PEG-PLGA	Sodium Cholate	AS1411(AP), a DNA aptamer		coumarin-6	n/r	n/r	*In vitro*: C6 glioma cells	Improved cellular association	Guo, Gao et al. 2011
			paclitaxel (PTX)		121	-23	*In vitro*: C6 glioma cells	Enhanced cytotoxicity of AP conjugated NP, IC 50 was determined	
		AP	paclitaxel (PTX)		156	-32.9	*In vivo*: rats bearing glioma xenografts and rats bearing intracranial C6 gliomas	target brain tumor, improved drug efficacy and prolong the life span of rats bearing gliomas	

Neuropathological examination of OVX rats proved that NPs treated groups prevented the expression of amyloid β-42 (Aβ42), which plays an important pathological role in AD development in the hippocampus region of brain (Mittal, Carswell et al. 2011).

Gelperina et al. (2010):

The efficacy of one nanoparticle delivery system is not only affected by the surface coating, but also by the core materials used in the NP synthesis such as stabilizer, drug and core polymer. Gelperina, S. et al compared doxorubicin/loperamide delivery to the brain using polysorbate 80 (Tween® 80, T80) or poloxamer 188 (Pluronic® F68) surfactant-coated PLGA nanoparticles. Two emulsifiers: poly (vinyl alcohol) (PVA) and human serum albumin (HSA) were used during synthesis, with HSA believed to be a safer surfactant. Tumor-bearing rats were prepared by tumor implantation to the adult male Wistar rats by injecting tumor cells into the cavity of the right lateral ventricle. The rats were treated for rat glioblastoma by using doxorubicin loaded NPs, administered by tail vein injection. PLGA/PVA coated with F68 (243.4 nm) showed the most effective anti-tumor effect: long-term remission in 40% (4/10) of the treated animals. PLGA/PVA coated with T80 (239.9 nm) was not as effective as PLGA-F68, only one rat survived the treatment. The analgesic effect of loperamide loaded nanoparticles was evaluated in female ICR mice or female Balb/c mice after intravenous injection. Tail-flick test which measured nociceptive threshold of mice were performed, and the maximal possible effect (% MPE) was determined to evaluate the analgesic effect. PLGA/PVA+F68 loaded with loperamide (168.5 nm) proved the maximum and most long-lasting antinociceptive effect: 80% MPE 15 min after injection and was maintained at 70 % for at least 60 min. PLGA/PVA+T80 provided a less prolonged analgesic compared to those with F68 (80% after 15 min and 40% after 60 min). Loperamide in solution of 1% F68 showed little effects while loperamide and F68

alone didn't show any antinociceptive effect. PVA-stabilized PLGA nanoparticles coated with F68 proved to be a promising brain delivery of the drugs (Gelperina, Maksimenko et al. 2010).

Sun et al. (2004):

Polysorbate 80 (Tween® 80, T80) has been proven to display a specific role in brain targeting. FITC loaded T80 coated surfactant-free PLA nanoparticles (FITC-T80-NP) were prepared (202.6 nm). Surfactant-free NPs with FITC and T80-coated NPs were synthesized as control groups. About 45 min after administration of 0.2 ml to mice by tail vein injection, the vascular perfusion and brain fixation was performed. Fluorescence studies of the brain found FITC-T80-NPs mainly located at the wall of brain micro-vessel endothelial cells, and indicating that NPs crossed the BBB via endocytosis mechanism. No fluorescence was found in the brain for the T80-NP with FITC-dextran , FITC-NPs, or mixture of free FITC and free T80, which confirmed the role of T80 coating on nanoparticles in brain delivery (Sun, Xie et al. 2004).

Kulkarni and Feng (2011)

Both polyvinyl alcohol (PVA) and D-α-tocopheryl polyethylene glycol 1000 succinate (vitamin E TPGS) were used as emulsifier to prepare PLGA nanoparticles. Poloxamer 188 (Pluronic® F68), polysorbate 80 (Tween® 80, T80) and poloxamer 407 (Pluronic® F127) were further coated on surface of PLGA NPs, and the effects of the surface modifications on the characteristics of the delivery system were investigated. The average diameters of all surface-modified NPs loaded with coumarin-6 were below 200 nm, and that of all surface-coated NPs with entrapped docetaxel was in the range of 220-250 nm. The *in vitro* release study of coumarin-6 from surface-modified NPs which used PVA as an emulsifier revealed that less than 10% of the coumarin-6 was released while 8% was released from TPGS NPs after incubation in 10 mM PBS (pH 7.4) at 37 ℃ for 24 h. The cellular uptake study of TPGS-emulsified and PVA-

emulsified PLGA NPs performed on Madin Darby canine kidney (MDCK) cells proved that TPGS was a better emulsifier which enhanced 1.5-fold more cellular uptake efficiency compared to the PVA emulsified NPs after 2 h incubation. Surface coated PLGA NPs with F68, F127 and T80 showed enhanced cellular uptake (26%, 25%, and 21%) versus unmodified NPs, and F68-modified PLGA NPs showed the highest uptake efficiency. The biodistribution study of surface modified PLGA NPs with entrapped coumarin-6 was carried out in rats 90 min after tail vein injection. The highest distribution was observed in the liver, lungs and spleen, and the percentages was: 29.9%, 34.9% and 18.4% for PVA-NPs; 1.19, 11.1 and 12.0% for TPGS-NPs, 3.94, 7.84 and 13.8% for T80-PVA-NPs, 8.17, 15.8 and 27.2% for F127-PVA-NPs, and 6.01, 7.84 and 11.2% for F68-PVA-NPs. TPGS-NPs also showed a higher distribution in the heart. It was demonstrated that surface functionalized PLGA NPs helped NPs reach the brain, and brain uptake of F68-PVA-PLGA was proved to be most efficient (6.29%) over NPs made with T80 (4.26%), F127 (5.07%), TPGS (4.20%) and PVA only (2.59%). The confocal microscopic studies of the brain after 90 min intravenous injections of the surface-coated NPs with entrapped coumarin-6 were performed. The green fluorescence was observed in the brain of the surface-coated NPs treated groups, which further confirmed surface-modified NPs delivered to the brain. The cell cytotoxicity of the docetaxel-loaded PLGA NPs coated with different surfactants was studied with the C6 glioma cell lines. The cell viability was determined after incubation for 24, 48 and 72 h. Cells exposed to drugs entrapped in the nano-delivery system showed lower viability than those exposed to free drug. Furthermore, IC_{50}, the concentration of the drug required to kill 50% cells in a fixed time period was determined to compare the drug delivery efficiency of different formations. The lowest IC_{50} in C6 glioma cells after 72 h was achieved by

the F68-PVA-NPs, which was 86.51 and 98.58% more efficient than that of PVA-NPs and free drug (Kulkarni and Feng 2011).

Tahara et al. (2011):

Efficacy of brain targeting with polysorbate 80 (Tween® 80, T80), poloxamer 188 (Pluronic® F68) and chitosan (CS) modified PLGA NPs (215 nm, 252 nm and 396 nm) was studied. *In vivo* studies were conducted in male Wister rats by left carotid artery or left jugular vein administration of 100 mg/ml NPs with coumarin-6 as fluorescence probe in different volumes (0.05, 0.10, 0.25 mL). The clearance of F68-NP from blood was faster than unmodified NPs, and the retention time of T80-NP was prolonged compared to other NPs for the carotid artery injection. Carotid artery administration was proved to be a more effective way of delivering all NP types into the brain, compared to jugular administration. Amount of NPs in the brain was quantified after 60 min administration via carotid artery, and brain slices were observed using confocal laser scanning microscopy (CLSM). T80-PLGA and CS-PLGA NPs accumulated more in the brain than uncoated and F68-coated PLGA NPs. CLSM of brain proved that T80-PLGA NP crossed the BBB, while CS-PLGA NP mainly adhered to endothelial cells. Most uncoated and F68-PLGA NP remained in the blood vessels, and very small amounts transported to the parenchyma (Tahara, Miyazaki et al. 2011).

Chen et al. (2011):

Chen Y.C.' group developed poloxamer 188 (P188) or polysorbate (P80) coated PLGA-PEG-PLGA nanoparticle delivery systems for brain delivery of loperamide. A novel PLGA-PEG-PLGA triblock copolymer was used and TPGS served as emulsifier for the preparation of the nanoparticles. The *in vitro* studies of loperamide loaded nanoparticles were carried out in rat brain endothelial cell line (RBE4) and C6 cells co-cultures after 4 h incubation at 37 ◦C. The

order of permeability ratio (%) of samples from highest to lowest was P188-coated NPs (147 nm), P80-coated NPs (149 nm), PLGA-PEG-PLGA (PEP) NPs (152 nm), PLGA NPs (173 nm) and loperamide in solution. *In vitro* cytotoxicity studies of all nanoparticles at the loperamide concentrations of 5, 10, 15 and 30 ng/ml showed no toxicity. Male ICR mice were used for the *in vivo* antinociception studies of nanoparticles incorporated with loperamide after i.v. administration at the dose of 5 mg/kg. Hot-plate test and formalin tests were employed, and the results showed P188-coated NPs had the best antinociceptive effects. Distribution of nanoparticles with entrapped courmarin-6 in the brain was further studied with male SD rats after administration through the tail vein at a dose of 0.5 mg/kg. Quantitative study demonstrated P188-coated NPs (200 nm) have the highest concentration in the brain followed by P80-coated NPs (190 nm), PEP NPs (196 nm) and PLGA NPs (224 nm). The result was similar to other reported study which claimed P188 showed better brain targeting delivery than P80 after surface coating on nanoparticles (Kreuter and Gelperina 2008; Kulkarni and Feng 2011). P188-coated PEP NPs showed the greatest cellular uptake, brain distribution and best antinociceptive effects over P80-coated NPs (Chen, Hsieh et al. 2011).

Xie et al. (2010):

To improve brain delivery of paclitaxel, PEG, TPGS, F127 and P80 were used as additives or for surface coatings during preparation of nanoparticles of around 200 nm via nanoprecipitation. Cellular uptake of all kinds of nanoparticulate formulations loaded with coumarin-6 were investigated with MDCK cell monolayer at a dose of 250 μg/ml 2h after incubation. Compared to uncoated PLGA NPs, NPs with additives showed enhanced cellular uptake, and NPs with the additives of P80 and TPGS demonstrated greatest cellular uptake. Surface-coated NPs were proved to be less effective in cellular uptake than those with additives.

Cytotoxicity of paclitaxel loaded nanoparticles (paclitaxel 30μg/well) was studied in C6 glioma cell line after 3-4 h incubation. The transendothelial electrical resistance (TEER) and cell viability were determined to evaluate paclitaxel delivery. Both results showed that NPs with TPGS and P80 as additives enhanced paclitaxel greater than other nanoparticulate formulations (Xie, Lei et al. 2010).

Ren et al. (2009):

Polysorbate 80 (Tween® 80, T80) was coated on the surface of PLA-b-PEG NPs loaded with Amphotericin B (AmB) to enhance brain delivery. The effect of different solvent and surfactant on size and entrapment efficiency of the drug in the NPs was studied. T80 coated NPs with DMSO as solvent (120 nm) achieved highest entrapment efficiency (50.7%). The *in vivo* study performed on *Cryptococcal Meningitis*-bearing mice after intravenous administration of designed NPs (6 mg/kg) showed brain delivery was greatly enhanced as the level of AmB in brain increased when compared to that observed with AmB injectable powder (1 mg/kg). Further recovery of fungus (*Cryptococcal Meningitis*) from brain also proved the result. The survival time of mice treated with NPs was twice longer than that of the AmB treated group. The toxicity of AmB to tissues including liver, kidney and blood system was measured and it was found that the accumulation of AmB in liver, spleen and kidney decreased significantly in the NP treated animals compared to that of AmB powder treated groups. AmB conjugated PLA-b-PEG NPs provided a brain targeting delivery with reduced toxicity of AmB and improved therapeutic efficiency (Ren, Xu et al. 2009).

Wang et al. (2010):

Trimethylated chitosan (TMC) conjugated PLGA nanoparticles were constructed for the delivery of coenzyme Q_{10} to the brain. Instead of using poly (vinyl alcohol) (PVA), vitamin E

succinated polyethylene glycol 1000 (vitamin E TPGS) was successfully used in the preparation of Co-Q_{10} loaded PLGA nanoparticles (147 nm). The conjugation of TMC was confirmed as zeta potential increased from -18.3 mV to 21.0 mV. Cytotoxicity was evaluated by MTT assay with SH-SY5Y cells; no significant cytotoxic effect of TMC conjugated PLGA NPs was found. The AD animal model, transgenic mice characterized by overexpression of Aβ and plaque accumulation was used. The biodistribution was investigated by fluorescent microscopy of brain sections after caudal vein injection of TMC-conjugated PLGA NPs loaded with coumarin-6 (136nm). A higher accumulation was observed in the brain parenchyma of the animals treated with TMC-conjugated PLGA NPs in comparison to the unconjugated PLGA NPs. According to the behavior studies, the memory impairment was greatly attenuated by the TMC-NPs loaded with Co-Q_{10}, while unconjugated PLGA –NP did not show any significant improvement over the control group. Senile plaque staining showed that senile plaques were reduced after the treatment of Co-Q_{10} loaded TMC-NPs. Behavior, senile and biochemical parameter tests of coenzyme Q_{10} loaded TMC-conjugated PLGA NPs (147nm) further confirmed the brain-targeted property and superior advantages of TMC/PLGA NPs over uncoated PLGA NPs. Biochemical parameters including oxidative stress, malondialdehyde (MDA), GSH-peroxydase (GSH-Px) and catalase (CAT) were determined. The MDA level in the brain decreased greatly in TMC-NPs treated groups compared to control and PLGA-NPs treated mice ($P<0.05$). The GSH-Px level and CAT level in the brain didn't show a difference from the control and unmodified NPs treated group, and the GSH-Px level and CAT level in TMC-NPs treated mice increased compared to PLGA-NPs treated group. (Wang, Wang et al. 2010).

Jalali et al. (2011):

Vitamin E polyethylene glycol 1000 succinate (vitamin E TPGS) was confirmed to be a better emulsifier than PVA by testing the *in vitro* cytotoxicity of the TPGS-coated PLGA nanoparticle tested in PC12 cells. Four concentrations of TPGS (0.02%, 0.06%, 0.12%, and 0.18%) were used for the preparation of TPGS-NPs (100-400 nm). The effects of different emulsifiers (TPGS, PVA, and mixture of both), stirring times on particle sizes, surface morphology and phase composition were investigated. *In vitro* cytotoxicity studies of TPGS-NPs in a PC12 cell line, a neural cell model, showed no obvious cytotoxicity. The more TPGS on the surface, the more effective therapeutic effects the TPGS-PLGA NPs showed (Jalali, Moztarzadeh et al. 2011).

Jaruszewski et al. (2012):

The accumulation of amyloid β (Aβ) proteins in the cerebral vasculature causes cerebral amyloid angiopathy (CAA) in patients suffering from Alzheimer's disease. A novel PLGA immuno-nanovehicle (265 nm) was designed by coating PLGA with chitosan to enhance stability and conjugating with an anti-Aβ antibody to the particles, for the treatment of Alzheimer's disease. Chitosan coated PLGA NP showed cubed-shaped NPs under scanning electron microscope (SEM), and the amount of chitosan adsorbed on the surface was 3.09 μg/mg NPs. The stability ratio was determined to evaluate the stability of NPs, and the immuno-nanoparticles showed the highest stabilities, followed by chitosan coated PLGA NPs and PLGA NPs. To evaluate the cellular uptake, polarized MDCK cell monolayer, a commonly used *in vitro* BBB model was used. With coumarin-6 as fluorescent marker, cellular internalization of immuno-nanoparticles was confirmed by the fluorescence images, which displayed higher fluorescence in modified chitosan-PLGA NPs than unmodified chitosan-PLGA NPs. After incubated with Aβ

proteins, immuno-nanoparticles demonstrated increased cellular uptake in the MDCK cell monolayer. The immuno-nanovehicles were transcytosed across the monolayer which demonstrated their ability to potentially cross the BBB (Jaruszewski, Ramakrishnan et al. 2012).

Parikh et al. (2010):

The effect of surface charge on brain delivery of sulpiride using surface modified pegylated nanoparticles was studied. Alexa Fluor 488 labeled thiolated cationized bovine serum albumin (CBSA) (329 nm, -19 mV) and bovine serum albumin (BSA) (308 nm) were conjugated to PEG-PLGA nanoparticles which were loaded with Sulpiride and Rhodamine-B. After administered to Sprague Dawley rats via tail vein, blood samples (0.5 mL) at 0.5, 1, 2, 4, 8, 16 and 24 h and total urine accumulated in 24 h were collected. Much less Sulpiride was released in plasma from CBSA-NPs in first 5 h compared to BSA-NPs and unconjugated NPs. The low drug level of urinary excretion for different formulations (19.26%) confirmed the possibility of particles being distributed in the body rather than being cleared. The fluorescent study showed that CBSA-NPs were cleared faster from plasma and reached the brain in higher concentrations compared to unconjugated NPs (218nm) and BSA NPs. The high uptake in the brain of CBSA-NPs compared to BSA-NPs proved that positive charge of the CBSA-NPs was the reason of higher brain uptake. Most endothelial cells of the BBB are negatively charged, and thus positively charged NPs could adsorb on cell surface and be taken up by adsorptive-mediated transcytosis (Parikh, Bommana et al. 2010).

Lu et al. (2007):

Lu, W.'s group investigated brain delivery of cationic bovine serum albumin (CBSA) conjugated PEG-PLA nanoparticles (CBSA-NP). In order to conjugate different concentrations of CBSA on the surface of NPs, different weight ratio of Mal-PEG-PLA to MPEG-PLA (1:20,

1:10 and 1:5) were used to form NPs measuring in average 105 nm. The BSA-NP was prepared with the ratio 1:10 and measured 97.4 nm. The brain transcytosis of CBSA-NP across the coculture of endothelial cells and astrocytes was confirmed using coumarin-6 as fluorescent probe after incubation for 5, 10, 20, 30 and 60 min. The permeability (Pe) of CBSA-NP was higher than that of unconjugated NP, and Pe values increased as the increasing amount of CBSA on the surface of NPs. Pre-incubation with 100 μg/ml free CBSA significantly decreased the Pe values of CBSA-NP to only 10%. Adsorptive mediated transcytosis (ATM) was believed to be the principle brain delivery pathway of CBSA-NP. A dose of 30 mg/kg of the three types of CBSA-NP, BSA-NP and unmodified NP with entrapped coumarin-6 as fluorescence probe were injected via tail vein in male BALB/c mice. Brain delivery of CBSA-NPs in mice was proved, and the optimal brain targeting nanoparticle was determined. The NPs with 110 CBSA/particle, with the maleimide-PEG-PLA/methoxy-PEG-PLA weight ratio 1:10 (105 nm) achieved 2.3-fold increasing of the percentage of injected dose per gram of brain (%/ID/g brain), compared with unmodified NP (Lu, Wan et al. 2007). In their previous study, the effect of particle size on transport of methotrexate across the BBB using polysorbate 80-coated polybutylcyanoacrylate nanoparticles (PBCA) was investigated, and an average size of 70 nm showed the highest accumulation of drug concentration for four different sizes of PBCA nanoparticles (Gao and Jiang 2006). The efficiency of brain delivery was lower with the co-injection of free CBSA with CBSA-NP compared to those without co-injection. CBSA-NPs were found to distribute more in liver and spleen than other organs, and NP clearance by liver and spleen increased with the increasing of CBSA content of NPs. Moreover, “accelerated blood clearance (ABC) phenomenon” was observed among single dose or over successive high doses of CBSA-NP treated profile via blood clearance testing. PEG-PLA NPs also showed an ability to induce the

ABC phenomenon in an inversely dose-dependent manner after one-dose treatment. Immunoglobulin binding to NP or CBSA-NP was determined via Western blotting analysis. It was observed that IgM was induced by both NP and CBSA-NP at day 10 after a dose of 0.005 mg/kg injection. For the successive treatment study, IgM and specific IgG were only induced by CBSA-NP (1:10) at day 10 after 5 successive injection at dose of 180 mg/kg/day. Mild acute inflammation of mice cerebrum, liver, spleen and kidney of intravenously injected CBSA-NP (1:10) at high dose (180 mg/kg/day) over 7 successive days was detected, it was concluded that potential toxicity of ABC phenomenon should be taken into consideration (Lu, Wan et al. 2007). Costantino et al. (2005):

Costantino, L. *et al*. conjugated five short peptides to PLGA respectively to form peptide-derivatized PLGA nanoparticles (162-211 nm) with poloxamer 188 (Pluronic® F68) as a emulsifier. Fluorescein or tetramethylrhodamine fluorescent probes were covalently linked to PLGA polymers, and fluorescent labeled polymers were used to prepare NPs. The ability of different nanoparticles to cross the BBB was investigated by the *in vivo* Rat Brain Perfusion Technique. A suspension of NPs (5 mg/mL saline per animal weighting 250 g) was perfused in rats in 20 s, and brain was collected after the rat was sacrificed. Fluorescent and confocal microscopy studies of brain showed four out of five peptide conjugated nanoparticles were able to penetrate the BBB into cerebral parenchyma while unconjugated PLGA nanoparticles were not. Moreover, one peptide (H_2N-Gly-L-Phe-D-Thr-Gly-L-Phe-L-Leu-L-Ser-*O*-β-D-glucose-$CONH_2$) conjugated NPs showed the highest distribution in the brain with the perfusion technique (Costantino, Gandolfi et al. 2005).

Li et al. (2011):

A phage-displayed peptide conjugated PEG-PLGA nanoparticles for brain targeting delivery was constructed. The 12-amino-acid-peptide (Pep TGN), a non-reported brain-target motif, was selected by 4 rounds of *in vivo* phage display screening with adult male ICR mice. Mice were injected in the tail vein with 10^{11} plaque forming units (pfu) of Ph.D.-12™ Phage Display Library in 100 μl Tris-buffered saline (TBS). The brain tissue was collected and homogenized 24 h after administration, then mixed with E. coli. After the final round of biopanning, a total of 20 peptides were screened, and a consensus sequence (TGN) was found in 60% of peptides via a multiple sequence-alignment analysis using Laser gene program. Both the competitive inhibitions and immunohistochemistry studies proved Pep TGN could be a promising ligand targeting the brain. Pep TGN was conjugated to PEG-PLGA NPs at 1:3 and 1:1 ratio to form 115.2 nm and 121.5 nm NPs respectively. *In vitro* cytotoxicity studies of NP, TGN-NP (1:3) and TGN-NP (1:1) with bEnd.3 cells after 4 h and 24 h incubation at 37 ℃ revealed low cytotoxicity. TGN-PLGA NP proved significant higher bEnd.3 cells uptake *in vitro*. After 1 h injection of treatment, enhanced brain targeting delivery of TGN-NPs *in vivo* was observed when compared to empty PLGA nanoparticles using coumarin-6 as fluorescence probe. The TGN-NPs with high concentration of TGN on the surface (1:1) displayed higher accumulation in the brain than TGN-NPs (1:3). The brain uptake of TGN-NP (1:3) and TGN-NP (1:1) was 55.2 ng/g and 95.1 ng/g at 1 h, about 2.1 and 3.6 times higher than that of unmodified NPs (26.3 ng/g). After 24 h, the brain uptake of TGN-NP (1:3) and TGN-NP (1:1) proved to be 2 and 4-fold higher than that of unconjugated NPs. The more TGN was conjugated on the surface, the higher brain delivery the NPs could achieve (Li, Peng et al. 2011).

Rao et al. (2008):

Protease inhibitors (PIs), used in the treatment of HIV are mostly known substrates of P-glycoprotein (P-gp), which hinders the transport across the BBB. Trans-activating transcriptor (TAT) peptide conjugated PLA nanoparticles (340 nm) were constructed to provide CNS delivery of ritonavir, an anti-HIV drug, to bypass the efflux action of P-gp. The amount of TAT peptide attached to the PLA NPs was 0.23 μg/mg NPs, corresponding to about 2012 peptide molecules per NP. Madine Darby canine kidney cells over-expressing P-gp (MDCK-MDR1) and wild type MDCK (MDCK-wt) were used to evaluate whether ritonavir loaded TAT-NPs bypassed the efflux action of P-gp with coumarin-6 as fluorescent marker. Permeability coefficient (P_{app}) was calculated after incubation for 5 h at 37 ℃. Approximately 40-fold increased uptake of ritonavir in MDCK-MDR1 using TAT-conjugated PLA nanoparticles (P_{app}, 2.4×10^{-5}, cm/s) than free ritonavir (P_{app}, 0.05×10^{-5}, cm/s) in solution was proved. TAT-NPs showed four-fold greater uptake of ritonavir in MDCK-MDR1 than in MDCK-wt cell lines while the uptake of free ritonavir was greater in MDCK-wt than in MDCK-MDR1. The brain drug level after intravenous administration of TAT-conjugated nanoparticles (80.3 μg/g of tissue) was 800-fold higher than that of drug in solution (0.1μg/g of tissue), and 7-fold higher than unconjugated NPs (12.2μg/g of tissue) at two weeks. TAT-NPs and unconjugated NPs were found to distribute in the brain, heart, spleen and kidney 1 day after administration, and greater amounts were found in the spleen than in other tissues. The drug level was sustained in heart and spleen from TAT-NPs treated groups for a longer period of time before drug clearance (4 weeks). The fluorescent microscopic analysis of brains and further histological analysis of TAT-conjugated nanoparticles showed that NPs first entered the brain vasculature, and then localized in the brain parenchyma without disrupting the BBB integrity (Rao, Reddy et al. 2008).

Tosi et al. (2010):

Sialic acid (SA) and similopioid peptide (g7) conjugated PLGA nanoparticles loaded with loperamide (LOP-SA-g7-NP) and a fluorescent dye, Rhodamine-123 (ROD), (ROD-SA-g7-NP), and labeled with tetramethylrhodamine (TMR-SA-g7-NP) made with poloxamer 188 (Pluronic® F68) as an emulsifier were synthesized to evaluate central nervous system targeting and distribution. LOP-SA-g7-NP (180 nm) was found to reach the brain 15 min after the administration and 30%-35% maximal possible effect (MPE) was reached as detected by the sudden opioid effect with the antinociceptive testing. The MPE values decreased to 20% after 30-60 min, increased to 50% after 6 h, and maintained at 30-50% for 15 h. After 24 h, the antinociceptive effect of NPs gradually decreased to 10-20% MPE. Compared to their previous studies, the effect of LOP-g7-NP was 57% MPE and lasted only 5 h after administration, the long-lasting effect of SA-LOP-g7-NP. Higher dose of drug delivered to the CNS provided higher MPE values. *In vivo* fluorescence studies of TRM-SA-g7-NP (154 nm) after intravenous administration at 0.5, 1, 2, and 6 h showed TMR-SA-g7-NP distributed in the cerebral parenchyma. The 3D confocal images further proved TMR-SA-g7-NP located close to the cerebral nuclei of brain cells, and some into the cytoplasm. The retention time of TMR-SA-g7-NP in the brain was studied by sacrificing rats 15 days, 1, or 2 months after administration. The TMR-SA-g7-NP could be detected in the CNS parenchyma after 15 days, but not any more after 1 month. The *in vivo* biodistribution studies with ROD-SA-g7-NP (197 nm) showed 4-6% of the injected TMR-SA-g7-NP was found into the CNS after 1 h, and it was maintained at this level for 6 h, then it decreased to 2% over 24 h. Compared to ROD-g7-NP (169 nm) which showed higher amount (13%) at 1.5 h, but decreased faster to 0.7% for 24 h, TMR-SA-g7-NP was proved to prolong retention time in brain. However, biodistribution *in vivo* also showed that

ROD-SA-g7-NP were greater accumulated in liver (10-20%), kidney (15-40%) and especially in lung (70% -30%) in the first five hours after administration compared to ROD-g7-NP and empty PLGA-NP, as SA coverage interacted with specific receptors for SA residues in other organs. This result explained the less accumulation of ROD-SA-g7-NP (6%) over ROD-g7-NP (13%) over 1 h in the brain (Tosi, Vergoni et al. 2010).

Mathew et al. (2012):

A targeting ligand Tet-1 peptide was conjugated to PLGA nanoparticles (150-200nm) to improve curcumin delivery to the brain. Curcumin incorporated in PLGA NPs was proved to conserve its anti-oxidant and anti-amyloid activity. Cytotoxicity studies of Tet-1 conjugated or unconjugated NPs were carried out with LAG cell line (mouse fibroblast like connective tissue) using Alamar Blue and MTT assays. No significant cytotoxic effects *in vitro* of both nanoformations were found according to the results. GI-1 glioma cells were used for the cellular uptake studies of Tet-1 grafted and unmodified NPs *in vitro*. Tet-1 conjugated PLGA NPs showed multiple folds increased uptake than the unconjugated NPs. Confocal laser scanning microscopy studies showed that Tet-1 targeted NPs distributed more around the cell soma and nucleus compared to unconjugated NPs. PLGA conjugated with Tet-1 peptide was proved to be a potential therapeutic carrier of curcumin for AD treatment (Mathew, Fukuda et al. 2012).

Geldenhuys et al. (2011):

Glutathione conjugated PEG-PLGA nanoparticles loaded with paclitaxel (200 nm) were constructed to enhance brain-targeted delivery. The effect of glutathione at different concentrations (1, 2 and 3% w/v) on average diameter of NPs was investigated first. Particle size of NPs decreased with increasing concentration of glutathione used for the synthesis. The concentration of 2% w/v glutathione was selected based on the size (237 nm) and PDI (0.74).

Intracellular uptake of glutathione modified PLGA-PEG NPs were investigated in RG2 cells, a rat glioma cell line, by using a coumarin-6 as fluorescent marker. Enhanced cellular uptake of glutathione-conjugated NPs was observed compared to uncoated NPs after incubation for 24 h. The cytotoxic efficacy of paclitaxel loaded glutathione-conjugated PLGA-PEG NPs were evaluated using MTT assay; higher cytotoxicity was proved for coated NPs compared with uncoated NP and free paclitaxel. As tubulin accumulation is induced by Paclitaxel, the immunofluorescence of tublin was performed using RG2 cells. Glutathione conjugated PLGA-PEG NPs showed higher accumulation of acetylated tubulin than uncoated NP and control. When compared to 1% Tween coated NPs, the cytotoxic effect and tubulin levels of 2% glutathione coated NPs were similar. Western blotting analysis further confirmed this result. *In vivo* brain uptake and biodistribution studies in brain tumor mouse model after 0.2 mL of 5 mg/kg NPs intraperitoneally administration, enhanced brain uptake compared with uncoated NPs was evidenced as well (Geldenhuys, Mbimba et al. 2011).

Chang et al. (2009):

The brain uptake mechanisms of transferrin (TF) conjugated PLGA NP with Dil as a fluorescent marker was studied. Fluorescent labeled Tween 20 and BSA coated PLGA NPs, and unmodified PLGA NPs were prepared as controls. Unmodified NPs without Tween 20 coalesced quickly, thus proteins were conjugated on the PLGA NPs to maintain NPs stable for at least 12 days at 37 ℃. The amount of Tf and BSA conjugated to the NPs was 89μg and 126 μg per mg NPs. Cytotoxicity studies on the integrity of BBB using either Lucifer Yellow or sucrose ^{14c} revealed high toxicity of Tween 20 coated PLGA NPs, and thus Tween 20 coated PLGA NPs were discarded in the following studies. An *in vitro* model of a co-culture of brain endothelial cells (BCECS) and astrocytes (glial cells) which mimic the BBB was prepared for the cellular

uptake study. Compared to unconjugated PLGA nanoparticles (63 nm) and BSA-coated PLGA nanoparticles (89 nm), uptake of Tf-coated PLGA nanoparticles (90 nm) was found 20-fold and 2-fold respectively greater after 1 h incubation. Endocytosis using an energy-dependent process was confirmed as the endocytosis of NPs was inhibited by low temperature and the presence of sodium azide and excess free Tf in solution. Inhibitors studies were carried out to investigate the mechanism of endocytosis. After incubated with filipin, a caveolae inhibitor, Tf-NPs showed significantly decreased cellular uptake compared to unconjugated NPs and BSA-NPs, which suggested a specific caveolae-mediated transcytosis of Tf-NPs and a adsorptive mediated endocytosis of unmodified NPs and BSA-conjugated NPs (Chang, Jallouli et al. 2009).

Gan and Feng (2010):

Transferring (Tf) conjugated nanoparticles of Poly (lactide)-D-α-Tocopheryl polyethylene glycol succinate diblock copolymer (PLA-TPGS) with entrapped docetaxel (Taxtere®) (137.6 nm) was prepared. Cellular uptake and cytotoxicity of the Tf-conjugated PLA-TPGS NPs with entrapped coumarin 6 as a fluorescent marker were evaluated and compared to unconjugated PLGA NPs in C6 glioma cell line for 4 h. The Tf conjugated PLA-TPGS NPs showed the highest cellular uptake, followed by unconjugated PLA-TPGS NPs and PLGA NPs. Following pre-incubation with an excess of Tf for 1 h, the cellular uptake of Tf-PLA-TPGS NPs decreased and was similar to that of the unconjugated PLA-TPGS NPs, which suggested that a receptor-mediated endocytosis process was involved. *In vivo* biodistribution of Tf-conjugated PLA-TPGS NPs was compared with that of PLGA NPs, PLA-TPGS NPs and docetaxel 24 h after intravenous injection in rats. Tf-conjugated PLA-TPGS NPs was proved to be able to cross the BBB, and showed a much higher concentration compared to unconjugated PLA-TPGS NPs. *In vitro* cytotoxicity of docetaxel loaded PLA-TPGS NPs with or without Tf

modification was evaluated with C6 glioma cells after incubation at 37 ℃ after 24 h, 48 h and 72 h. Tf conjugated PLA-TPGS NPs proved the lowest cytotoxicity compared with unconjugated PLA-TPGS, PLGA NPs and solution docetaxel. Furthermore, IC_{50}, a quantitative index of inhibitory concentration was employed to demonstrate the advantages of the Tf-conjugated PLA-TPGS NPs. Based on the IC_{50} data of the designed NPs loaded with docetaxel, it was concluded that Tf-conjugated PLA-TPGS NPs could be 23.4%, 16.9% and 229% more efficient than unconjugated PLGA NPs, PLA-TPGS NPs and docetaxel respectively (Gan and Feng 2010).

Jain et al. (2011):

Transferrin (Tf) was conjugated on the surface of PEG-PLGA NPs (121 nm) to improve temozolomide delivery to brain. *In vitro* cytotoxicity studies of Tf-PEG-PLGA NPs with incorporated temozolomide were investigated with eight human cancer cell lines of six different human cancer tissues including prostate, colon, breast, neuroblastoma, CNS and lungs after incubation for 48 h. Cells exposed to PEG-PLGA NPs and Tf-PEG-PLGA NPs showed the lowest cell viability compared to those exposed to PLGA NPs. Confocal laser scanning microscopy (CLSM) of brain 4h after i.v. administration of all formations of nanoparticles showed PEG-PLGA NPs and Tf-PEG-PLGA NPs distributed in the brain, and Tf-PEG-PLGA NPs were found within the brain parenchyma. All these results demonstrated Tf conjugated PEG-PLGA NPs improved brain delivery of temozolomide (Jain, Chasoo et al. 2011).

Kuo et al. (2011):

Transferrin (Tf) grafted PLGA NPs (170-200nm) were synthesized with dioctadecyldimethylammonium bromide (DODAB) as emulsifier to enhance nevirapine (NVP) delivery across human brain microvascular endothelial cells (HBMECs). The effects of Tf and DODAB on cell viability of HBMECs at a dose of 0.0125% (w/v) NVP loaded Tf-PLGA NPs

were investigated. An increase of DODAB concentration (33%-100%) in Tf-NPs reduced the cell viability of HBMECs to 70-75%. Tolerable toxicity and mild secretion of TNF-α were observed. Permeability studies of NVP loaded Tf-PLGA NPs with the concentration of 0.05 mg/ml revealed nanoparticles with 67% DODAB reached the highest permeability followed by 100% and 0% DODAB emulsified NPs. The uptake of fluorescent Tf-PLGA NPs loaded with NVP was 3.2 times greater than unmodified NPs. According to all results, the optimum condition for NVP delivery with Tf-PLGA NPs for this study was 67% DODAB, 0.05% NVP and 0.1% Tf (Kuo, Lin et al. 2011).

Carroll et al. (2010):

A transferring antibody (OX 26) was covalently linked to PLGA-PEG NPs (105 nm) to enhance brain delivery of entrapped Tempol. P-gp-ATP assay was employed to study the ability of the NPs to prevent P-gp efflux. Incubated NPs with P-gp didn't show any increase in ATPase use, which indicated the OX 26 conjugated NPs were not the substrate for P-gp. An enhanced cellular uptake of conjugated NPs was observed compared to unconjugated NPs in RG2 rat glioma cells using coumarin 6 as a fluorescence label. Cell proliferation study via MTT assay proved conjugated PLGA NPs were more efficient in preventing cell viability than unconjugated NPs and free Tempol in RG2 rat glioma cells after incubation for 24 h at 37 ℃ (Carroll, Bhatia et al. 2010).

Grabrucker et al. (2011):

Grabrucker A.M. el al developed glycopeptides-conjugated PLGA NPs (BBB-NPs) for Zn^{2+} (190-210 nm) delivery to CNS. Cytotoxicity studies of unloaded or Zn^{2+} loaded PLGA NPs and BBB-NPs were carried out with neuronal/glial cultures. Unloaded PLGA NPs and BBB-NPs showed no significant toxic effects on cells at a concentration of 625 μg/ml, and double or triple

this concentration. However, a significant reduction of cell viability was observed at 8× (BBB-NPs) and 10× (both NPs). Uptake studies revealed that BBB-NPs improved endocytosis compared to unconjugated NPs with tetramethylrhodamine covalently linked with NPs. To achieve selective targeting to neurons (NCAM1 labeled) or glial cells (CD44 labeled), anti-NCAM1 antibody and anti-CD44 antibody were conjugated on the surface of nanoparticles, respectively. Specific targeting of antibody modified NPs was observed (Grabrucker, Garner et al. 2011).

Hu et al. (2011):

Lactoferrin (Lf) conjugated PEG-PLGA nanoparticles (Lf NP) entrapped with urocortin (UCN) were synthesized and both *in vitro* and *in vivo* targeting delivery was evaluated. Coumarin-6 incorporated in the NPs (120nm) was used as a fluorescence probe. *In vitro* cellular uptake was carried out in bEnd.3 cells, a model of the BBB, after incubation with coumarin-6 loaded Lf-NPs and unconjugated NPs for 0.25, 0.5 and 1 h at 37 ℃. A time-, temperature-, and concentration-dependent cellular uptake was confirmed. About 3.9-fold higher cellular uptake of Lf-NP was observed over unconjugated NPs at 4 h. Excess free Lf was added to evaluate the inhibitory effect of Lf on Lf-NPs uptake. The efficiency of Lf-NPs in the presence of excess Lf decreased to 30% of the efficiency of NPs without free Lf. Further inhibitory studies with chlorpromazine which inhibits clathrin-dependent process and filipin which inhibit caveolae-dependent process were carried out. The uptake method of Lf NP was proved to be an additional clathrin-mediated endocytosis processes induced by Lf. After intravenous administration in 6-OHDA rat model of Parkinson's disease, Lf-NPs accumulated more in heart and spleen but less in kidney compared to unmodified NPs. Moreover, Lf-NP showed 2.49-fold of coumarin-6 accumulation in the brain of rats than unconjugated NP in 24 h, and mainly distributed in the

cortex, substantia nigra and striatum region. Urocortin (UCN) was entrapped in the Lf-NPs to study the therapeutic effect on 6-OHDA rat model of Parkinson's disease. The behavior test was carried out at 7, 14 and 21 days after the rats were injected with UCN loaded Lf-NPs and unconjugated NPs. Immunohistochemistry stain of tyrosine hydroxylase and striatal transmitter contents were also used to evaluate the therapeutic effects of the NPs. The rotation behavior of 6-OHDA was greatly attenuated by UCN loaded LF-NPs after intravenous administration. The TH-immunoreactivity was significantly improved after LF-NP with entrapped UCN compared to other treatment groups. The percentage of DA in the striatum was significantly increased after Lf-NPs injection at 21 days. Lf-NP showed relatively low toxicity via *in vitro* cell viability experiment. *In vivo* CD 68 immunohistochemistry, which was used to investigate the acute inflammation of NPs showed dose-dependent inflammatory reactions in liver, spleen and kidney at 24 h which disappeared at 48 h after successive administration of LF-NP for 7 days, but no obvious inflammatory reactions to other tissues. The results proved Lf NPs was a promising brain delivery carrier for drug with low toxicity (Hu, Shi et al. 2011).

Kuo and Yu (2011):

Biodegradable poly-(γ-glutamic acid) (γ-PGA), a natto mucilage from certain strains of *Bacillus subtilis* was used to enhance cellular internalization. In this study, γ-PGA was grafted to the surface of PLGA nanoparticles to enhance the transport of saquinavir (SQV) across the BBB. Three kinds of γ-PGA of three molecular weight: 6, 14 and 52 kDa measuring 188.8, 218.1, and 307.6 nm respectively were used for the preparation of γ-PGA PLGA NPs with didecyl dimethylammonium bromide (DDAB) and 1,2-distearoyl-sn-glycero-3-phosphoethanolamine-N-[carboxy(polyethylene glycol)-2000] (DSPE-PEG(2000)-carboxylic acid) as stabilizer. The effect of percentage of DDAB used for the synthesis on the average particles diameter of γ-PGA

conjugated PLGA NPs was studied as well. An increase in the concentration of DDAB (0.02, 0.04, and 0.06%) increased the average size of NPs and the conjugation efficiency due to electrostatic interaction. The permeability of γ-PGA NPs with entrapped SQV was studied in the co-cultured Human brain-microvascular endothelial cells (HBMEC)/human astrocyte (HA) system. The effects of different molecular weights and grafting efficiency of γ-PGA to the permeability of SQV across a monolayer of human brain-microvascular endothelial cells (HBMECs) were investigated, and proved that the maximal permeability was achieved by the 6kDa of γ-PGA conjugated PLGA NPs (85.2% grafting efficiency, 180 nm) which was 6 times enhanced over that of free SQV. The abilities of γ-PGA to promote the endocytosis of NPs and expression of ornithine decarboxylase (ODC) by HBMECs, which could enhance the delivery to the CNS, were also demonstrated. An increase of γ-PGA on the surface of NPs enhanced the uptake of γ-PGA conjugated NPs (Kuo and Yu 2011).

Guo et al. (2011):

AS1411 (Ap), a DNA aptamer was conjugated to the PEG-PLGA nanoparticles (156 nm) to enhance the brain delivery of paclitaxel (PTX, Taxol®) for the treatment of glioma. The conjugation of Ap to NP was confirmed using Urea polyacrylamide gel electrophoresis (PAGE) and X-ray photoelectron spectroscopy. *In vitro* PTX release from Ap-PTX-NP was 43.3% in PBS and 46.8% in plasma after 24 h, which was quite similar to that from PTX-NP. Fluorescently labeled Ap-NPs were proved to enhance cellular association in C6 glioma cells compared to unmodified NPs. Cellular uptake was reduced when incubated with excess Ap. Cell viability of C6 cells was evaluated using MTT assay, showing significantly enhanced cytotoxicity of PTX when loaded in Ap-NP over free PTX (2.59, 4.18 and 4.67 times) and unconjugated PTX loaded NP (2.92, 3.32, and 2.67 times) after incubation for 24 h, 48 h and 96

h, respectively. A pharmacokinetic study showed prolonged retention time of NPs after intravenous administration at a dose of 3 mg/kg in rats for 0.1, 0.25, 0.5, 0.75, 1, 2, 4, 8, 12 and 24 h. The highest concentration of PTX in the tissue from Ap-PTX-NP was found in the liver compared to those treated with PTX-NP and PTX. Ap-PTX-NP showed the highest efficiency of drug delivery to the tumor, which was 1.57-fold over that of PTX-NP and 2.44-fold than that of PTX respectively after 24 h. Rats bearing glioma xenograft and intracranial glioma were used to investigate biodistribution and anti-glioma efficacy of PTX loaded AP-NP *in vivo*. After intravenous administration of treatment for 20 days, growth, volume, and weight of xenograft tumors were characterized. The average tumor inhibition of Ap-PTX-NP, PTX-NP and PTX for tumor volume was 81.6, 66.9 and 68.6%, and 79.3, 68.6, and 48.2% for tumor weight. The survival times of Wistar rats bearing intracranial C6 glioma with the treatment of saline, PTX, PTX-NP and Ap-PTX-NP were 18, 24, 27 and 31 day respectively. Ap-PTX-NP proved to inhibit tumor more effectively and greatly prolonged survival time of the animals (Guo, Gao et al. 2011).

2.3. Discussion

Among 29 papers cited in this review, nine papers performed *in vitro* studies (Chang, Jallouli et al. 2009; Carroll, Bhatia et al. 2010; Xie, Lei et al. 2010; Grabrucker, Garner et al. 2011; Jalali, Moztarzadeh et al. 2011; Kuo, Lin et al. 2011; Kuo and Yu 2011; Jaruszewski, Ramakrishnan et al. 2012; Mathew, Fukuda et al. 2012), 8 papers focused on *in vivo* studies (Sun, Xie et al. 2004; Costantino, Gandolfi et al. 2005; Ren, Xu et al. 2009; Gelperina, Maksimenko et al. 2010; Parikh, Bommana et al. 2010; Tosi, Vergoni et al. 2010; Tahara, Miyazaki et al. 2011; Tsai, Chien et al. 2011), and 12 papers did both *in vitro* and *in vivo* studies (Lu, Wan et al. 2007; Rao, Reddy et al. 2008; Gan and Feng 2010; Wang, Wang et al. 2010; Chen, Hsieh et al. 2011;

Geldenhuys, Mbimba et al. 2011; Guo, Gao et al. 2011; Hu, Shi et al. 2011; Jain, Chasoo et al. 2011; Kulkarni and Feng 2011; Li, Peng et al. 2011; Mittal, Carswell et al. 2011).

2.3.1. *In vitro* studies

In vitro studies were usually conducted in brain endothelial cell lines (bovine, human and rat), Madin-Darby Canine kidney cells and glioma cells. *In vitro* studies were performed to investigate cytotoxicity, uptake efficiency, endocytosis mechanism and drug efficiency with different cell lines. All the aspects are discussed in the following sections.

2.3.1.1. Cytotoxicity

The uptake efficiency, internalization mechanisms, and cytotoxicity of nanoparticles have been studied with different cell lines. In addition to naked NPs, PLGA/PLA NPs were coated to change the surface property or linked with a targeting ligands to trigger adsorptive-mediated or receptor-mediated transcytosis to the CNS (Patel, Zhou et al. 2011). The cytotoxicity studies of TMC-TPGS-PLGA NPs (136 nm) with SH-SY5Y cells (Wang, Wang et al. 2010), TPGS-PLGA NPs (250 nm) with PC 12 cell line (Jalali, Moztarzadeh et al. 2011), TGN-PEG-PLGA NPs (119 nm) with bEnd.3 cells (Li, Peng et al. 2011), Tet-1 PLGA NPs (150-200) with LAG cell line (mouse fibroblast like connective tissue) (Mathew, Fukuda et al. 2012) and Lf-PEG-PLGA (120 nm) with bEnd.3 cells (Hu, Shi et al. 2011) demonstrated no significant cytotoxicity of all formations of nanoparticles at a dose range of 0.075-8000 μg/ml.

2.3.1.2. Uptake efficiency

Cellular uptake was investigated by fluorescent or confocal microscopy studies, showing enhanced internalization of surface modified nanoparticles compared to unmodified nanoparticles. Different cells including MDCK cells (Rao, Reddy et al. 2008; Xie, Lei et al. 2010; Kulkarni and Feng 2011; Jaruszewski, Ramakrishnan et al. 2012), BCEC cells (Lu, Wan et al.

2007; Chang, Jallouli et al. 2009; Chen, Hsieh et al. 2011; Kuo, Lin et al. 2011; Kuo and Yu 2011), bEnd.3 cells (Hu, Shi et al. 2011; Li, Peng et al. 2011), and glioma cells (Carroll, Bhatia et al. 2010; Gan and Feng 2010; Xie, Lei et al. 2010; Guo, Gao et al. 2011) were used as *in vitro* cell models treated at dose ranging from 10 to 15000 μg/ml. Decreasing size, positive charge and less hydrophilic NPs were associated with enhanced cellular uptake (Kulkarni and Feng 2011). After coating with TMC, a cationic ligand, zeta potential of NPs increased from -18 to 21 mV, and the active transport of NPs via AMT was confirmed (Wang, Wang et al. 2010). TPGS and surfactants such as T80 and F68 coated NPs have been proven to have an improved cellular uptake due to changes of NP surface properties such as surface charge and surface hydrophilicity (Kulkarni and Feng 2011). MDCK cellular uptake of TPGS-PLGA NPs (222nm) showed 1.5-fold higher than PVA-emulsified NPs 4h after incubation (Kulkarni and Feng 2011). The permeation percentages of loperamide entrapped F68- and T80-PLGA NPs (21% and 14.5%) were significantly increased compared to loperamide loaded PLGA NPs (4.5%) and free loperamide (0.4%) (Chen, Hsieh et al. 2011).

Targeted ligands conjugated on the surface could provide a receptor-mediated endocytosis as opposed to non-specific endocytosis. Cellular uptake of Tf-PLGA NPs (90 nm) was found 20-fold and 2-fold respectively greater than unmodified PLGA NPs and BSA-PLGA NPs (88 nm) 1h after incubation with BCECS. In one study, anti NCAM1 antibody conjugated PLGA NPs (190-210 nm) distributed more in neurons labeled with NCAM1 while anti-CD44 antibody conjugated PLGA NPs (190-210 nm) targeted more glial cells labeled with CD44 (Grabrucker, Garner et al. 2011).

The endocytosis process was proven by changing the temperature-, concentration-, and time-dependent uptake and co-incubating cells with free targeting ligand and NaN_3 which stops

energy-dependent processes indicating active endocytosis process (Chang, Jallouli et al. 2009; Hu, Shi et al. 2011). Furthermore, the uptake mechanisms of different ligand-conjugated nanoparticles were studied with cells pre-incubated with inhibitors. By using chlorpromazine which inhibits clathrin-dependent and caveolae-dependent pathway, colchicines which inhibits macropinocytosis pathway, and BFA which inhibits Golgi apparatus and lysosome related endocytosis process, transport of Lf-TPGS-PLA NPs (120 nm) across the membrane was proved to be clathrin mediated endocytosis (Hu, Shi et al. 2011). The mechanism of uptake of Tf-PLGA NPs (90 nm) was confirmed as caveoale-dependent by co-incubating cells with filipin, a caveolae inhibitor, and other different types of inhibitors. Co-incubated blank NPs with filipin did not show inhibition of NP cellular uptake which indicated that endocytosis of blank NPs might be adsorptive mediated endocytosis (Chang, Jallouli et al. 2009).

2.3.1.3. Therapeutic efficacy

A number of *in vitro* experiments have proved that surface functionalized nanoparticles enhanced the therapeutic efficacy of antitumor drugs against the glioma cells such as RG2 and C6 glioma cells when compared to that of the free drugs in solution and unmodified nanoparticles with entrapped drugs (Carroll, Bhatia et al. 2010; Xie, Lei et al. 2010; Geldenhuys, Mbimba et al. 2011; Guo, Gao et al. 2011; Kulkarni and Feng 2011; Li, Peng et al. 2011). Besides the cell viability, IC_{50}, the concentration of the drug required to kill 50% of the incubated cells over a fixed time period, was employed to quantify and evaluate the cytotoxicity of NPs loaded with chemotherapeutic drugs, and their therapeutic efficiency. The lowest IC_{50} (1.63 μg/ml) for surfactant coated NPs with entrapped docetaxel was achieved with the F68-PLGA NPs (196 nm) after 24 h in C6 glioma cell lines, which was 94.30% more efficient than docetaxel (Kulkarni and Feng 2011). AP-PEG-PLGA with entrapped paclitaxel NPs (156 nm)

showed 2-4 times lower IC_{50} than unmodified NPs and free drug (Guo, Gao et al. 2011). Glutathione-coated PEG-PLGA NPs (237 nm) with entrapped paclitaxel showed significantly higher therapeutic efficiency than uncoated NPs and paclitaxel solution. Tubulin immunofluorescent and western blotting studies also confirmed the enhanced therapeutic efficacy of paclitaxel entrapped glutathione-coated NPs (Geldenhuys, Mbimba et al. 2011).

2.3.2. *In vivo* studies

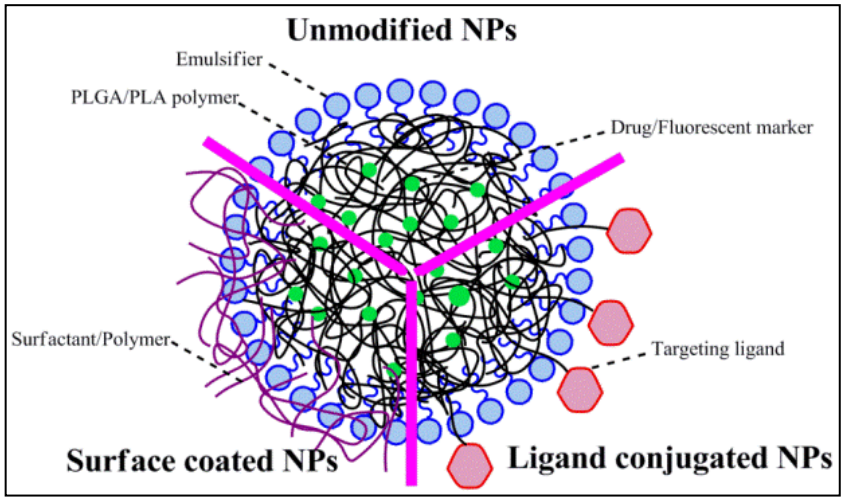

Figure 2.1 Schematic of three categories of PLGA/PLA NPs. Three types of PLGA/PLA NPs are discussed in this review: unmodified NPs, surface coated NPs and ligand conjugated NPs.

In vivo studies were conducted in rats or mice after administration (oral, carotid artery, or intravenous) of the nanoparticles. Several experiments including brain uptake quantification, confocal laser scanning microscopy, behavior studies, therapeutic efficacy of drugs and *in vivo* toxicity were carried out. The % brain uptake was calculated when the results were not reported and expressed as percentage of dose administered per animal, and data was plotted over a 24 hr time span (Lu, Wan et al. 2007; Rao, Reddy et al. 2008; Ren, Xu et al. 2009; Gan and Feng 2010; Tosi, Vergoni et al. 2010; Hu, Shi et al. 2011; Kulkarni and Feng 2011; Mittal, Carswell et al.

2011; Tahara, Miyazaki et al. 2011; Tsai, Chien et al. 2011). In all cases, the brain weights of rat and mice used to convert % dose/g reported by some authors to % dose were 2 g and 400 mg, respectively (Rosen GD 2000). NP types were divided into three categories: unmodified PLGA/PLA NPs, surface-coated NPs, and ligand-conjugated NPs (Figure 2.1). Brain uptake of unmodified PLGA/PLA NPs which were the control group in most cases, was important to confirm the safety of PLGA/PLA NPs. After synthesis of PLGA/PLA NPs, surfactants such as polysorbate 80 and polymers such as TMC could be coated on the surface of NPs to enhance brain uptake; this was for the second category "surface coated" NPs. Specific ligands which interact with surface receptors on brain endothelial cells could also be covalently linked to NPs and thus provide a brain targeted delivery; the third category: targeting ligand conjugated NPs. Polyethylene glycol (PEG), a hydrophilic polymer was commonly used to improve brain delivery. PEG-containing NPs were proved to have advantages such as stability, prolonged blood circulation time, reduced liver distribution and enhanced brain uptake (Chen and Liu 2011). In this review, PEGylated NPs PEG-PLGA and PEG-PLA were reported in 10 papers (Lu, Wan et al. 2007; Ren, Xu et al. 2009; Carroll, Bhatia et al. 2010; Parikh, Bommana et al. 2010; Chen, Hsieh et al. 2011; Geldenhuys, Mbimba et al. 2011; Guo, Gao et al. 2011; Hu, Shi et al. 2011; Jain, Chasoo et al. 2011; Li, Peng et al. 2011), and are included in the discussion.

2.3.2.1. Unmodified PLGA/PLA NPs

Brain uptake of PLGA/PLA nanoparticles (100-300 nm) were tested at different doses, ranging between 0.02 to 5.25 mg/animal, by quantifying concentration of entrapped drug (Rao, Reddy et al. 2008; Mittal, Carswell et al. 2011; Tsai, Chien et al. 2011) or fluorescent marker (Lu, Wan et al. 2007; Gan and Feng 2010; Tosi, Vergoni et al. 2010; Hu, Shi et al. 2011; Kulkarni and Feng 2011; Tahara, Miyazaki et al. 2011) after administration to rats (Gan and

Feng 2010; Tosi, Vergoni et al. 2010; Kulkarni and Feng 2011; Mittal, Carswell et al. 2011; Tahara, Miyazaki et al. 2011; Tsai, Chien et al. 2011) or mice (Lu, Wan et al. 2007; Rao, Reddy et al. 2008; Hu, Shi et al. 2011) (Figure 2.2). In all cases, the percentage of dose administered that was transported to the CNS was below 4%, and the majority of the studies (7 out of 9 reported in this review) showed percentages lower than 1%. The highest brain uptake (4%) was achieved 1 h after carotid artery administration of PLGA-NPs (200 nm) at a dose of 5 mg with coumarin 6 as an entrapped fluorescent marker (Tahara, Miyazaki et al. 2011). Carotid artery administration was proven to be more effective than intravenous administration for brain delivery as expected, since NPs could be transported directly to the brain after carotid artery administration (Tahara, Miyazaki et al. 2011). Oral administered PLGA NPs (134 nm) could only reach the brain at a 0.09% of the initial dose 24 h after administration (Mittal, Carswell et al. 2011). Curcumin-loaded PLGA NPs (163 nm) were found to have the lowest brain uptake (about 0.02%) according to quantification of drug level in the brain 1 hr after intravenous administration (Tsai, Chien et al. 2011). In the cases which measured level of entrapped drug were used to determine brain uptake of NPs, brain uptakes of NPs was less than 0.17% (Mittal, Carswell et al. 2011; Tsai, Chien et al. 2011). However, the study that employed PLA NPs loaded with ^{3}H-ritonavir, a radioactive labeled drug (300 nm) indicated a higher % (0.6-1.7% initial dose) reached the brain 24 h post administration (Rao, Reddy et al. 2008). Considering the potential degradation of drugs *in vivo* and the sensitivity of the equipment or method used to measure the concentration of drugs, the lower dose of NPs detected in the brain was expected when the method of detection was based on entrapped unmodified drug versus radiolabeled drug.

Three papers claimed there was no evidence showing that unmodified NPs crossed the BBB by detecting fluorescence in the brain (Sun, Xie et al. 2004; Costantino, Gandolfi et al.

2005; Wang, Wang et al. 2010). Two studies reported low intensity of a fluorescent probe loaded in unmodified nanoparticles after administration in the brain (Parikh, Bommana et al. 2010; Geldenhuys, Mbimba et al. 2011). In most cases (11 out of 14 papers), unmodified PLGA/PLA NPs were found to cross the BBB at a relatively low percentage even after i.v. administration of a high NP dose (5 mg/animal). Regardless of the emulsifiers used to prepare nanoparticles, different administration methods and quantification methods (drug or fluorescent marker), the uptake was always less than 4 % and in most cases lower than 1 %.

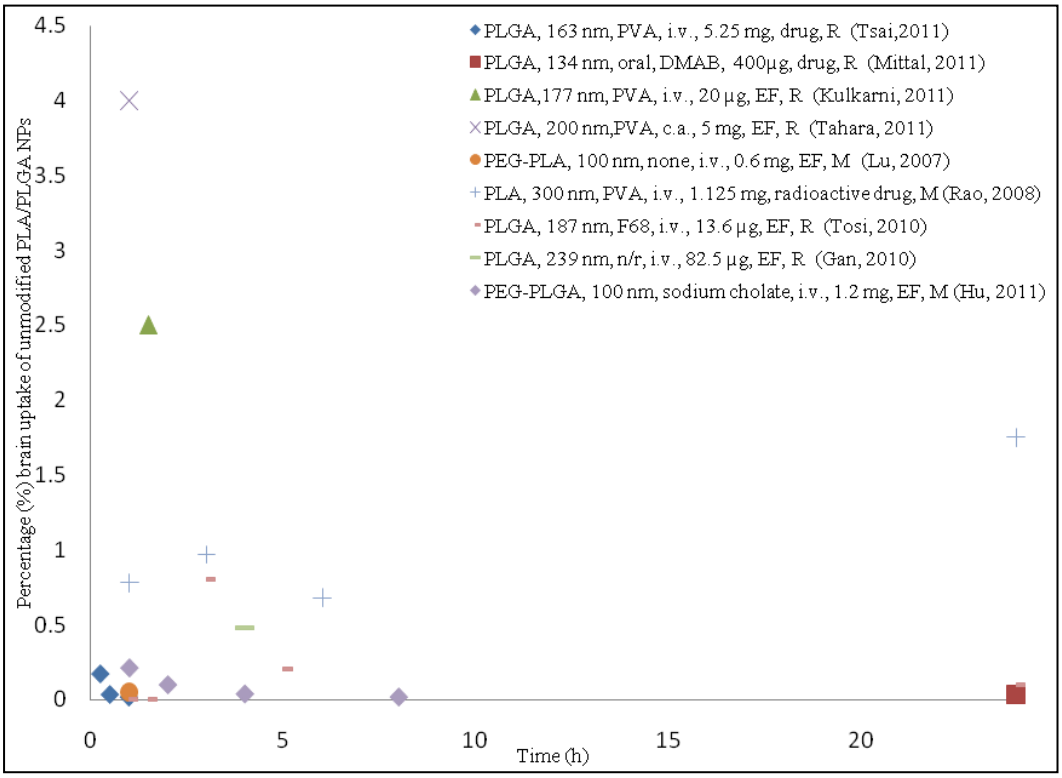

Figure 2.2. Percentage (%) unmodifided NPs brain uptake of dose administered versus time.The legend information is presented in the following order: NP type, size, emulsifier (n/r- not reported), administration (i.v.-intravenous administration; c.a.-carotid artery), dose, quantification method (EF- entrapped fluorescence marker) and animal model (M-mice; R-rats).

Table 2.2 Percentage (%) brain uptake of surface coated PLGA/PLA NPs. Size (nm), administration, dose (μg/dose), quantification method, animal model, and percentage brain uptake are listed.

						Percentage brain uptake (%)						
NPs	Size (nm)	Admin.	Dose (μg/ml)	Quant.	Animal model	0.5h	1h	1.5h	3h	6h	12h	24h
1% T80-PLGA NPs (Mittal, Carswell et al. 2011)	138	Oral	100/200/400	Drug	Rats							0.078/0.052/0.037
4% T80-PLGA NPs (Mittal, Carswell et al. 2011)	157	Oral	100/200/400									0.166/0.112/0.088
1% T80-PLGA NPs (Mittal, Carswell et al. 2011)	138	i.v.	100									0.38
TPGS-PLGA NPs (Kulkarni and Feng 2011)	165	i.v.	20	EF	Rats			4.2				
T80-PLGA NPs (Kulkarni and Feng 2011)	194	i.v.	20					4.3				
F127-PGLA NPs (Kulkarni and Feng 2011)	188	i.v.	20					5.5				
F68-PLGA NPs (Kulkarni and Feng 2011)	196	i.v.	20					6.2				
CS-PLGA NPs (Tahara, Miyazaki et al. 2011)	396	c.a.	5000/10000/25000	EF	Rats		16/7.6/4.0					
T80-PLGA NPs (Tahara, Miyazaki et al. 2011)	231	c.a.	5000/10000/25000				6.4/6/4.6					
F68-PLGA NPs (Tahara, Miyazaki et al. 2011)	252	c.a.	5000/10000/25000				3.2/3.4/1.5					
T80-PLA-PEG NPs (Ren, Xu et al. 2009)	120	i.v.	150	Drug	Mice	3.52	11.9		13.5	15.7	17.3	11.9
TPGS-PLGA NPs (Gan and Feng 2010)	121	i.v.	N/A	EF	Rats		1					

Abbreviation: Admin.-administration; c.a.-carotid artery; CS-chitosan; EF-entrapped fluorescence marker; F127-poloxamer 407; F68-poloxamer 188; i.v.-intravenous; N/A-not available; Quant.-quantification method; T80-Tween 80/polysorbate 80; TPGS- D-α-tocopheryl polyethylene glycol 1000 succinate

2.3.2.2. Surface coated nanoparticles

Brain uptake:

Besides changing the surfactant used in NP synthesis, the surface of the NP can bemodified by the addition of other compounds, such as chitosan or PEG, in an attempt to improve brain NP uptake (Table 2). TPGS has been successfully used to prepare NPs, and It was found that TPGS was a more effective and safer emulsifier than PVA, and could improve adsorption of NPS by the gastrointestinal tract to improve bioavailability of the delivered drug (Jalali, Moztarzadeh et al. 2011). TPGS-PLGA NPs demonstrated modest increase of brain uptake (1%) 1h after i.v. administration compared to PVA-PLGA NPs (0.5%) (Gan and Feng 2010). Brain delivery of modified PLGA/PLA NPs was improved when positively charged compared to unmodified NPs. The highest brain uptake (16%) was achieved with CS-PLGA NPs (396 nm) after carotid artery administration for 1 h (Tahara, Miyazaki et al. 2011). The same group demonstrated that although CS-PLGA NPs (396 nm) reached the highest brain uptake, NPs were only observed on vascular endothelial cells and considering that CS could open intracellular tight juctions, it was concluded that CS-PLGA NPs might not be a good brain delivery system (Tahara, Miyazaki et al. 2011). Carotid artery administration was proven to be the most efficient for improved brain uptake, followed by intravenous administration, and oral delivery (Mittal, Carswell et al. 2011; Tahara, Miyazaki et al. 2011).

The amount of NPs transported to the brain (μg/g tissue) reported in the literature increased as the increase of dose administered while percentage (%) of dose calculated by the author did not show a dose-dependent increase. For example, F68-PLGA NPs remaining in the brain 60 min after NP administration via carotid artery was 0.08, 0.17 and 0.19 mg/g tissue at injected doses of 5, 10 and 25 mg/ml respectively which corresponded to 3.2, 3.4 and 1.5%.

Among all the surfactants used to enhance brain delivery, T80 was the most commonly used. T80 coating could adsorb apolipoprotein E/B from the blood on the nanoparticle surface and thus provided a receptor-mediated active endocytosis of the NPs (Wohlfart, Gelperina et al. 2011). For i.v. administration of surfactant coated PLGA NPs, F68 was confirmed to be a better targeting agent than T80 (Kreuter 2001; Gelperina, Maksimenko et al. 2010). Kulkarni, S.A. and S.S. Feng compared the brain uptake of F68, F127 and T80 coated PLGA NPs, and found that F68-PLGA NPs (252 nm) reached the highest brain distribution (6.2%) via i.v. injection (Kulkarni and Feng 2011). When comparing the anti-tumor effect of drug loaded in T80 and F68 coated PLGA NPs, Gelperina, S. *et al* found as well that F68-coated NPs (168 nm) had a higher therepeutical efficacy than T80-PLGA NPs after i.v. administration (Gelperina, Maksimenko et al. 2010). Kreuter J. and Gelperina S. demonstrated that F68 appeared to be a very promising coating agent for both PLGA and PBCA NPs, while T80 was only effective in the case of PBCA NPs comparing Kulkarni's finding (Kreuter and Gelperina 2008). However, c.a. administration showed a different delivery trend between T80 and F68 coated NPs: T80-PLGA NPs (231 nm) proved to be delivered at a higher percentage (6%) than F68-PLGA NPs (252 nm)(3%) (Tahara, Miyazaki et al. 2011). For the same surfactant and same administration, the more surfactant coated on the nanoparticle surface, the higher the brain nanoparticles uptake (Mittal, Carswell et al. 2011).

Location of NPs in the brain:

Fluorescent microscopy studies focused on identifying the location of the NPs in the brain revealed that T80-PLGA NPs with entrapped coumarin-6 (215 nm) and very small amount of F68-PLGA NPs (252 nm) distributed in the parenchyma (Tahara, Miyazaki et al. 2011), and

highTMC-PLGA loaded with coumarin-6 (136 nm) NPs were found in the cortex, paracoele, the third ventricle and choroid plexus epithelium (Wang, Wang et al. 2010).

Therapeutic efficacy:

Therapeutic efficacy of certain drugs was evaluated in different animal models. T80-PLGA NPs with entrapped estradiol (150 nm) were administered to an ovariectomized (OVX) rat model of Alzheimer's disease (AD). Behavior studies and neuropathological examination results indicated enhanced oral delivery of estradiol to rat brain with the NPs (Mittal, Carswell et al. 2011). Another AD animal model APP/PS1 double transgenic mice was exposed to NPs introduced to investigate the delivery efficacy of Q_{10} loaded in TMC-PLGA NPs (146 nm) to the brain; behavior, senil plaque staining , and biochemical parameters were studied. Therapeutic efficacy of the drug was greatly enhanced when it was entrapped in TMC-PLGA NPs (Wang, Wang et al. 2010). Anti-tumor effect of T80- and F68-coated NPs with entrapped doxorubicin was demonstrated in tumor-bearing rats, and the analgesic effect of loperamide loaded T80- and F68-coated NPs was confirmed in mice. The maximal possible effect (% MPE) was determinied to evaluate the analgesic effect. F68-PLGA loaded with loperamide provided 80% MPE after 15 min and 70% MPE for at least 60 min after administration while T80-PLGA NPS with entrapped loperamide reached 80% MPE and only 40% MPE after 60 min. Free loperamide showed little antinociceptive effect (Gelperina, Maksimenko et al. 2010). *In vivo* antinociception studies of P188-, P80-coated and PLGA-PEG-PLGA NPs with entrapped loperamide were conducted after i.v. administration at a dose of 0.5 mg/kg. The results of hot-plate test and formalin tests showed P188-coated NPs had the best antinociceptive efficacy (Chen, Hsieh et al. 2011). P188 was proved to be a better brain targeting agent for PLGA NPs than P80 after i.v. administration in

several reported studies (Kreuter and Gelperina 2008; Gelperina, Maksimenko et al. 2010; Chen, Hsieh et al. 2011; Kulkarni and Feng 2011).

2.3.2.3. Targeting ligand conjugated nanoparticles

Brain uptake:

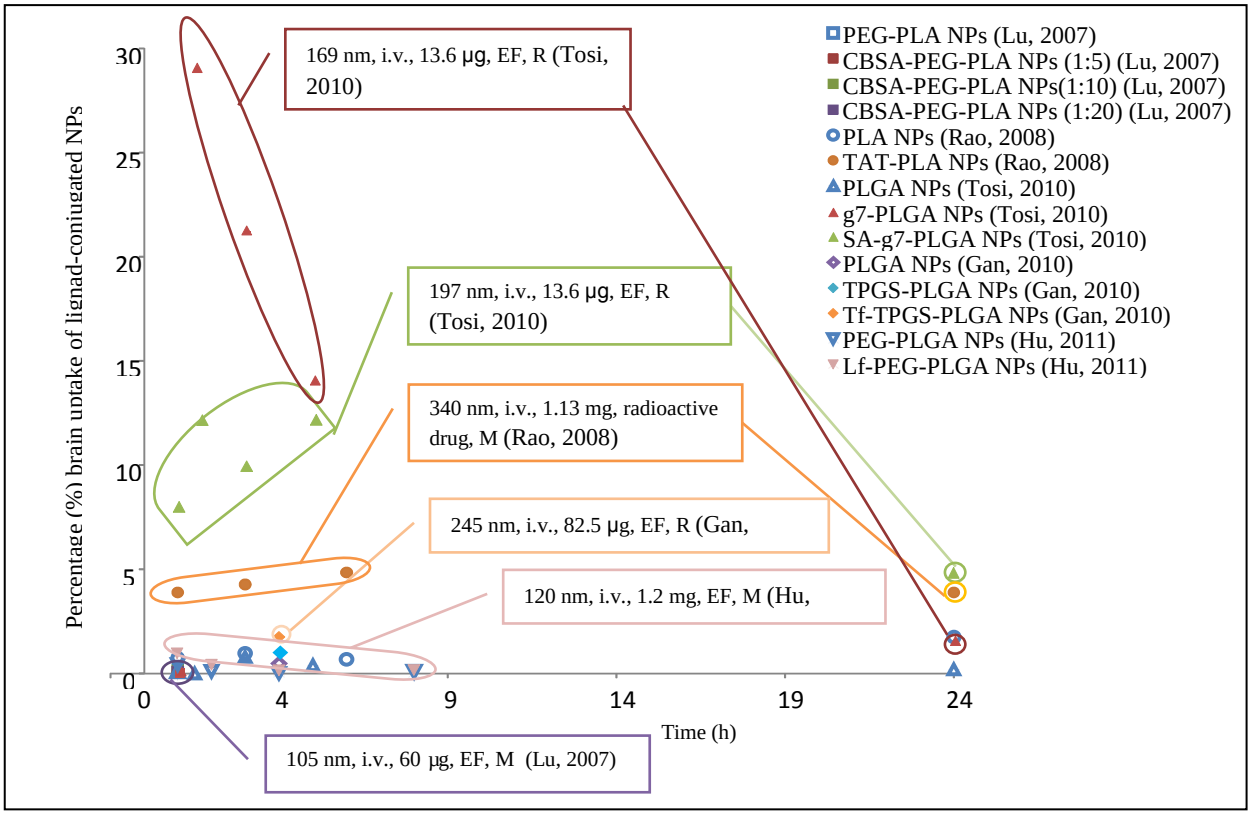

Fig.3. Percentage (%) ligand-conjugated NPs brain uptake of dose administered versus time. The marked information is presented in the following order: size, administration (I.v.- intravenous administration), dose, quantification method (EF- entrapped fluorescence marker) and animal model (M- mice; R-rats).

Brain delivery of specific ligand-conjugated nanoparticles was greatly enhanced compared to that of unconjugated nanoparticles (Figure 2.2). The percentage of NP dose in the brain reached as high as 29% for g7-PLGA NPs (169 nm) at 1.5 h after i.v. administration at a dose of 13.6 µg in rats (Tosi, Vergoni et al. 2010), which is the highest brain uptake reported in the literature. Uptake of g7-PLGA NPs was found to be receptor-mediated endocytosis. The

lowest value for % dose NPs in the brain was reported for CBSA-conjugated nanoparticles: the uptake process was confirmed to be absorptive mediated transcytosis, and the uptake efficiency reached 0.3%/g brain, 2.3-fold more than that of unmodified NPs (Lu, Wan et al. 2007). Different peptides functionalized nanoparticles were constructed to activate receptor-mediated endocytosis, which could enhance brain-targeted delivery. Four synthetic opioid peptides (Costantino, Gandolfi et al. 2005), a 120 amino-acid-peptide screened from *in vivo* phage display (Li, Peng et al. 2011), trans-activating transcriptor (TAT) peptide (Rao, Reddy et al. 2008) and a simil-opioid peptide (g7) (Tosi, Vergoni et al. 2010) were successfully conjugated to PLGA/PLA NPs and the conjugation was showed to improve brain delivery of nano-carriers. Transferrin (Tf) is another commonly used ligand for targeted brain delivery as Tf was proven to interact with corresponding receptor in the brain to induce receptor-mediated transcytosis (Chang, Jallouli et al. 2009; Gan and Feng 2010; Jain, Chasoo et al. 2011; Kuo, Lin et al. 2011). Other specific ligands conjugated to successfully increase brain uptake included transferring antibody (Carroll, Bhatia et al. 2010), sialic acid residue (Tosi, Vergoni et al. 2010), lactoferrin (Hu, Shi et al. 2011), poly-(γ-glutamic acid) (Kuo and Yu 2011), and DNA aptamer (Guo, Gao et al. 2011).

In all cases, targeting ligand succeeded to provide a receptor-mediated endocytosis of surface functionalized NPs, and brain uptake of modified NPs greatly increased (the highest one reached 29%) when compared to unconjugated NPs (<1%) after i.v. administration.

Location of NPs in the brain:

Fluorescence studies on the location of NPs in the brain demonstrated that three peptide-derived NPs (162-211 nm) with covalently linked fluorescent probe (Costantino, Gandolfi et al. 2005), TAT-PLA NPs with coumarin-6 as fluorescent marker (340 nm) (Rao, Reddy et al. 2008), tetramethylrhodamine-linked SA-g7-PLGA NPs (154 nm) (Tosi, Vergoni et al. 2010) and Tf-

PEG-PLGA (121 nm) with entrapped rhodamine 6G (Jain, Chasoo et al. 2011) all reached cerebral parenchyma, which proved the ability of targeted NPs to cross the BBB.

Therapeutic efficacy:

Besides direct-observation of nanoparticles in the brain, several experiments were performed to prove enhanced brain delivery of the drug in disease animal models. The antinociceptive effects of SA-g7-PLGA NPs with entrapped loperamide was tested and MPE values maintained at 30-50% for 15h while the effect of loperamide loaded g7-PLGA NPs was 57% for only 5h after administration (Tosi, Vergoni et al. 2010).Therapeutic effect of urocortin (UCN) loaded in Lf-NPs on 6-OHDA rat model of Parkinson's disease was investigated. The behavior, immunohistochemistry and transmitter contents of the brain results confirmed the improved efficiency of UCN loaded Lf-NPs to attenuate the striatum lesion compared to the control group after i.v. administration (Hu, Shi et al. 2011). *In vivo* anti-tumor efficacy was carried out on rats bearing glioma xenografts and rats bearing intracranial C6 gliomas. After intravenous administration of paclitaxel (PTX) loaded aptamer-conjugated NPs (Ap-PTX-NP), tumor size, body weight and survival time were recorded to evaluate the anti-glioma efficacy. The average tumor inhibition of Ap-PTX-NP and free Taxol for tumor volume was 81.6 and 68.6%, and for tumor weight was 79.3 and 48.2%. The survival time of Ap-PTX-NP treated rats bearing glioma was 7 days longer than PTX treated group and 13 days longer than saline treated group (Guo, Gao et al. 2011). In all cases, therapeutic effect of the drug was greatly improved after the drug was incorporated into surface-modified NPs.

2.4. Conclusions

In recent years, polymeric nanoparticles were well investigated and the technology has developed at a rapid pace. PLGA/PLA nanoparticles (100-300 nm) have been proven as potential

carriers for drug delivery across the BBB with advantages of both enhanced drug efficiency and safety. NPs offer superior alternatives to oral and i.v. administration of free drugs that cannot otherwise transport across the BBB, which is definitely a significant breakthrough for brain delivery.

For *in vitro* studies, cytotoxicity, cellular uptake, mechanism of uptake, and therapeutic efficiency were investigated. *In vitro* toxicity studies showed no toxicity of PLGA NPs for doses of 0.075 to 8000 μg/ml. The cellular uptake efficiency was greatly improved with the modification of PLGA NPs. The permeation percentages of loperamide entrapped F68- and T80 surface modified PLGA NPs (21% and 14.5%) in rat brain endothelial cell line and C6 co-cultures were significantly increased compared to loperamide loaded unmodified PLGA NPs (4.5%) and free loperamide (0.4%) (Chen, Hsieh et al. 2011). A significant decrease in cell viability of glioma cells treated with drug loaded modified NPs was proven, supporting the improved uptake and efficacy of drugs loaded in PLGA NPs. Endocytosis mechanisms were unveiled for specific systems. For example, the uptake of Lf-TPGS-PLA NPs was proved to be clathrin mediated endocytosis and endocytosis of Tf-PLGA NPs was confirmed as caveolae mediated endocytosis.

In vivo biodistribution studies were conducted in either rats or mice after NP administration (oral, carotid artery and i.v.), to determine brain uptake of various NPs. PLGA/PLA NPs showed very low (<1%) brain uptake without modification, which alleviated the concern that unmodified PLGA/PLA NPs used for applications other than CNS delivery cross the BBB. Surface modifications of PLGA NPs such surface-coating and the addition of targeting ligands improved brain delivery of drugs compared with unmodified PLGA NPs. Ligands, covalently linked to the surface of the particles improved brain uptake of NP the most.

The highest brain uptake was achieved by g7-PLGA NPs (169 nm) (14% /g tissue) which were characterized as instant high brain delivery with a short retention time (Tosi, Vergoni et al. 2010). The presence of modified PLGA/PLA NPs within rats/mice brain parenchyma after systemic administration was confirmed by microscopy studies. Besides brain uptake, behavior studies of treated animals and therapeutic efficacy studies after NP administration supported the enhancement of brain delivery of modified PLGA NPs as compared to unmodified NPs or free drug.

It was evident that *in vitro* and *in vivo* information on delivery of drugs with PLGA/PLA NPs (100-300 nm) to CNS was available and sufficient to confirm the enhanced brain uptake and therapeutic efficacy of certain drugs entrapped in PLGA NPs. These studies suggest that multiple strategies could be applied to construct an optimum brain delivery system based on PLGA. However, the literature is lacking in several aspects. First, *in vivo* long-term toxicity studies of modified NPs including their effects on the brain were not found in the literature and should be evaluated. It is important to assess the safety and potential risks of brain-targeted PLGA/PLA NPs, especially for systems that are associated with highly improved brain uptake. Second, the amount of data is not sufficient in the literature to understand NP brain uptake as a function of concentration of the NPs administered, or their properties (size, charge). It is unclear if brain uptake of NPs is concentration-dependent, and if saturation would be reached as the dose administered was increased. Size appears to affect uptake, with small NP size being more favorable, but it is hard to compare uptake across studies when other parameters (charge, method of administration or detection) are not uniform. Brain uptake is also enhanced for NPs that are more hydrophobic and if they carry a positive charge. However, because of the lack of systematic studies, comparisons between systems reported in the literature so far are not possible.

Lastly, information on the location of NPs modified by different strategies in the brain after they cross the BBB is not readily available, as well. Location of the NPs within the brain may affect the efficacy of the entrapped drug.

It is clear that even though much is yet to be done to understand brain uptake of polymeric NPs, and their impact on drug efficacy and safety, the design of safe nano carriers for improved drug delivery to certain location in the brain, and an enhanced drug efficacy and low toxicity is certainly possible. Design of such targeted delivery systems to the CNS will aid in treatment of CNS diseases.

2.5. References

Begley, D. J. (2004). "Delivery of therapeutic agents to the central nervous system: the problems and the possibilities." Pharmacol Ther **104**(1): 29-45.

Carroll, R. T., D. Bhatia, et al. (2010). "Brain-targeted delivery of Tempol-loaded nanoparticles for neurological disorders." J Drug Target **18**(9): 665-674.

Chang, J., Y. Jallouli, et al. (2009). "Characterization of endocytosis of transferrin-coated PLGA nanoparticles by the blood-brain barrier." Int J Pharm **379**(2): 285-292.

Chen, Y. and L. Liu (2011). "Modern methods for delivery of drugs across the blood-brain barrier." Adv Drug Deliv Rev.

Chen, Y. C., W. Y. Hsieh, et al. (2011). "Effects of surface modification of PLGA-PEG-PLGA nanoparticles on loperamide delivery efficiency across the blood-brain barrier." J Biomater Appl.

Costantino, L. and D. Boraschi (2012). "Is there a clinical future for polymeric nanoparticles as brain-targeting drug delivery agents?" Drug Discov Today **17**(7-8): 367-378.

Costantino, L., F. Gandolfi, et al. (2005). "Peptide-derivatized biodegradable nanoparticles able to cross the blood-brain barrier." J Control Release **108**(1): 84-96.

Gan, C. W. and S. S. Feng (2010). "Transferrin-conjugated nanoparticles of Poly(lactide)-D-alpha-Tocopheryl polyethylene glycol succinate diblock copolymer for targeted drug delivery across the blood-brain barrier." Biomaterials **31**(30): 7748-7757.

Gao, K. and X. Jiang (2006). "Influence of particle size on transport of methotrexate across blood brain barrier by polysorbate 80-coated polybutylcyanoacrylate nanoparticles." Int J Pharm **310**(1-2): 213-219.

Geldenhuys, W., T. Mbimba, et al. (2011). "Brain-targeted delivery of paclitaxel using glutathione-coated nanoparticles for brain cancers." Journal of Drug Targeting **19**(9): 837-845.

Gelperina, S., O. Maksimenko, et al. (2010). "Drug delivery to the brain using surfactant-coated poly(lactide-co-glycolide) nanoparticles: influence of the formulation parameters." Eur J Pharm Biopharm **74**(2): 157-163.

Grabrucker, A. M., C. C. Garner, et al. (2011). "Development of novel Zn2+ loaded nanoparticles designed for cell-type targeted drug release in CNS neurons: *in vitro* evidences." PLoS One **6**(3): e17851.

Guo, J., X. Gao, et al. (2011). "Aptamer-functionalized PEG-PLGA nanoparticles for enhanced anti-glioma drug delivery." Biomaterials **32**(31): 8010-8020.

Hu, K., Y. Shi, et al. (2011). "Lactoferrin conjugated PEG-PLGA nanoparticles for brain delivery: preparation, characterization and efficacy in Parkinson's disease." Int J Pharm **415**(1-2): 273-283.

Jain, A., G. Chasoo, et al. (2011). "Transferrin-appended PEGylated nanoparticles for temozolomide delivery to brain: *in vitro* characterisation." J Microencapsul **28**(1): 21-28.

Jalali, N., F. Moztarzadeh, et al. (2011). "Surface modification of poly(lactide-co-glycolide) nanoparticles by D-alpha-tocopheryl polyethylene glycol 1000 succinate as potential carrier for the delivery of drugs to the brain." Colloids and Surfaces a-Physicochemical and Engineering Aspects **392**(1): 335-342.

Jaruszewski, K. M., S. Ramakrishnan, et al. (2012). "Chitosan enhances the stability and targeting of immuno-nanovehicles to cerebro-vascular deposits of Alzheimer's disease amyloid protein." Nanomedicine-Nanotechnology Biology and Medicine **8**(2): 250-260.

Kreuter, J. (2001). "Nanoparticulate systems for brain delivery of drugs." Adv Drug Deliv Rev **47**(1): 65-81.

Kreuter, J. and S. Gelperina (2008). "Use of nanoparticles for cerebral cancer." Tumori **94**(2): 271-277.

Kulkarni, S. A. and S. S. Feng (2011). "Effects of surface modification on delivery efficiency of biodegradable nanoparticles across the blood-brain barrier." Nanomedicine **6**(2): 377-394.

Kuo, Y. C., P. I. Lin, et al. (2011). "Targeting nevirapine delivery across human brain microvascular endothelial cells using transferrin-grafted poly(lactide-co-glycolide) nanoparticles." Nanomedicine (Lond) **6**(6): 1011-1026.

Kuo, Y. C. and H. W. Yu (2011). "Transport of saquinavir across human brain-microvascular endothelial cells by poly(lactide-co-glycolide) nanoparticles with surface poly-(gamma-glutamic acid)." International Journal of Pharmaceutics **416**(1): 365-375.

Li, H. M., R. R. Peng, et al. (2011). "HIV Incidence among Men Who Have Sex with Men in China: A Meta-Analysis of Published Studies." PLoS One **6**(8): e23431.

Lu, W., J. Wan, et al. (2007). "Brain delivery property and accelerated blood clearance of cationic albumin conjugated pegylated nanoparticle." J Control Release **118**(1): 38-53.

Mathew, A., T. Fukuda, et al. (2012). "Curcumin loaded-PLGA nanoparticles conjugated with Tet-1 peptide for potential use in Alzheimer's disease." PLoS One **7**(3): e32616.

Mistry, A., S. Stolnik, et al. (2009). "Nanoparticles for direct nose-to-brain delivery of drugs." Int J Pharm **379**(1): 146-157.

Mittal, G., H. Carswell, et al. (2011). "Development and evaluation of polymer nanoparticles for oral delivery of estradiol to rat brain in a model of Alzheimer's pathology." J Control Release **150**(2): 220-228.

Olivier, J. C. (2005). "Drug transport to brain with targeted nanoparticles." NeuroRx **2**(1): 108-119.

Parikh, T., M. M. Bommana, et al. (2010). "Efficacy of surface charge in targeting pegylated nanoparticles of sulpiride to the brain." Eur J Pharm Biopharm **74**(3): 442-450.

Park, K. (2008). "Trojan monocytes for improved drug delivery to the brain." J Control Release **132**(2): 75.

Patel, T., J. Zhou, et al. (2011). "Polymeric nanoparticles for drug delivery to the central nervous system." Adv Drug Deliv Rev.

Rao, K. S., M. K. Reddy, et al. (2008). "TAT-conjugated nanoparticles for the CNS delivery of anti-HIV drugs." Biomaterials **29**(33): 4429-4438.

Ren, T. B., N. Xu, et al. (2009). "Preparation and Therapeutic Efficacy of Polysorbate-80-Coated Amphotericin B/PLA-b-PEG Nanoparticles." Journal of Biomaterials Science-Polymer Edition **20**(10): 1369-1380.

Rip, J., G. J. Schenk, et al. (2009). "Differential receptor-mediated drug targeting to the diseased brain." Expert Opin Drug Deliv **6**(3): 227-237.

Roney, C., P. Kulkarni, et al. (2005). "Targeted nanoparticles for drug delivery through the blood-brain barrier for Alzheimer's disease." J Control Release **108**(2-3): 193-214.

Rosen GD, W. A., Capra JA, Connolly MT, Cruz B, Lu L, Airey DC, Kulkarni K, Williams RW (2000). The Mouse Brain Library @ www.mbl.org., Int Mouse Genome Conference 14: 166.

Silva, G. A. (2007). "Nanotechnology approaches for drug and small molecule delivery across the blood brain barrier." Surg Neurol **67**(2): 113-116.

Sun, W. Q., C. S. Xie, et al. (2004). "Specific role of polysorbate 80 coating on the targeting of nanoparticles to the brain." Biomaterials **25**(15): 3065-3071.

Tahara, K., Y. Miyazaki, et al. (2011). "Brain targeting with surface-modified poly(D,L-lactic-co-glycolic acid) nanoparticles delivered via carotid artery administration." Eur J Pharm Biopharm **77**(1): 84-88.

Tosi, G., A. V. Vergoni, et al. (2010). "Sialic acid and glycopeptides conjugated PLGA nanoparticles for central nervous system targeting: *In vivo* pharmacological evidence and biodistribution." J Control Release **145**(1): 49-57.

Tsai, Y. M., C. F. Chien, et al. (2011). "Curcumin and its nano-formulation: the kinetics of tissue distribution and blood-brain barrier penetration." Int J Pharm **416**(1): 331-338.

Wang, Z. H., Z. Y. Wang, et al. (2010). "Trimethylated chitosan-conjugated PLGA nanoparticles for the delivery of drugs to the brain." Biomaterials **31**(5): 908-915.

Wohlfart, S., S. Gelperina, et al. (2011). "Transport of drugs across the blood-brain barrier by nanoparticles." J Control Release.

Xie, J., C. Lei, et al. (2010). "Nanoparticulate formulations for paclitaxel delivery across MDCK cell monolayer." Curr Pharm Des **16**(21): 2331-2340.

CHAPTER 3 WHEAT GERM AGGLUTININ CONJUGATED PLGA NANOPARTICLES FOR ENHANCED NEURON DELIVERY IN *C.ELEGANS*

3.1. Introduction

Parkinson's disease (PD), a neurodegenerative disorder of the central nervous system, is the second most common neurodegenerative disease after Alzheimer's disease (Alves, Forsaa et al. 2008). PD impairs motor skills, cognitive processes, and other body functions (Wolters 2009). According to current studies, nigral dopamine deficiency-related dysfunction of the basal ganglia is regarded as the cause of the major PD symptoms (Wolters 2009).

As dopamine cannot across Blood Brain Barrier (BBB), current treatments are effective at managing motor symptoms through the use of levodopa (L-DOPA), dopamine agonists and Monoamine oxidase B (MAO-B) inhibitors (Schapira 2005). However, delivery of these drugs is quite poor. For instance, only 5-10% of L-DOPA orally administered is able to cross the blood-brain barrier. The remaining is often metabolized to dopamine by enzymes, i.e. decarboxylases, in the stomach or blood, causing a wide variety of side effects, such as nausea, dyskinesias and stiffness(Factor 2008). Many severe side effects may be induced by the undesirable distribution of any antiparkinsonian drug in health tissues, including psychiatric distribution and dyskinesias(Ceravolo, Frosini et al. 2009). This greatly limits the maximum allowable dose of the drug.

To reduce the harmful side effects of the undesirable accumulation of drugs, improved delivery systems must be developed for treatment of PD. Among the advanced technology, nanotechnology appears promising in developing drug delivery systems of targeting and controlled-release characteristics beneficial for drug delivery such as L-DOPA(Linazasoro 2008). The advantages of nanoparticles as drug delivery systems include time controlled drug delivery,

reduced drug toxicity, improved bioavailability and enhanced therapeutic efficacy and biodistribution of the drug(Ravi Kumar 2000). Polymeric nanoparticles range in size from about 10-1000nm (Kreuter 2001), and can be modified with different ligands to create a smart targeting delivery system. For example, to further improve the delivery efficacy of L-DOPA; a targeted delivery system should be designed to enhance brain delivery of this drug. Wang's group synthesized trimethylated chitosan modified PLGA nanoparticles for the delivery of drugs to the brain, and showed that the conjugated nanoparticles were able to cross the blood brain barrier with low toxicity (Wang, Wang et al. 2010). Hu K's group developed lactoferrin conjugated polyethylene glycol-polylactide-polyglycolide (PEG-PLGA) nanoparticles which targeted mice brain 3 fold more than empty nanoparticles (Hu, Shi et al. 2011). Endocytosis of Transferring-coated PLGA nanoparticles by BBB endothelial cells was found 20-fold higher than that of blank PLGA nanoparticles(Chang, Jallouli et al. 2009).

Lectins have been conjugated with drugs to enhance drug absorption in the gastrointestinal tract or to target drug to a certain kind of cells including intestine cells, cancer cells and brain endothelial cells (Ratzinger, Wang et al. 2010). Chunxia Wang's group has designed wheat germ agglutinin-conjugated PLGA nanoparticles for enhanced intracellular delivery of paclitaxel to colon cancer cells. Conjugated PLGA nanoparticles demonstrated 1.67 fold in the Caco-2 (30% of uptake) and 1.48 fold HT-29 (40% of uptake) cells more than non-targeted nanoparticles (Wang, Ho et al. 2010). Xiaoling Gao *et al*. developed an enhanced delivery of vasoactive intestinal peptide with nanoparticles conjugated with wheat germ agglutinin (Gao, Wu et al. 2007). The delivery of incorporated vasoactive intestinal peptide by PLGA nanoparticles and WGA conjugated PLGA nanoparticles was greatly improved 3.5 to 4.7 folds and 5.6 to 7.7 folds respectively when compared to the free drug. Wen Z. *et al* conjugated

odorranalectin (OL) to PEG-PLGA nanoparticles to improve nose-to-brain drug delivery in the treatment of central neuron systems disorders(Wen, Yan et al. 2011).

Various lectins have been used as components of oral drug delivery systems including tomato lectin, peanut agglutinin and wheat germ agglutinin (WGA) (Gao, Wu et al. 2007). WGA comes from Triticum vulgaris, and shows a special affinity to N-Acetyl-glucosamine (GlcNAc) and sialic acid which are the major glycoproteins on the surface of most cells. WGA is regarded as a promising carrier for oral drugs because of its biochemical characteristics and non-toxic property(Irache, Durrer et al. 1994).

Several protocols have been developed to conjugate WGA with PLGA nanoparticles. Liu's group coupled WGA to PLGA nanoparticles by activating the hydroxyl group of poly (vinyl alcohol) (PVA) with glutaraldehyde (Liu, Wang et al. 2010). Another commonly used method is to activate the free carboxyl groups on the nanoparticle suface by carbodiimide reagents and then linking it with amino groups of WGA (Weissenbock, Wirth et al. 2004; Mo and Lim 2005; Yin, Chen et al. 2006). However, surface functionalization of nanoparticles could be hard to achieve as limited number of carboxyl groups is available and might be masked due to the presence of surface additives (Yin, Chen et al. 2006).Yin's group synthesized a novel WGA-PLGA conjugate by covalently linking the amine groups of WGA with the carbodiimide-activated carboxylic group of PLGA, and prepared nanoparticles with these conjugates (Yin, Chen et al. 2006).

Caenorhabditis elegans (*C.elegans*) is a model commonly used to study neuron drug delivery (Braungart, Gerlach et al. 2004; Nass, Merchant et al. 2008) as the hermaphroditic *C.elegans* organism contains only eight dopamine neurons, thereby largely simplifying a wide array of investigations (Nass, Hall et al. 2002). Worms that express the green fluorescent protein

(GFP) can be used when the *in vivo* visualization of cellular processes is necessary. Other advantages of using *C.elegans* in laboratory studies include a short generation time, and ease of growth (Wood 1988; Riddle 1997; Wintle and Van Tol 2001).

The hypothesis of this study was that WGA-conjugated PLGA nanoparticles will enhance targeted delivery of PLGA nanoparticles to the neurons of *C. elegans*. WGA conjugated PLGA nanoparticles were synthesized and characterized in terms of physical properties and conjugation efficiency. The ability of the nanoparticles to target the neurons and the effect of the nanoparticles on pumping rate, travel distance, size of *C. elegans*, as well as area and intensity of DAergic neurons were tested. Co-localization of DAergic neurons and PLGA-tWGA nanoparticles was demonstrated by fluorescent images.

3.2. Objectives

1. Synthesis of TRITC conjugated poly (lactide-co-glycolide) nanoparticles (PLGA-t NPs) and tWGA conjugated PLGA nanoparticles (PLGA-tWGA NPs) by emulsion evaporation method, with PVA as surfactant.
2. Charaterization of PLGA-t NPs and PLGA-tWGA NPs in terms of size, size distribution, zeta potential (DLS), morphology (TEM) and conjugation efficiency.
3. Analysis of the effect of tWGA, PLGA-t NPs and PLGA-tWGA NPs on pumping rate, size, and number, intensity and area of GFP-DAergic neurons with *C.elegans*.

3.3. Materials and methods

3.3.1. Chemicals and materials

PLGA 50:50 with an average molecular weight of 45 000–75 000, PVA with an average molecular weight of 30 000–70 000, 1-Ethyl-3-(3-dimethylaminopropyl)carbodiimide (EDC), N-hydroxysuccinimide (NHS), Ethylenediamine, Diethylether, Dimethyl sulfoxide (DMSO), Ethyl

Acetate, tetrahydrofuran (THF) and Ethanol were purchased from Sigma-alorich (St.louis, USA). TRITC was purchased from Thermoscientific (IL, USA). DCM was obtained from Mallinckwdt, chemicals (NJ, USA). TRITC-WGA and N-acetyl-glucosamine were acquired from Vector Laboratories, INC (CA, USA).

3.3.2. Preparation of TRITC-labeled PLGA conjugates

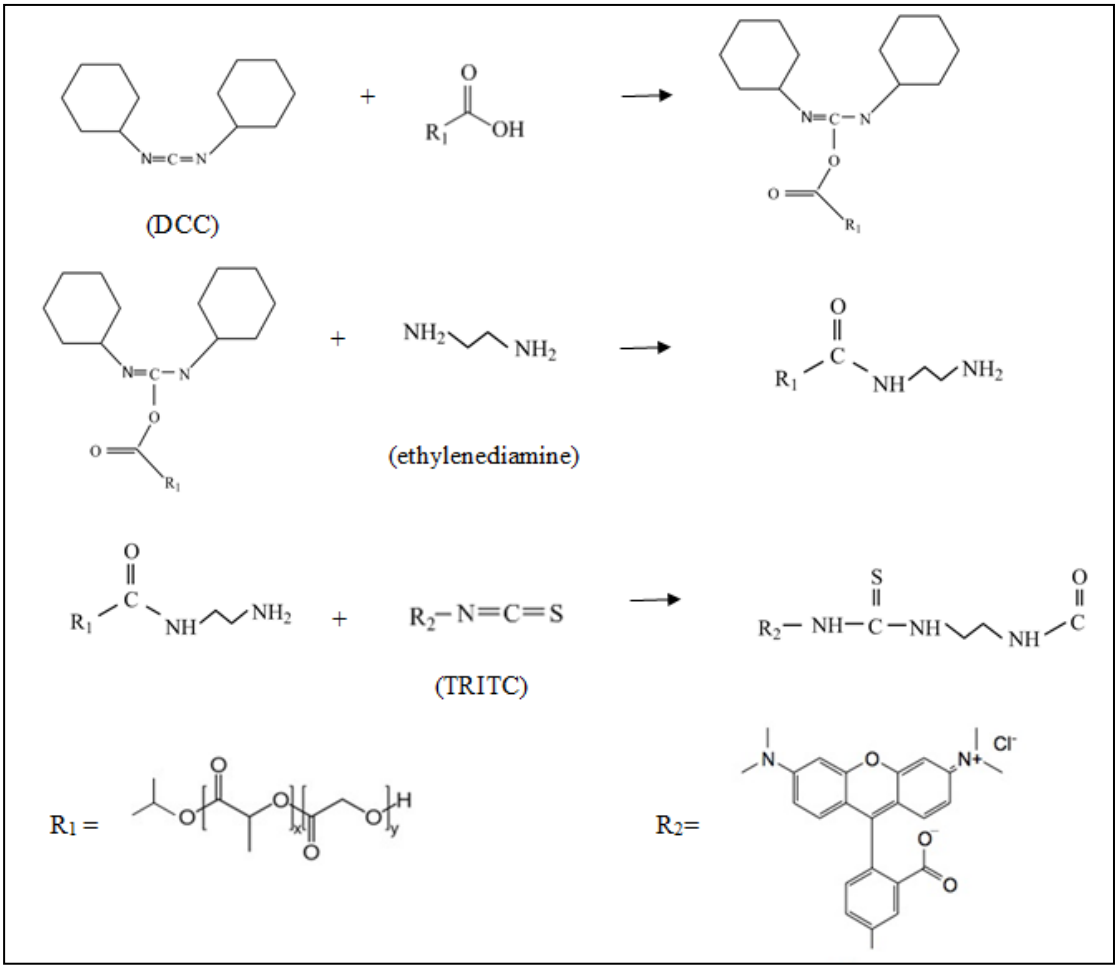

Figure 3.1 PLGA-t conjugation reactions

For preparation of fluorescent PLGA nanoparticles, TRITC was covalently conjugated to the PLGA chains by a carbodiimide method (Figure 3.1) (Chung, Kim et al. 2010) . In this method, 200 mg PLGA was dissolved in 10ml DCM, and 4.1mg DCC (20 µmol) and 2.3 mg NHS (20 µmol) were added to activate the carboxylic groups of PLGA. Then, 10 fold excess

ethylenediamine (3.3 µL, 50 µmol) was added to convert the succinimidyl ester group into a primary amine group. Next, 4.0 mg TRITC was added at room temperature to the PLGA. The product was precipitated in excess ethanol to remove unreacted TRITC, and then dried under vacuum.

3.3.3. Sythesis of PLGA-WGA conjugates

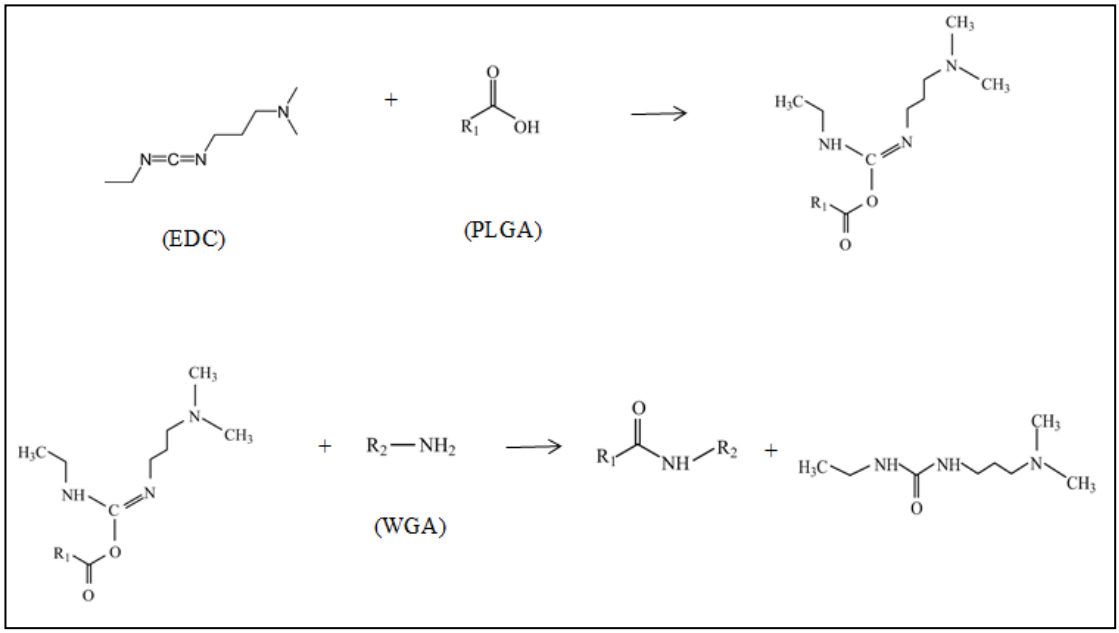

Figure 3.2 PLGA-tWGA conjugation reation

To conjugate TRITC-WGA (tWGA) with PLGA, a similar carbodiimide method was performed (Figure 3.2) (Yin, Chen et al. 2006). First, 100 mg PLGA was dissolved in 10 ml tetrahydrofuran (THF). Then, 2 ml PBS (0.01 M, pH 6.0) with 3.88 mg 1-Ethyl-3-(3-dimethylaminopropyl) carbodiimide (EDC) and 2.88 mg N-hydroxysulfosuccinimide (NHS) were injected. The activation of PLGA was carried out at room temperature overnight. Afterwards, the mixture was dried under vacuum, and washed with 3 ml nanopure water to remove excess carbordiimide reagents three times. Then, 5 mg tWGA was added and incubated

at room temperature for three days. Free tWGA was removed by water-dichloromethane (DCM) extraction performed three times. The product was dried under vacuum for 2 days.

3.3.4. Synthesis of PLGA-t nanoparticles

An amount of 20 mg of TRITC-labeled PLGA and 20 mg non-tagged PLGA were dissolved in 2 ml dichloromethane to form an organic phase. An aqueous phase was formed with 0.3% PVA dissolved in nanopure water. Then, the organic phase was added in droplets to the aqueous phase, and the emulsion was sonicated in an ice bath at 4 ◦C with a probetype sonicator (VC505, Sonics & Materials Inc., Wilmington, NC, USA) set at 750 W for 10 min, in pulse mode at 38% amplitude. Dichloromethane was evaporated under vacuum and nitrogen flow for 5 min in a rotoevaporator (Buchi R-124, Buchi Analytical Inc., New Castle, DE, USA). Following synthesis, centrifugation was carried out to remove the excess surfactant. After purification, nanoparticles were kept for 2 h at 80 ℃ and freeze-dried at 4 ℃ under 110 mm Hg of vacuum for 48 h in a Freezone 4.5 (Labconco Corp., Kansas City, MO, USA). Trehalose was be added to the nanoparticles suspension before precooling at a ratio of 1:1 (w/w) relative to the amount of nanoparticles. Finally, the lyophilized samples were stored in desiccators placed in the refrigerator for further use.

3.3.5. Synthesis of PLGA-tWGA nanoparticles

PLGA-t nanoparticles and PLGA-tWGA nanoparticles were prepared by an emulsion evaporation method(Zigoneanu, Astete et al. 2008). First, 40 mg PLGA-tWGA conjugates were dissolved in 2 ml DCM as organic phase. Then the organic phase was injected to 10 ml 0.3 % polyvinyl alcohol (PVA) in an ice-bath with sonication (VC505, Sonics & Materials Inc., Wilmington, NC, USA) for 10 minutes, followed by removing organic solvents under vacuum

for 5 minutes. Excess PVA was removed by dialysis for 2 days. Trehalose was added at a ratio of 1:1. The final products were lyophilized for 2 days and stored at 4 ℃.

3.3.6. Characterization of nanoparticles

An amount of 5.0 mg nanoparticles was resuspended in nanopure water. The average size, polydispersity index (PDI) and zeta potential of the resuspension were determined by dynamic light scattering (DLS). The morphology of nanoparticles was determined by transmission electron microscopy.

The amount of TRITC conjugated to PLGA-t NPs was determined by using a spectrofluorometer (Wallac 1420 VICTOR, Perkin Elmer Inc., Waltham, Massachusetts, USA). The volume of 0.1 mL standard TRITC solution was pipetted to each well. The intensity of the standard solution was measured at different concentrations at the absorbance 531/572 nm with nano pure water as blank. The amount of 1 mg PLGA-t NPs was resuspended in 1 ml nano pure water and measured under the same condition. The concentration of TRITC conjugated on PLGA NPs was determined according to the standard curve of TRITC.

The conjugation efficiency of PLGA-tWGA NPs is determined by BCA protein assay (BCA protein assay kit, Thermo Scientific, Rockford, IL, USA) (Mo and Lim 2005). An enhanced test tube protocol with working range at 5-250 μg/ml was used. A series of albumin (BSA) were prepared for a standard curve. Accurately weighed PLGA-tWGA NPs (5 mg) were dissolved in 1 mL nano pure water. The volume of 0.1 ml of each standard BSA solution, PLGA-tWGA solution were pipetted to each labeled tube, and 2.0 ml fresh prepared BCA working reagent was added to each tube. The mixtures were incubated at 60 ℃ for 30 minutes, and cooled to room temperature. The absorbance of all the samples was measured with the spectrophotometer set at 562 nm within 10 minutes. A cuvette filled only with water was set as blank. The protein concentration was determined according to the standard curve and it was expressed as the weight of WGA relative to the weight of nanoparticles (μg WGA/ mg NPs).

3.3.7. Effect of targeting on *C.elegans*

Age synchronized *C. elegans* was cultured in agar dish, and fed with freshly cultured *E. coli* (OP500) and Luria-Bertani Medium (LB) in the presence of the treatments including tWGA, PLGA-t nanoparticles, PLGA-tWGA nanoparticles. The applied treatments were compared with the control (no treatment). Concentration of the free tWGA used as a control was determined according to the conjugation efficiency of PLGA-tWGA NPs.

The following characteristics of *C. elegans* were monitored during their life span, pumping rate, body size, and on the number, area and intensity of DAergic neurons.

3.3.7.1. Pharyngeal pumping rate

Animals were examined three times a week using a stereomicroscope (Nikon SMZ-U). The pumping rate of five worms was recorded manually for 1 min. The pumping rate data was compared with the control.

3.3.7.2. Size of C. elegans

C. elegans BZ555 was cultured in agar dishes at 20°C and fed with freshly cultured *E. coli* (OP50) or with *E.coli* mixed with nanoparticles for 10-15 days. Digital video was captured daily using a digital camera (Redica 4000R) and a stereomicroscope (Nikon SMZ-U). Offline analysis was performed with ImagePro (Mediacy) to measure length over time (n=10-20).

3.3.7.3. Number, intensity, and area of GFP-DAergic neurons and co-localization

Staining was performed to locate PLGA-t NPs and PLGA-tWGA NPs as follows. After pumping rate reached a level lower than 60/min, worms treated with PLGA-t NPs and PLGA-tWGA NPs were washed with S-Basal (1ml /dish), fixed with 4% paraformaldehyde for 30 min, washed with PBS, and kept at 4°C overnight. 10 µl of the sample and 10µl of Fluoromount-G (anti fading mounting medium) was applied on to a glass slide and mounted with a cover glass. Micrographs of the slides were taken using a fluorescence microscope (Nikon Eclipse Ti-S) equipped with a digital camera Retiga 400-R, and

FITC/TRITC filters. The co-localization of the GFP-DAergic neurons (green) and nanoparticles (red) was determined by imaging.

Number, fluorescent area (μm^2), and mean intensity of DAergic neurons were quantified with NIS analyze, and compared between control group and treated groups (n=20). The number and area of GFP-DAergic neurons per animal were indicated by the appearance of GFPs expressed in eight DAergic neurons. The intensity of DAergic neurons was determined by the fluorescent intensity of GFP per neuron per animal.

A time study was also carried out to evaluate the effect of GFP-DAergic neurons over time. A number of 5 worms was picked out every other day, stained on a glass slide, and number, area, and intensity were determined with the method described above.

Co-localization of fluorescent nanoparticles to labeled GFP-DAergic neurons, and nanoparticle routing was identified with a Zeiss LSM510 laser scanning microscope.

3.3.8. Statistics

Ancova Test in SAS was used to assess significance of pumping rate, body size and time study. Statistics of intensity, area and number of GFP-DAergic neurons were performed by anova test in SAS. Significant difference was declared at p-values lower than 0.05.

3.4. Results and Discussion

3.4.1. Nanoparticle physical-chemical characteristics

In this study, both fluorescent nanoparticles and WGA conjugated nanoparticles were prepared. The main characteristics of PLGA-t NPs and PLGA-tWGA NPs are summarized in Table 3.1. Mean diameters of these nanoparticles ranged from 208 nm (PLGA-t NPs) to 221 nm (PLGA-tWGA NPs) with a polydispersity index of 0.11 and 0.08, respectively. These nanoparticles were negatively charged, and zeta potential ranged from -34.5 mV (PLGA-t NPs)

to -42.0 mV (PLGA-tWGA NPs) at neutral pH. The amount of TRITC conjugated PLGA-t NPs was 1.2 μg /mg NP. Morphology of the NPs was examined under a transmission electron microscope. The TEM images showed that all nanoparticles appeared relatively spherical in shape (Figure 3.3).

Table 3.1 Physical characteristic of nanoparticles

Formulation	Size (nm)	PdI	Zeta potential (mV)	WGA conjugation efficiency (μg WGA /mg NP)
PLGA-t NP	208.0±2.9	0.11±0.01	-34.5±0.5	-
PLGA-tWGA NP	221.0±0.1	0.08±0.01	-42.0±0.4	4.9±1.1

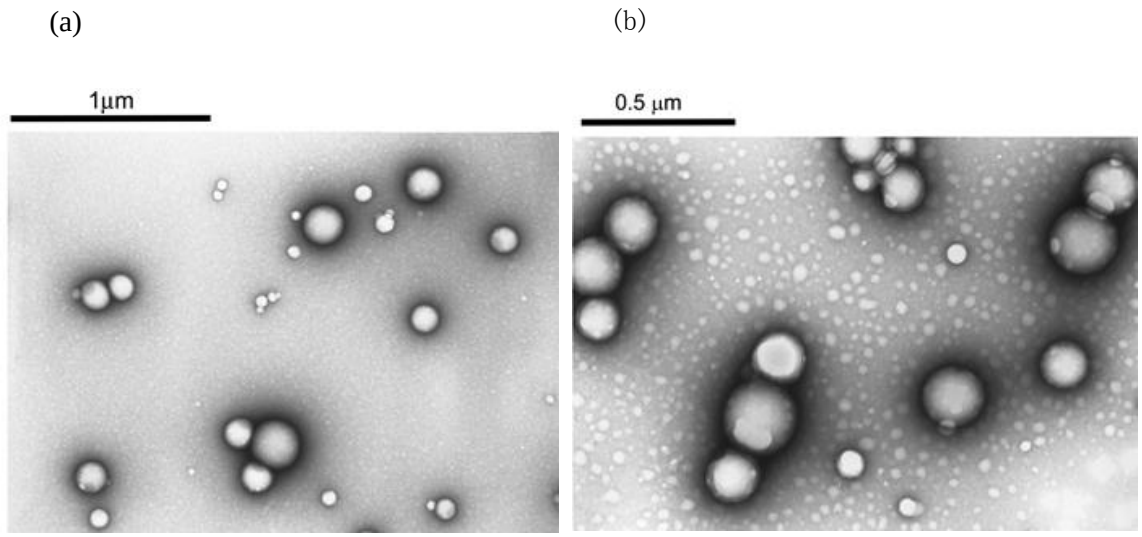

Figure 3.3 TEM pictures of (a) PLGA-t NP at magnificent of 33,000× and (b) PLGA-tWGA NP at magnificent of 50,000×

3.4.2. WGA conjugation efficiency

After freeze drying, both nanoparticle suspensions PLGA-t and PLGA-tWGA displayed a pink color which indicated success of conjugation. The conjugation efficiency was 4.9 μg WGA/mg NP as determined by spectrophotometry (Table 1). The conjugation efficiency of

WGA was lower compared to another method which coupled WGA to the surface of already synthesized PLGA nanoparticles (18.1±2.5 µg WGA/mg nanoparticles) (Wang, Ho et al. 2010), but of similar order of magnitude. TRITC labeled WGA was used in the synthesis, rather than free WGA, in order to visualize nanoparticles and in the TRITC-WGA construct, amine groups of WGA, reaction groups important for the PLGA conjugation, were mostly occupied by TRITC, which might lead to low conjugation of TRITC-WGA to PLGA.

3.4.3. Effect of targeting on *C. elegans*

In order to measure the ability of WGA conjugated PLGA nanoparticles (PLGA-tWGA NPs) to target neurons in *C. elegans*, the effect of PLGA-tWGA nanoparticles on *C. elegans* behavior was tested and compared with that of free tWGA. PLGA-t NPs were also tested to evaluate the effect of unconjugated PLGA NPs. The following characteristics were monitored in *C. elegans* during its life span (about 14 days), pharyngeal pumping rate, size (length/width), number, area and intensity of GFP-DAergic neurons, and transport of nanoparticles (co-localization).

3.4.3.1. Pharyngeal pumping rate

E. coli (OP50), food for *C.elegans* is ingested by the pharynx, a neuromuscular organ in the head (Wolkow 2006). Feeding behavior of *C.elegans* can be monitored by counting the contraction rate of the pharynx muscle.

It is well known that the pharyngeal pumping rate slows as the pharynx muscles deteriorate during aging(Wolkow 2006). It was not surprising therefore that pumping rate of the control and treated groups decreased over the 14 days study (Figure 3.4). Pumping rate for the control group decreased from 282/min to 18/min in 15 days while pumping rate in 1.0 mg/ml and

2.0 mg/ml PLGA-t NPs treated groups decreased from 280/min-288/min to 18/min-19/min over the same period of time (Figure 3.4a). Statistically, no significant difference was found in the pumping rate between the control group and the treated groups (P>0.05). More than half of worms treated with a higher concentration of PLGA-t NPs, 3.0 mg/ml PLGA-t NPs were found dead within 8 days. However, *C.elegans* treated with PLGA NPs that was not covalently linked with TRITC at the same concentration survived the same life span as the control group. The short life span of PLGA-t treated worms at a high concentration indicated that the high amount of TRITC conjugated to PLGA caused earlier death of the worms.

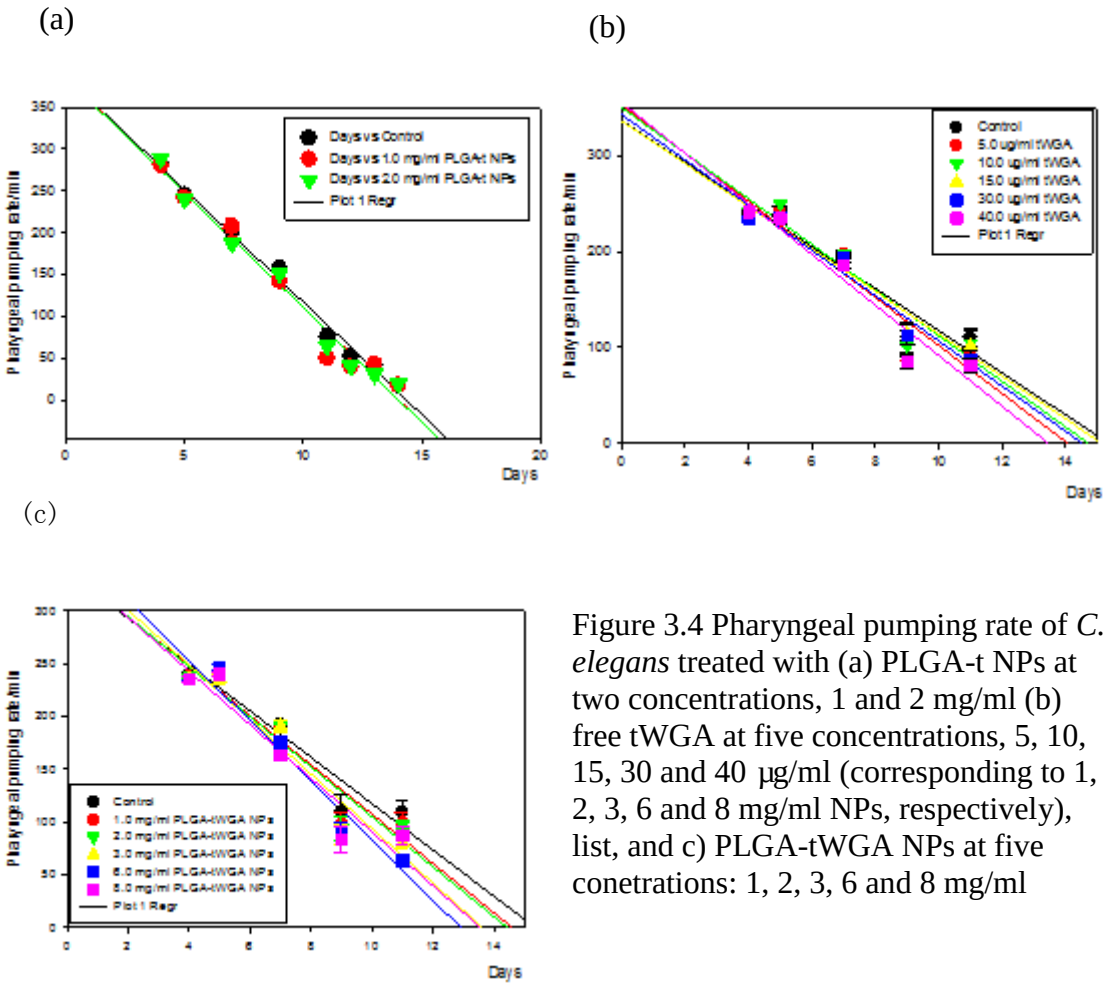

Figure 3.4 Pharyngeal pumping rate of *C. elegans* treated with (a) PLGA-t NPs at two concentrations, 1 and 2 mg/ml (b) free tWGA at five concentrations, 5, 10, 15, 30 and 40 μg/ml (corresponding to 1, 2, 3, 6 and 8 mg/ml NPs, respectively), list, and c) PLGA-tWGA NPs at five conetrations: 1, 2, 3, 6 and 8 mg/ml

Pumping rate of the *C.elegans* treated at five concentrations of free tWGA decreased from 241/min to 81/min while that of control group decreased from 239 to 109/min within 12 days (Figure 3.4b). For PLGA-tWGA NPs treated group, pumping rate was reduced from 238/min to 63/min over 12 days. The values for the pumping rate are in good agreement with the literature, which reports that in young adults, the parynx pumps 200-300 times/min and declines greatly with aging (Chow, Glenn et al. 2006). Several factors might contribute to the decrease of pumping rate including contraction related muscle deterioration in the pharynx and microbial infection (Chow, Glenn et al. 2006). Statistically, compared with the control group, a significant difference was found only at the highest concentration of free tWGA, 40 μg/ml tWGA; for all other tWGA concentrations pumping rate was not significantly different than the control. For PLGA-tWGA NPs treated animals, three groups treated with the highest concentrations of NPs, 3, 6, and 8 mg/ml PLGA-tWGA NPs were significantly different from the control ($P<0.05$).

To facilitate comparison between treatments, worms were treated with PLGA-tWGA NPs and corresponding concentrations of tWGA. No significant difference was observed except between 15.0 μg/ml tWGA treated group and the equivalent 3.0 mg/ml PLGA-tWGA NPs treated group ($P=0.0135$), and between 30.0 μg/ml tWGA and the equivalent 6.0 mg/ml PLGA-tWGA NPs treated groups ($P=0.0017$). This result confirmed that while free tWGA affected pumping rate solely at the highest concentration (40 μg/ml), PLGA-tWGA NPs showed a significant effect on pumping rate starting at 3 mg/ml, an equivalent of only 15 ug/ml tWGA. At the smallest tWGA concentrations, the targeting agent did not have an effect on pumping rate, whether in free or conjugated form. It is apparent that a minimum tWGA is required to have an effect on the neurons, and that this effect is noted at lower concentrations for tWGA when conjugated to PLGA nanoparticles than in free form.

As dopamine neurons are mechanosensory neurons, involved in locomotion, feeding, egg-laying and so on, pumping rate could be used as an indicator of the effect of the nanoparticle treatment on dopamine neurons (Collins, Huang et al.). The significant difference in pumping rate caused by free tWGA only at the highest concentration (40 µg/ml) and PLGA-tWGA NPs at three highest concentrations (3, 6, and 8 mg/ml equivalent to 15, 30, and 40 ug/ml tWGA) compared to control group indicated that tWGA conjugated to PLGA NPs affected more pumping rate of the worms than the equivalent concentration of free tWGA.

3.4.3.2. Size of *C. elegans*

Both length and width of *C.elegans* were measured using ImagePro and the values were compared to size of the control group (Figure 3.5). Measurements were performed three days after the worms were age synchronized and incubated at 20 ◦C. Length and width of all groups were found to be in average 480 µm in length and 150 µm in width. Both length and width of *C.elegans* increased during aging. For the control group, size increased to 900 µm in length and 250 µm in width over a period of 14 days. *C. elegans* is reported to measure up to 1000 µm at adulthood with variations in size due to the software used in the measurement and type of worms studied (Meyer, Lord et al. 2010).

Size of the worms treated with PLGA-t NPs increased from 423-432 µm (day 1) to 759-855 µm (day 14) in length, and from 173-194 µm to 279-287 µm in width (Figure 3.5a), whereas length of the control group increased from 457±4 µm (day 4) to 819±3 µm (day 14). Width of control group increased from 180 µm to 280 µm from day 4 to day 14. Statistics showed that for both length and width of PLGA-t NPs treated group, no significant difference was found at both concentrations tested ($P>0.5$). The experiments were done at the lowest two concentrations of

PLGA-t NPs to avoid early death of animals as observed at the highest concentrations of TRITC labeled PLGA NPs, noted earlier.

Length of tWGA treated worms were initially 437-473 µm at day 4, and it increased to 866-922 µm at day 14 (Figure 3.5b), whereas PLGA-tWGA treated groups increased in length from 416-473 µm to 692-899 µm (Figure 3.5c). Width from day 4 to day 14 of the three concentrations of tWGA treated groups increased from 80-197 µm to 262-300 µm (Figure 3.5b) while the length of three concentrations of PLGA-tWGA treated groups varied from 186-191 µm to 252-277 µm (Figure 3.5c). Most of tWGA and PLGA-tWGA NPs treated worms showed significantly different length and width when compared to the control group. The presence of tWGA in free or conjugated form affected length of *C. elegans*, but no specific trend was identified. The size increased or decreased depending on the treatment and the size changes were found minimal.

For *C.elegans*, growth is not controlled by the dopamine neurons, instead body size is mainly affected by genetic factors and environmental factors, of which food and temperature are most important (So, Miyahara et al. 2011). Hence, body size is not an indicator of targeting, but it could be an indicator of treatment toxicity. The trend of size increasing versus time did show a significant difference between control and nanoparticles treated group. However, at each time point, both width and length varied only slightly relative to the control. For all treatments both length and width stayed within the normal body size of *C.elegans*, and hence tWGA and PLGA-tWGA NPs were believed to be nontoxic to *C.elegans* at the concentrations tested.

(a)

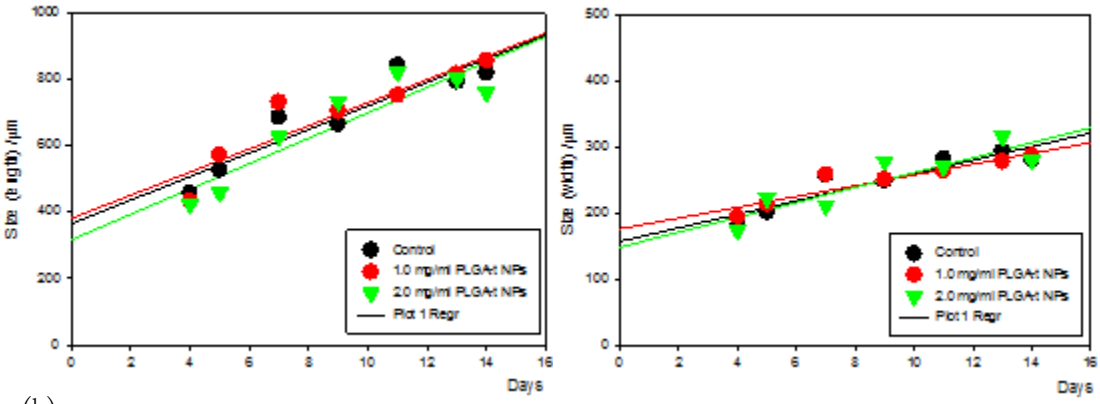

(b)

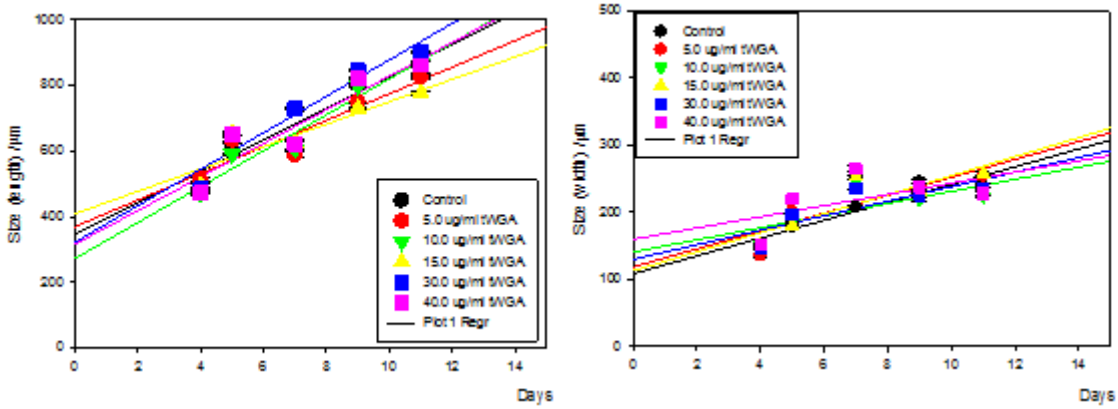

(c)

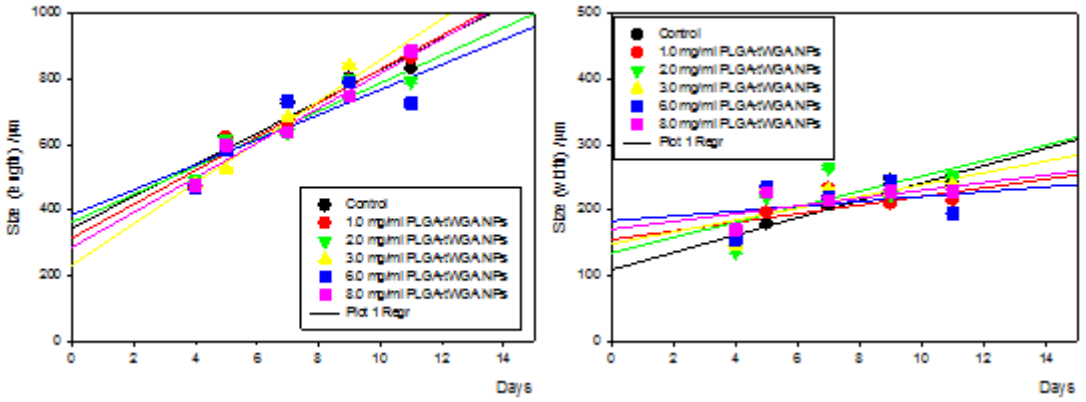

Figure 3.5 Size (length/width) of control group and (a) two concentrations of PLGA-t NPs treated groups, (b) five concentrations of tWGA NPs (5.0 μg WGA/mg NPs) treated groups, and (c) five concentrations of PLGA-tWGA NPs (5.0 μg WGA/mg NPs) treated groups

3.4.3.3. Area, mean intensity and number of GFP-DAergic neurons

The *C. elegans* strain BZ555 was used in this study because it expressed green fluorescent protein in the dopamine neurons, allowing visualization of DAergic neurons. If nervous system of *C.elegans* shows minimal changes during aging (Collins, Huang et al.), then a change in the number, area or intensity of the DAergic neurons of nanoparticle-treated worms could be an indication of successful delivery of the nanoparticles to the neurons.Fluorescent intensity and area of GFP-DAergic neurons were used as an indicator of the presence of fluorescent nanoparticles transported to GFP-DAergic neurons.

The number of GFP-DAergic neurons of tWGA treated groups was in the range of 6.0-6.6, and for the PLGA-tWGA NPs treated group the number of identifiable neurons was 6.0-6.4, similar to the control (6.2/animal). It is known that *C. elegans* hemaphrodites have eight DAergic neurons, however in average only six neurons were identifiable in the strain BZ555 after aging with the fluorescence microscopic technique described earlier. Statistically, no significant difference was observed in the number of neurons for all concentrations when compared to the control ($P>0.5$) (Figure 3.6a).

For tWGA treated groups, area of GFP-DAergic neurons was 5.6– 7.8 μm^2 (Figure 3.6b). No significant difference was found between the neuron area of tWGA treated group at five concentrations (5.0, 10.0, 15.0, 30 and 40 µg/ml (5.6-7.8 μm^2) and that of the control (7.3 μm^2). PLGA-tWGA NPs showed a significant effect on area of GFP-DAergic neurons compared to the control. Area of GFP-DAergic neurons was significantly lower for the PLGA-tWGA NPs treated worms at 1.0 mg/ml (4.9 μm^2) and 3.0 mg/ml (4.7 μm^2) ($P=0.04$, 0.03 respectively). The lowest value reached was 4.5 μm^2 for 6 mg/ml PLGA-tWGA treated group ($P=0.0053$).

(a)

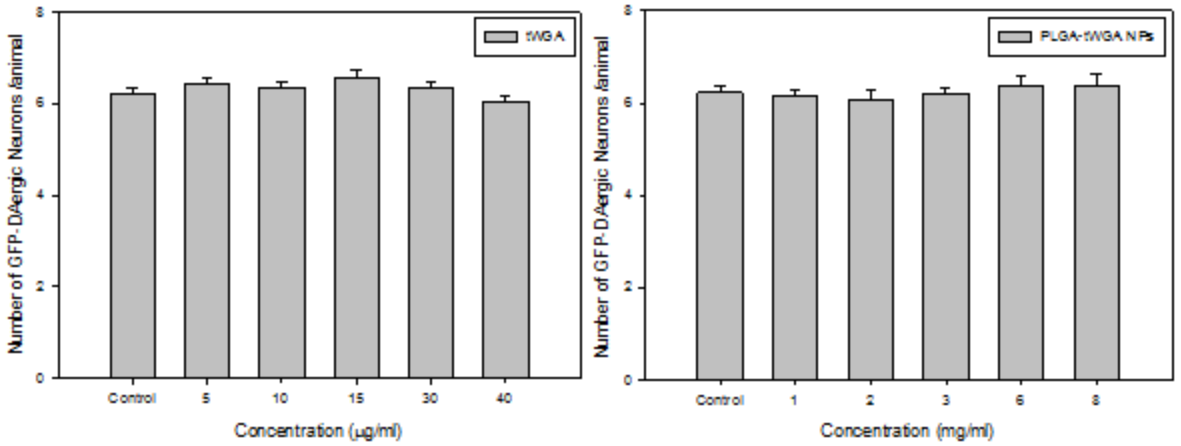

(b)

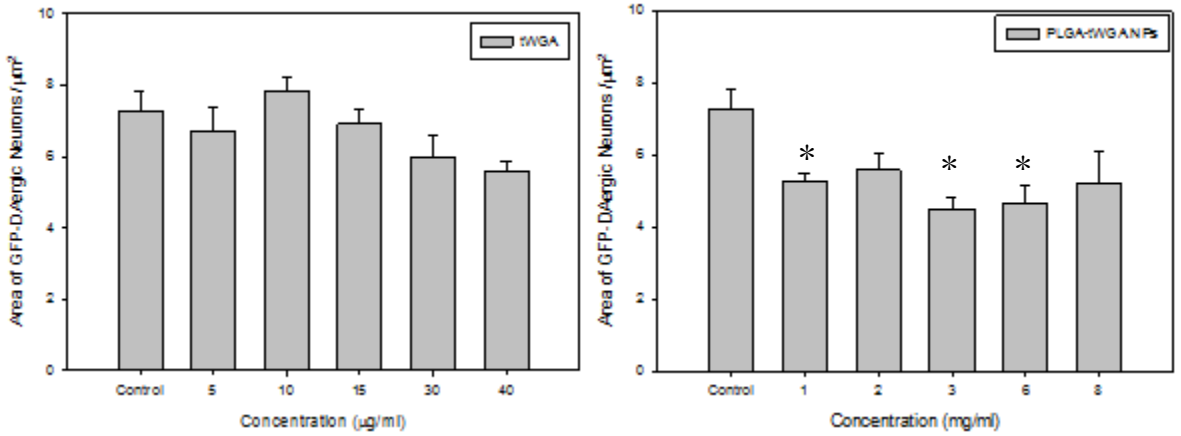

(c)

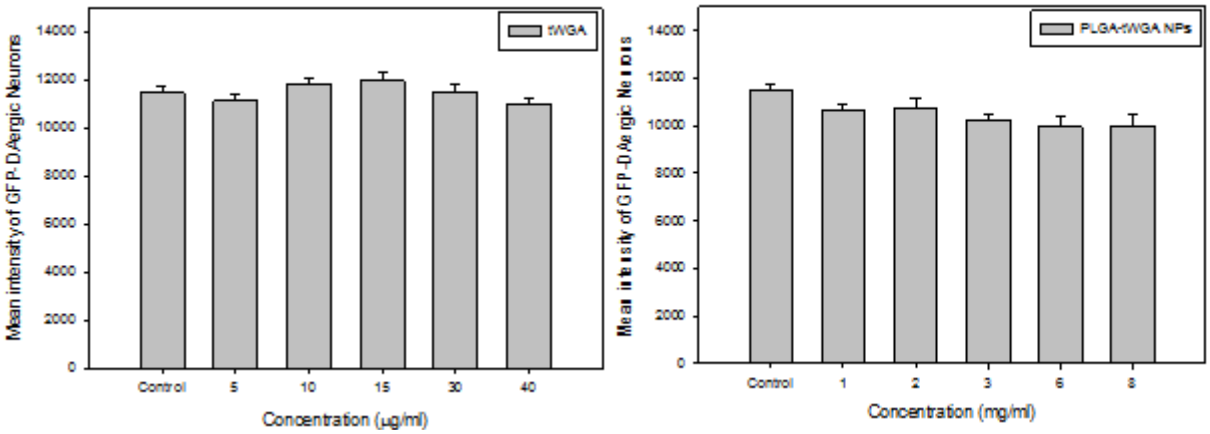

Figure 3.6 (a) Number, (b) mean area and (c) mean intensity of GFP-DAergic neurons. * $P<0.05$

(a)

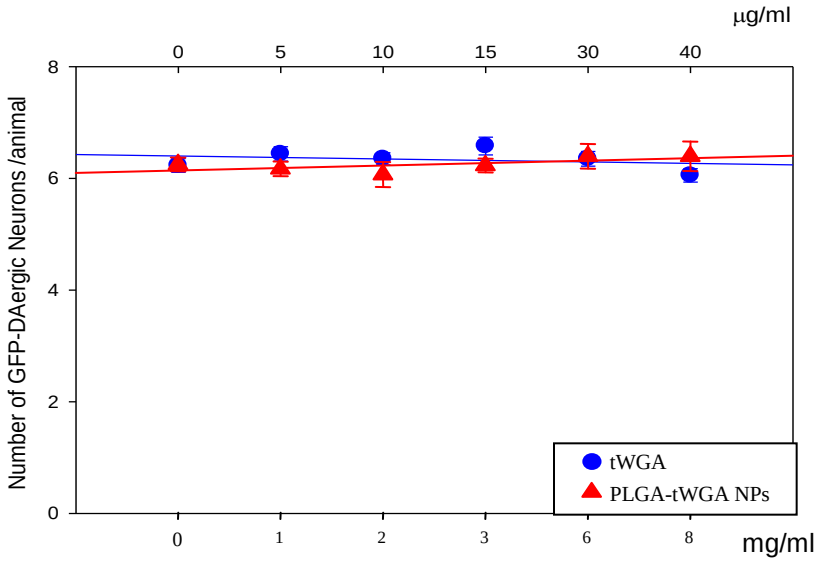

(b)

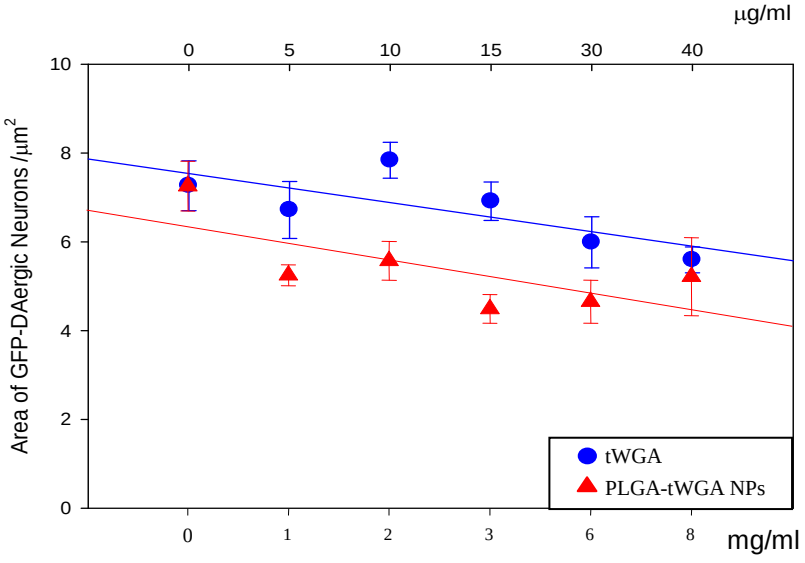

(c)

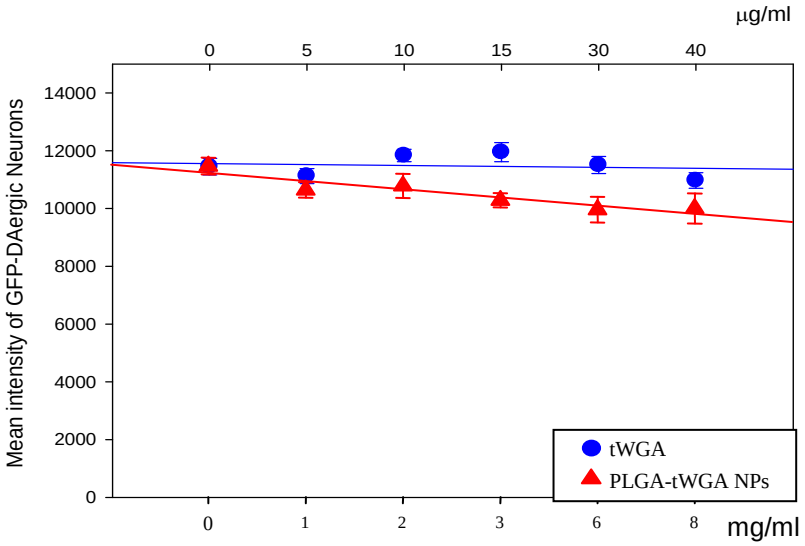

Figure 3.7 (a) Number, (b) mean area and (c) mean intensity of GFP-DAergic neurons versus concentration.

For tWGA treated group, the average intensity of GFP-DAergic neurons decreased from 11,448 (control) to 10,970-11,949 ($P>0.08$) (Figure 3.6c). The intensity of GFP-DAergic neurons over five concentrations of PLGA-tWGA NPs (1, 2, 3, 6, and 8 mg/ml) decreased in a dose dependent manner from 11,448 (control) to 9,941 -10,763, but no significant difference was found ($P>0.05$) between the treatments and the control.

The comparison between PLGA-tWGA NPs and same amount of tWGA was also performed. No significant difference was found in the number of neurons between PLGA-tWGA NPs treatment and the equivalent amount of free tWGA treatment. As for the area, 2.0 mg/ml and 3 mg/ml PLGA-tWGA NPs showed a greater effect on decreasing the area of the neurons than the equivalent amount of free tWGA ($P=0.03$ and 0.006 respectively). In terms of intensity of GFP-DAergic neurons, no significant difference was observed except for the 3.0 mg/ml PLGA-tWGA NPstreated groups and equivalent concentration of tWGA ($P=0.01$).

The concentration-dependent trend of all treatments was assessed by comparing the number, area and intensity of GFP-DAergic neurons change as a function of concentration (Figure 3.7). Number of GFP-DAergic neurons for both treatments maintained at similar level over the concentration range studied (Figure 3.7a, $P=0.6$). Area of GFP-DAergic neurons of worms treated with tWGA and PLGA-tWGA NPs showed a dose dependent decrease (Figure 7b). PLGA-tWGA NPs treated group showed a significant decrease compared to tWGA treated worms ($P<0.0001$). Dose dependent trend was also found for the intensity of GFP-DAergic neurons (Figure 3.7c). After treatment with tWGA, intensity of GFP-DAergic neurons slightly decreased while PLGA-tWGA NPs treated group showed a much more pronounced dose-dependent decrease ($P<0.0001$).

The number and intensity of GFP DAergic Neurons did not change for all treatments compared to the control group, whereas the area changed for PLGA-tWGA NPs, indicating that particles did reach the neurons and had an effect that resulted in a smaller area of possibly damaged DAergic neurons. PLGA-tWGA NPs may damage the DAergic neurons, especially at the highest concentrations (> 3mg/ml) with an effect on pumping rate as seen earlier,. It was implied that the significant decrease of pumping rate for the PLGA-tWGA NPs treatments at the highest concentrations was the result of targeted transport of PLGA-tWGA NPs to DAergic neurons. The decrease in the area of the GPF DAergic neurons of PLGA-tWGA treated worms, confirmed the findings, supporting the targeting ability of the PLGA-tWGA NPs. The same amount of free tWGA did not show an equivalent strong effect on both pumping rate and area of DAergic neurons. Dose-dependent PLGA-tWGA NPs effects on DAergic neurons were proven to be stronger than that of free tWGA.

A time study of number, size and area of neurons treated at concentration of NPs (3 mg/ml for PLGA-t NPs and PLGA-tWGA NPs) and equivalent free tWGA concentration (15.0 μg/ml for tWGA) were conducted, as well (Figure 3.8). Generally, number, area and intensity decreased during aging. However, except for area of PLGA-tWGA treated group compared with control (P=0.002), no significant difference was observed for the other treatments and parameters studied. Both tWGA and PLGA-t NPs did not cause significant effects on GFP-DAergic neurons in terms of number, area and intensity while PLGA-tWGA did. GFP-DAergic neurons studies along with time study indicated PLGA-tWGA NPs had significant effect especially at high concentrations (>3 mg/ml) on GFP-DAergic neurons. The significant changes observed in the area of neurons in PLGA-tWGA treated worms indicated that PLGA-tWGA NPs successfully

transported to DAergic neurons and showed a concentration-dependent effect on DAergic neuron cell.

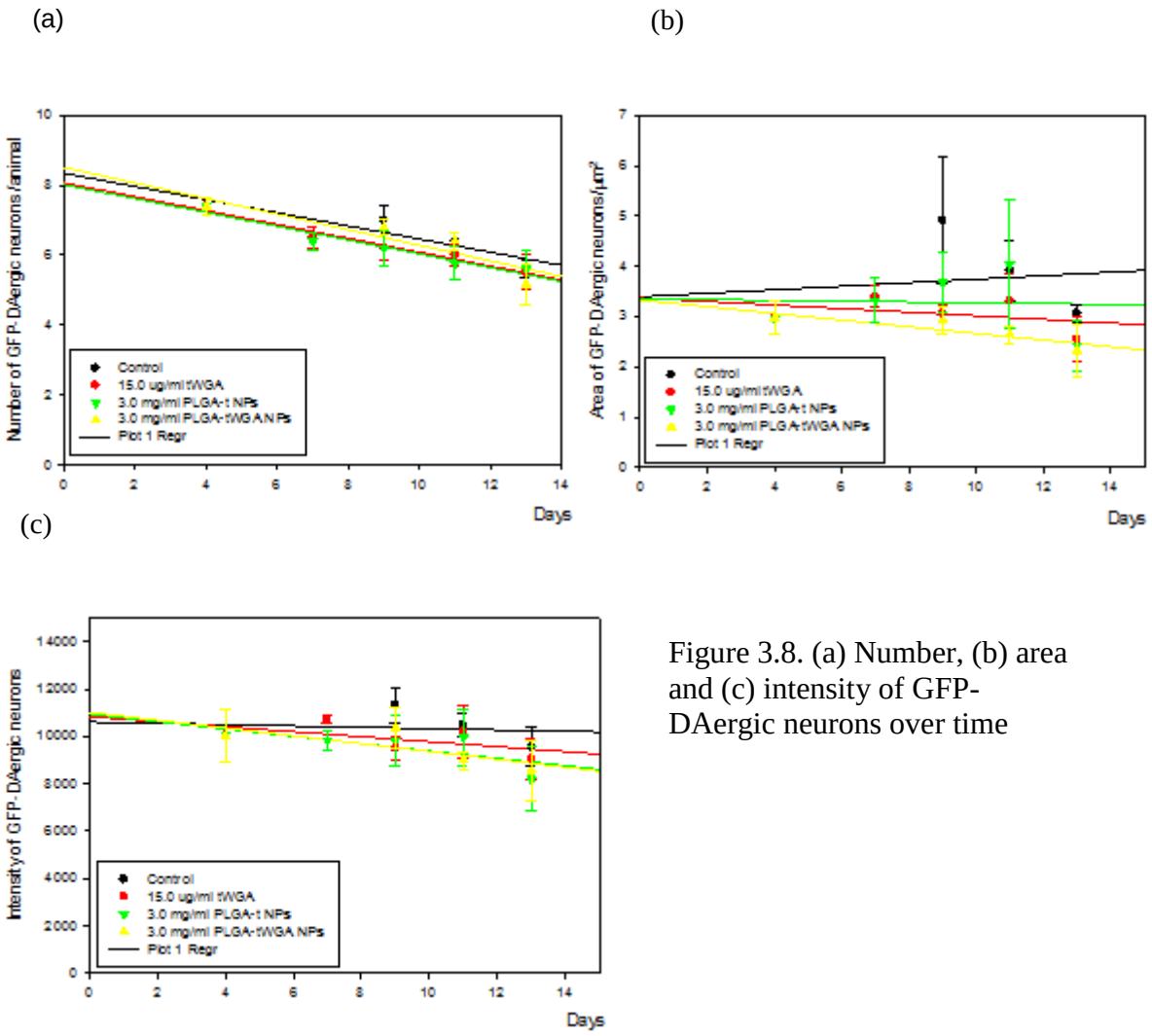

Figure 3.8. (a) Number, (b) area and (c) intensity of GFP-DAergic neurons over time

3.4.3.4. Co-localization

For all treatments (free WGA and WGA-conjugated NPs, all labeled with TRITC), a Zeiss LSM510 laser scanning microscope was used to confirm *in vivo* targeting and NP distribution. For PLGA-t NPs treated group, PLGA-t NPs were located along the mouth and intestine of worms while PLGA-tWGA NPs showed up less in the intestine (Figure 3.9).

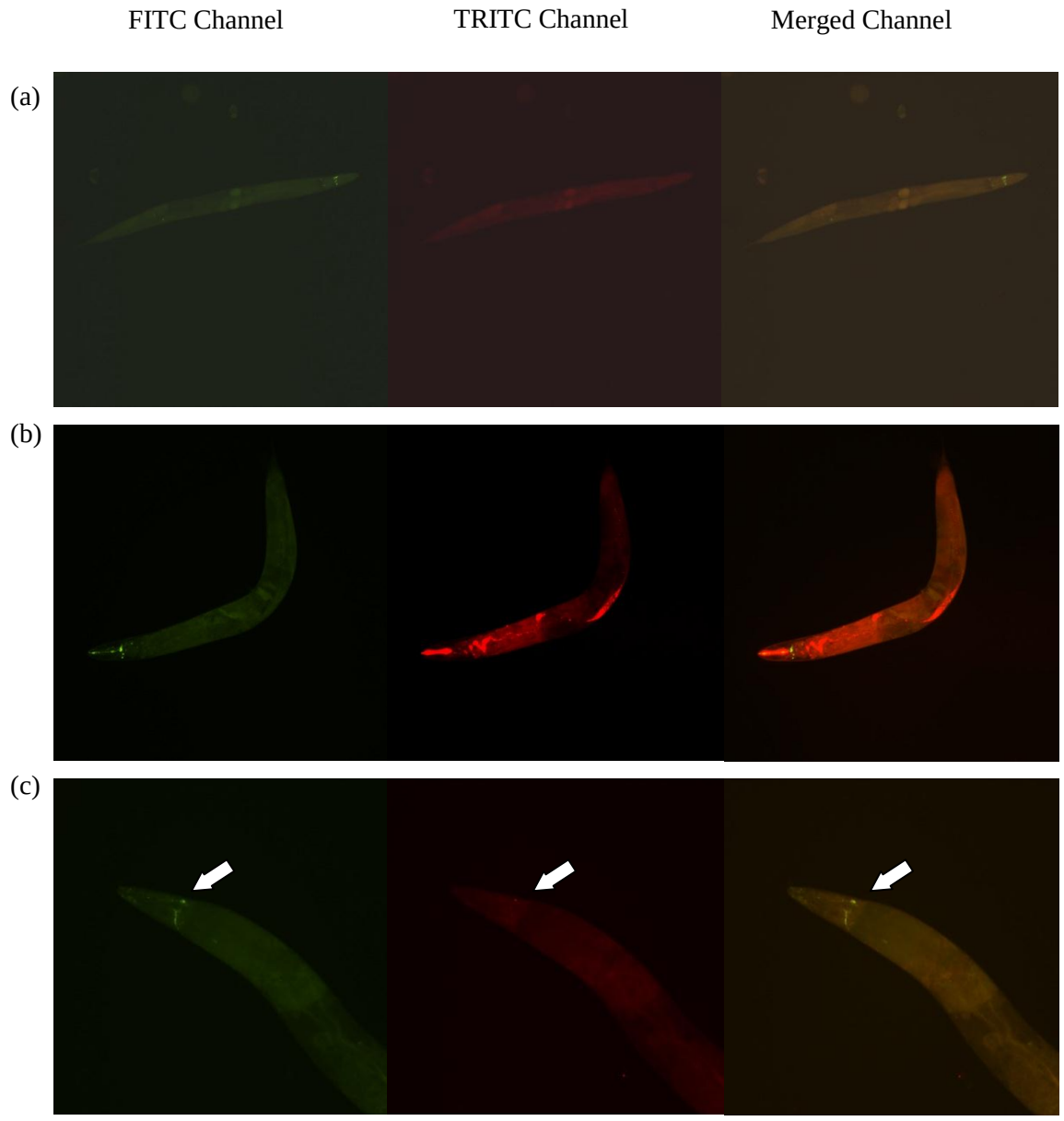

Figure 3.9. Fluorescent pictures of (a) control group (×10), (b) 2.0 mg/ml PLGA-t NPs treated group (×10), and (c) 1.0 mg/ml PLGA-tWGA NPs treated group (×20). Green fluorescence represented GFP-Daergic Neurons, and red fluorescence represented nanoparticles

Very faint fluorescence was detected in the free tWGA treated worms over all concentrations tested as lectins might be readily digested or excreted out of the body. PLGA-tWGA NPs were proved to co-localize with the GFP-DAergic neurons as indicated by green fluorescence partially overlapped with red fluorescence (labeled nanoparticles) (Figure 3.9c).

Co-localization was not observed in PLGA-t NPs treated group or most tWGA treated worms but only in PLGA-tWGA NPs treated groups, which demonstrated that tWGA conjugated to PLGA NPs were able to target neurons.

N-acetyl-glucosamine and sialic acid are abundant on most cell surface including intestinal mucus and cerebral capillary endothelium (Bies, Lehr et al. 2004; Gabor, Bogner et al. 2004) and are binding moieties of WGA. The interaction between the glycoproteins on cell surface and WGA was hypothesized to enhance cellular binding and endocytosis of WGA-conjugated nanoparticles by receptor-mediated pathway (Bies, Lehr et al. 2004). Compared to PLGA-t NPs, PLGA-tWGA NPs showed stronger effect on both pumping rate and GFP-DAergic neurons, as expected. Co-localization pictures further confirmed that the conjugation of tWGA improved targeted transport of nanoparticles to DAergic neurons. Interestingly, when conjugated to NPs, transport ability of tWGA was greater than that of free tWGA. Significant decreasing in pumping rate and area of GFP-DAergic neurons with PLGA-tWGA NPs treatment indicated a higher effect on DAergic neurons of covalently linked tWGA over free tWGA. An *in vitro* study of transcytosis of WGA-conjugated NPs in Caco-2 cells also revealed that WGA-conjugated NPs had a higher transcytosis than free WGA (Russell-Jones, Veitch et al. 1999). The enhanced transcytosis could be due to a possibly different trafficking route of PLGA-tWGA NPs when compared to free tWGA or enhanced receptor clustering which was induced by multiple tWGA binding on the surface of nanoparticles (Russell-Jones, Veitch et al. 1999; Gabor, Bogner et al. 2004). Similarly, more PLGA-tWGA NPs were possibly transcytosed into systemic circulation than free tWGA after PLGA-tWGA NPs in *C.elegans* from the intestine, and therefore provided a better chance to target DAergic neurons. Enhanced targeted delivery of PLGA-tWGA NPs to neurons compared with tWGA and PLGA-t NPs was confirmed in *C.elegans*, making PLGA-

tWGA NPs ideal targeted neural delivery systems that could be used to deliver drugs to neurons and fight neurodegenerative disease such as Parkinson's disease.

3.5. Conclusion

A DAergic neuron targeting delivery system was successfully constructed by conjugating tWGA with PLGA NPs. PLGA-tWGA polymer was synthesized first and then used to prepare nanoparticles of 221 nm (5 μg tWGA /mg NPs); nanoparticles were tested in *C.elegans*. PLGA-tWGA NPs did not show a significant effect on pumping rate and life span of *C. elegans* at low concentration (<3 mg/ml). For tWGA treated worms, only the highest concentration resulted in a significant effect on pumping rate. Both length and width of *C. elegans* over all concentration of tWGA and PLGA-tWGA NPs treatment were only slightly affected. Due to the high concentration TRITC, PLGA-t NPs proved toxic to the worms at concentrations higher than 3 mg/ml. Fluorescent studies of GFP-DAergic neurons revealed that area of GFP-DAergic neurons of worms treated with high concentrations PLGA-tWGA NPs (>3mg/ml) was significantly decreased. Number and mean intensity of GFP-DAergic neurons also decreased, but no significant difference was found compared with control group. WGA conjugated PLGA NPs at low concentrations (<3mg/ml) was proved to target DAergic neurons without negative effects. The decreasing values of GFP-DAergic neurons in terms of area and intensity along with the co-localization of the fluorescent particles with the GFP-DAergic neurons of treated worms proved targeting property of PLGA-tWGA nanoparticles to DAergic neurons. However, the mechanism of tWGA transport to DAergic neurons when conjugated to PLGA NPs has not been thoroughly understood as a result of this study. Future studies should consider unveiling the mechanism of NPs uptake and transport to the neurons, as well as the effect of different sizes of nanoparticles and different amounts of tWGA on targeting neurons in *C. elegans*.

3.6. References

Alves, G., E. B. Forsaa, et al. (2008). "Epidemiology of Parkinson's disease." J Neurol **255 Suppl 5**: 18-32.

Bies, C., C. M. Lehr, et al. (2004). "Lectin-mediated drug targeting: history and applications." Adv Drug Deliv Rev **56**(4): 425-435.

Braungart, E., M. Gerlach, et al. (2004). "Caenorhabditis elegans MPP+ model of Parkinson's disease for high-throughput drug screenings." Neurodegener Dis **1**(4-5): 175-183.

Ceravolo, R., D. Frosini, et al. (2009). "Impulse control disorders in Parkinson's disease: definition, epidemiology, risk factors, neurobiology and management." Parkinsonism Relat Disord **15 Suppl 4**: S111-115.

Chang, J., Y. Jallouli, et al. (2009). "Characterization of endocytosis of transferrin-coated PLGA nanoparticles by the blood-brain barrier." Int J Pharm **379**(2): 285-292.

Chow, D. K., C. F. Glenn, et al. (2006). "Sarcopenia in the Caenorhabditis elegans pharynx correlates with muscle contraction rate over lifespan." Exp Gerontol **41**(3): 252-260.

Chung, Y. I., J. C. Kim, et al. (2010). "The effect of surface functionalization of PLGA nanoparticles by heparin- or chitosan-conjugated Pluronic on tumor targeting." J Control Release **143**(3): 374-382.

Collins, J. J., C. Huang, et al. The measurement and analysis of age-related changes in Caenorhabditis elegans. WormBook. T. C. e. R. Community, WormBook.

Factor, S. A. (2008). "Current status of symptomatic medical therapy in Parkinson's disease." Neurotherapeutics **5**(2): 164-180.

Gabor, F., E. Bogner, et al. (2004). "The lectin-cell interaction and its implications to intestinal lectin-mediated drug delivery." Adv Drug Deliv Rev **56**(4): 459-480.

Gao, X., B. Wu, et al. (2007). "Brain delivery of vasoactive intestinal peptide enhanced with the nanoparticles conjugated with wheat germ agglutinin following intranasal administration." J Control Release **121**(3): 156-167.

Hu, K., Y. Shi, et al. (2011). "Lactoferrin conjugated PEG-PLGA nanoparticles for brain delivery: preparation, characterization and efficacy in Parkinson's disease." Int J Pharm **415**(1-2): 273-283.

Irache, J. M., C. Durrer, et al. (1994). "Preparation and characterization of lectin-latex conjugates for specific bioadhesion." Biomaterials **15**(11): 899-904.
Kreuter, J. (2001). "Nanoparticulate systems for brain delivery of drugs." Adv Drug Deliv Rev **47**(1): 65-81.

Linazasoro, G. (2008). "Potential applications of nanotechnologies to Parkinson's disease therapy." Parkinsonism Relat Disord **14**(5): 383-392.

Liu, Y., P. Wang, et al. (2010). "Wheat germ agglutinin-grafted lipid nanoparticles: preparation and *in vitro* evaluation of the association with Caco-2 monolayers." Int J Pharm **397**(1-2): 155-163.

Meyer, J. N., C. A. Lord, et al. (2010). "Intracellular uptake and associated toxicity of silver nanoparticles in Caenorhabditis elegans." Aquat Toxicol **100**(2): 140-150.

Mo, Y. and L. Y. Lim (2005). "Paclitaxel-loaded PLGA nanoparticles: potentiation of anticancer activity by surface conjugation with wheat germ agglutinin." J Control Release **108**(2-3): 244-262.

Mo, Y. and L. Y. Lim (2005). "Preparation and *in vitro* anticancer activity of wheat germ agglutinin (WGA)-conjugated PLGA nanoparticles loaded with paclitaxel and isopropyl myristate." J Control Release **107**(1): 30-42.

Nass, R., D. H. Hall, et al. (2002). "Neurotoxin-induced degeneration of dopamine neurons in Caenorhabditis elegans." Proc Natl Acad Sci U S A **99**(5): 3264-3269.

Nass, R., K. M. Merchant, et al. (2008). "Caenohabditis elegans in Parkinson's disease drug discovery: addressing an unmet medical need." Mol Interv **8**(6): 284-293.

Ratzinger, G., X. Wang, et al. (2010). "Targeted PLGA microparticles as a novel concept for treatment of lactose intolerance." J Control Release **147**(2): 187-192.

Ravi Kumar, M. N. (2000). "Nano and microparticles as controlled drug delivery devices." J Pharm Pharm Sci **3**(2): 234-258.

Riddle, D. L. (1997). C. elegans II. Plainview, N.Y., Cold Spring Harbor Laboratory Press.

Russell-Jones, G. J., H. Veitch, et al. (1999). "Lectin-mediated transport of nanoparticles across Caco-2 and OK cells." Int J Pharm **190**(2): 165-174.

Schapira, A. H. (2005). "Present and future drug treatment for Parkinson's disease." J Neurol Neurosurg Psychiatry **76**(11): 1472-1478.

So, S., K. Miyahara, et al. (2011). "Control of body size in C. elegans dependent on food and insulin/IGF-1 signal." Genes Cells **16**(6): 639-651.

Wang, C., P. C. Ho, et al. (2010). "Wheat germ agglutinin-conjugated PLGA nanoparticles for enhanced intracellular delivery of paclitaxel to colon cancer cells." Int J Pharm **400**(1-2): 201-210.

Wang, Z. H., Z. Y. Wang, et al. (2010). "Trimethylated chitosan-conjugated PLGA nanoparticles for the delivery of drugs to the brain." Biomaterials **31**(5): 908-915.
Weissenbock, A., M. Wirth, et al. (2004). "WGA-grafted PLGA-nanospheres: preparation and association with Caco-2 single cells." J Control Release **99**(3): 383-392.

Wen, Z., Z. Yan, et al. (2011). "Odorranalectin-conjugated nanoparticles: preparation, brain delivery and pharmacodynamic study on Parkinson's disease following intranasal administration." J Control Release **151**(2): 131-138.

Wintle, R. F. and H. H. Van Tol (2001). "Dopamine signaling in Caenorhabditis elegans-potential for parkinsonism research." Parkinsonism Relat Disord **7**(3): 177-183.

Wolkow, C. A. (2006). "Identifying factors that promote functional aging in Caenorhabditis elegans." Exp Gerontol **41**(10): 1001-1006.

Wolters, E. (2009). "Non-motor extranigral signs and symptoms in Parkinson's disease." Parkinsonism Relat Disord **15 Suppl 3**: S6-12.

Wood, W. B. (1988). The Nematode Caenorhabditis elegans. Cold Spring Harbor, N.Y., Cold Spring Harbor Laboratory.

Yin, Y., D. Chen, et al. (2006). "Preparation and evaluation of lectin-conjugated PLGA nanoparticles for oral delivery of thymopentin." J Control Release **116**(3): 337-345.

Zigoneanu, I. G., C. E. Astete, et al. (2008). "Nanoparticles with entrapped alpha-tocopherol: synthesis, characterization, and controlled release." Nanotechnology **19**(10): 105606.

CHAPTER 4. CONCLUSION

In recent years, polymeric nanoparticles were well investigated and the technology has developed at a rapid pace. PLGA/PLA nanoparticles (100-300 nm) have been proven as potential carriers for drug delivery across the BBB with advantages of both enhanced drug efficiency and safety. Both *in vitro* and *in vivo* studies on delivery of drugs with surface modified PLGA/PLA NPs (100-300 nm) to CNS confirmed the enhanced brain uptake and therapeutic efficacy of certain drugs entrapped in PLGA NPs.

A DAergic neuron targeting delivery system was successfully constructed by conjugating tWGA with PLGA NPs. PLGA-tWGA polymer was synthesized first and then used to prepare nanoparticles of 221 nm (5 μg tWGA /mg NPs). The following tests in *C.elegans* showed that PLGA-tWGA NPs did not have significant effect on pumping rate and life span of *C.elegans* as low concentration (<3 mg/ml). Fluorescent studies of GFP-DAergic neurons revealed that area of GFP-DAergic neurons of worms treated with high concentrations PLGA-tWGA NPs (>3mg/ml) was significantly decreased. Number and mean intensity of GFP-DAergic neurons also decreased, but no significant difference was found compared with control group. The co-localization of PLGA-tWGA NPs with the GFP-DAergic neurons of treated worms along with locomotion and neuron studies of *C.elegans* proved that WGA conjugated PLGA NPs at low concentrations (<3mg/ml) targeted DAergic neurons without negative effects.

CHAPTER 5. FUTURE WORK

The mechanism of tWGA transport to DAergic neurons when conjugated to PLGA NPs has not been thoroughly understood as a result of this study. Future studies should consider unveiling the mechanism of NPs uptake and transport to the neurons, as well as the effect of different sizes of nanoparticles and different amounts of tWGA on targeting neurons in *C. elegans*. Furthermore, PLGA-tWGA NPs with entrapped L-DOPA should be synthesized and investigated for the drug efficacy in *C.elegans*. Other animal studies such as mice or rats should also be considered to determine the ability of PLGA-tWGA NPs cross the BBB. It is necessary to assess the safety and potential risks of PLGA-tWGA NPs in vertebrate especially after long-term exposure.

APPENDIX. STANDARD CURVES

1. Standard Curve for WGA

The conjugation efficiency of PLGA-tWGA NPs was determined by BCA protein assay (BCA protein assay kit, Thermo Scientific, Rockford, IL, USA) (Mo and Lim 2005). An enhanced test tube protocol with working range at 5-250 μg/ml was used. A series of albumin (BSA) solutions were prepared for a standard curve. The volume of 0.1 ml of each standard BSA solution, PLGA-tWGA solution were pipetted to each labeled tube, and 2.0 ml freshly prepared BCA working reagent was added to each tube. The mixtures were incubated at 60 ℃ for 30 minutes, and cooled to room temperature. The absorbance of all samples was measured with a spectrophotometer set at 562 nm within 10 minutes. A cuvette filled only with water was set as blank. The experiment was done in triplicate.

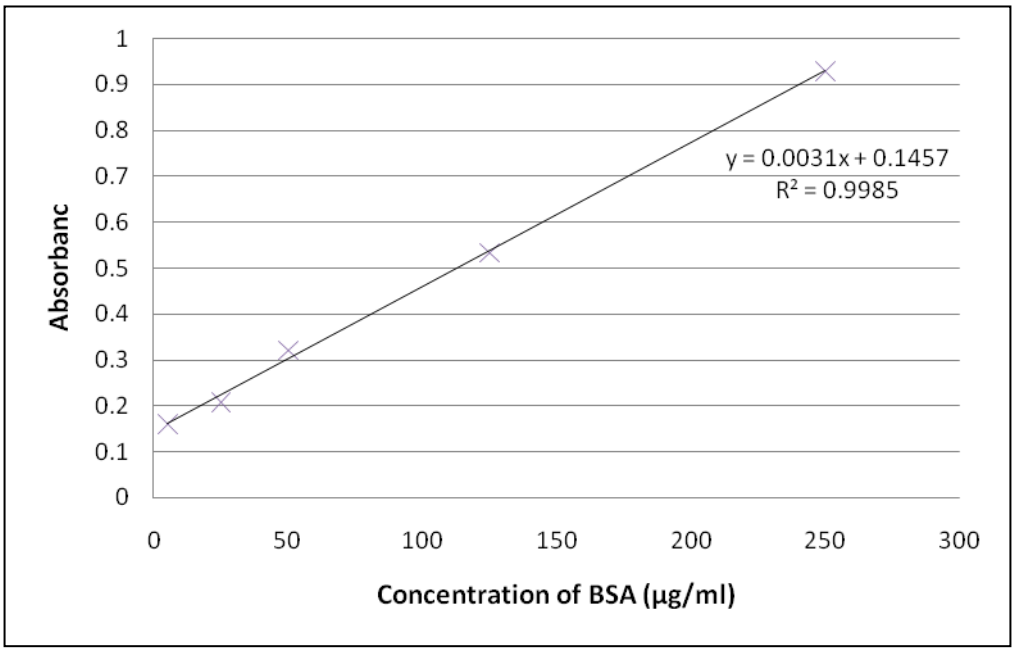

Figure A.1. Standard curve for WGA

2. Standard Curve for TRITC

The amount of TRITC conjugated to PLGA-t NPs was determined by using a spectrofluorometer (Wallac 1420 VICTOR, Perkin Elmer Inc., Waltham, Massachusetts, USA). The volume of 0.1 mL standard TRITC solution was pipetted to each well. The intensity of the standard solution was measured at different concentrations at the absorbance 531/572 nm with nano pure water as blank. A number of x replicates was

used.

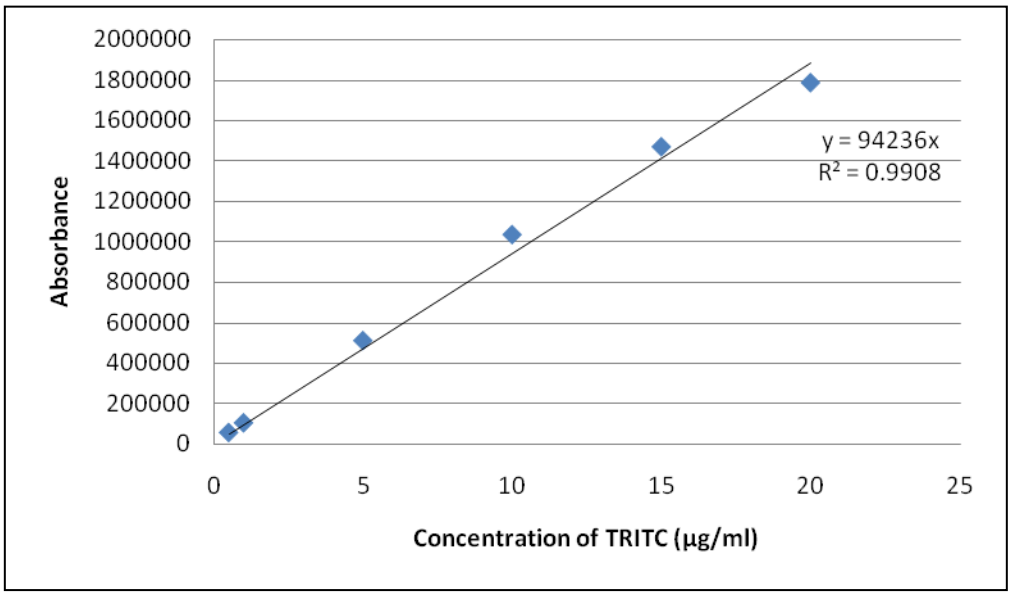

Figure A.2 Standard Curve for TRITC

VITA

Jingyan Li reveived her undergraduate degree in bioengineering in June 2010 from East China University of Science and Technology. In spring 2010, she was accepted for a master's program in the Department of Biological and Agricultural Engineering at Louisiana State University, Baton Rouge, Louisiana. She is an active member of the Phi Kappa Phi honor society.

Jingyan Li will be awarded the degree of Master of Science in Biological and Agricultural Engineering from Louisiana State Univeristy in December 2012.